LBL-12670
SAC-54
UC-70

SWEDISH-AMERICAN COOPERATIVE PROGRAM ON RADIOACTIVE WASTE STORAGE IN MINED CAVERNS IN CRYSTALLINE ROCK

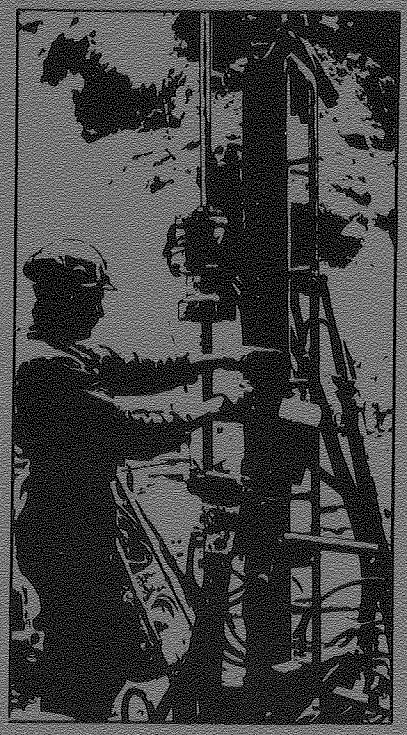

Technical Information Report No. 54

ASSESSMENT OF THERMOCOUPLE TEMPERATURE MEASUREMENTS DURING IN SITU HEATER EXPERIMENTS AT STRIPA, SWEDEN

E. Binnall and M. McEvoy

October 1985

A Joint Project of

Swedish Nuclear Fuel Supply Co.
Fack 10240 Stockholm, Sweden

Operated for the Swedish
Nuclear Power Utility Industry

Lawrence Berkeley Laboratory
Earth Sciences Division
University of California
Berkeley, California 94720, USA

Operated for the U.S. Department of
Energy under Contract DE-AC03-76SF00098.

DISCLAIMER

LBL-12670
SAC-54
UC-70

ASSESSMENT OF THERMOCOUPLE TEMPERATURE MEASUREMENTS DURING IN SITU HEATER EXPERIMENTS AT STRIPA, SWEDEN

Eugene Binnall and Maurice McEvoy

October, 1985

Earth Sciences Division
Lawrence Berkeley Laboratory
University of California
Berkeley, California 94720

This work was supported by the Assistant Secretary for Nuclear Energy, Office of Civilian Waste Management of the U.S. Department of Energy under Contract No. DE-AC03-76SF00098. Funding for this project is administered by the Office of Crystalline Repository Development at Battelle Memorial Institute.

GLOSSARY

This glossary is included to provide the reader with a quick reference to uncommon terms or terms that normally have wider meanings but are used in a restrictive sense in this report.

AD-9	Acurex Autodata-Nine data logger
ANSI	American National Standards Institute
B&F	Data logger used for USBM gauges and some thermocouples
DAS	Data acquisition systems
DVM	Digital voltmeter
Engineering data	Experimental data that were converted to engineering units using computer programs written at LBL. Data on the PDT are time-averaged engineering data
Experiment 1	Full-scale experiment with 3.6 kW heater (H9)
Experiment 2	Full-scale experiment with 5 kW heater (H10) and eight additional peripheral heaters (H11-H18)
Experiment 3	Time-scaled experiment
F.S.	Full-scale
IRAD gauge	Vibrating wire stress-meter, manufactured by IRAD Gage, Inc., Lebanon, New Hamshire
IOIS	Modcomp's Input/Output Interface Subsystem
IPR	Ice-point reference
I/O	Input and Output
LBL	Lawrence Berkeley Laboratory, University of California, Berkeley, California
LLNL	Lawrence Livermore National Laboratory
Logger data	Data printed on paper tapes by data loggers; also referred to as "data-logger data"

ModComp	Modular Computer Systems, Inc., computer manufacturer
MUX	Multiplexer
NBS	National Bureau of Standards, U.S.A.
PCI	Peripheral Controller Interface
PDT	Public-domain data tapes. Two 800 bpi, 2400 ft. magnetic tapes (for computer use) containing digital data from the Stripa heater experiments; available to the public
ppm	Parts per million
Raw data	Unprocessed experimental data recorded by the computer-based data acquisition system
REMAC	Remote Data Acquisition Subsystem, manufactured by ModComp
RFS	Richmond Field Station, University of California
rms	root-mean-square
RTD	Resistance temperature device. A temperature-sensing transducer that changes in electrical resistance as a function of temperature
RTV	Room Temperature Vulcanizing material
SAC	Swedish-American Cooperative Program on Radioactive Waste Storage in Mined Caverns in Crystalline Rock
S/N	Serial number
SPF	Sensor Parameter File. Location of data in computer files. Sometimes called "sensor number."
TC or T/C	Thermocouple
Thermocouple	Chromel-Alumel type K thermocouple
T.S.	Time-Scaled
USBM gauge	U.S. Bureau of Mines borehole deformation gauge
WRRAIS	Wide-Range Relay Analog-Input Subsystem, manufactured by ModComp

LIST OF FIGURES

LIST OF TABLES

ABSTRACT

Heater experiments were conducted in a granite body adjacent to a recently inactivated iron ore mine at Stripa, Sweden, to investigate the response of a hard rock mass to thermal loading. Electrical heaters were installed to simulate thermal loading by canisters of high-level nuclear waste. Extensometers, borehole deformation gauges, vibrating wire stressmeters, and thermocouples were used to monitor the thermomechanical response of the granite. A computer based data acquisition system recorded data, performed on-line computations and provided graphic output. Heating commenced on June 1, 1978 and lasted approximately one year in each of three experiment areas. Monitoring of the rock cool-down response continued for half a year after the heaters were turned off. In-situ post-experiment recalibrations of instrumentation were completed by June, 1980.

This report assesses the performance of the thermocouples that were used during the experiment to measure the temperature field in the granite surrounding the electrical heaters. Calibration methods, setup, and error sources are described. Difficulties encountered with the thermocouples are discussed and the accuracy of the temperature measurements is estimated. Calibration data are presented to illustrate the variability among thermocouples. Comparison, over time, of data independently acquired using a computer and data loggers illustrates the long-term variabilities of the temperature measurements.

1.0 INTRODUCTION

Field experiments were conducted in Sweden to investigate the effects of thermal loading on design parameters for repositories of high-level radioactive waste. The heat generated by radioactive decay must be accounted for when assessing the structural integrity of a waste repository and when estimating the likelihood of any waste returning to the biosphere while still significantly radioactive. Electrical heaters were installed in specially mined drifts at the Stripa mine to simulate the heat produced by actual radioactive-waste canisters. Experiments were designed using these heaters to test both short-term and long-term thermal loading effects on granite. These experiments were conducted as part of a Swedish-United States cooperative program to study radioactive waste storage (Witherspoon and Degerman, 1978; Witherspoon et al., 1980).

The first heater was turned-on June 1, 1978, and the last heater was turned-off September 26, 1979. Rock cool-down measurements continued through February, 1980. Rock temperatures of over 300°C were measured and the mechanical response of the rock was measured at temperatures to 150°C. Measured heater canister skin temperatures approached 500°C.

The heater experiments were located in two drifts 340 meters below the surface. A time-scaled experiment was located in one of the drifts and two full-scale experiments in opposite ends of the other drift, as shown in Fig. 1. An extensometer drift ran parallel to the full-scale drift, but at a lower elevation, to provide access for installation of horizontal instrumentation in the rock surrounding the full-scale heaters. Heater power controllers, instrument signal conditioning

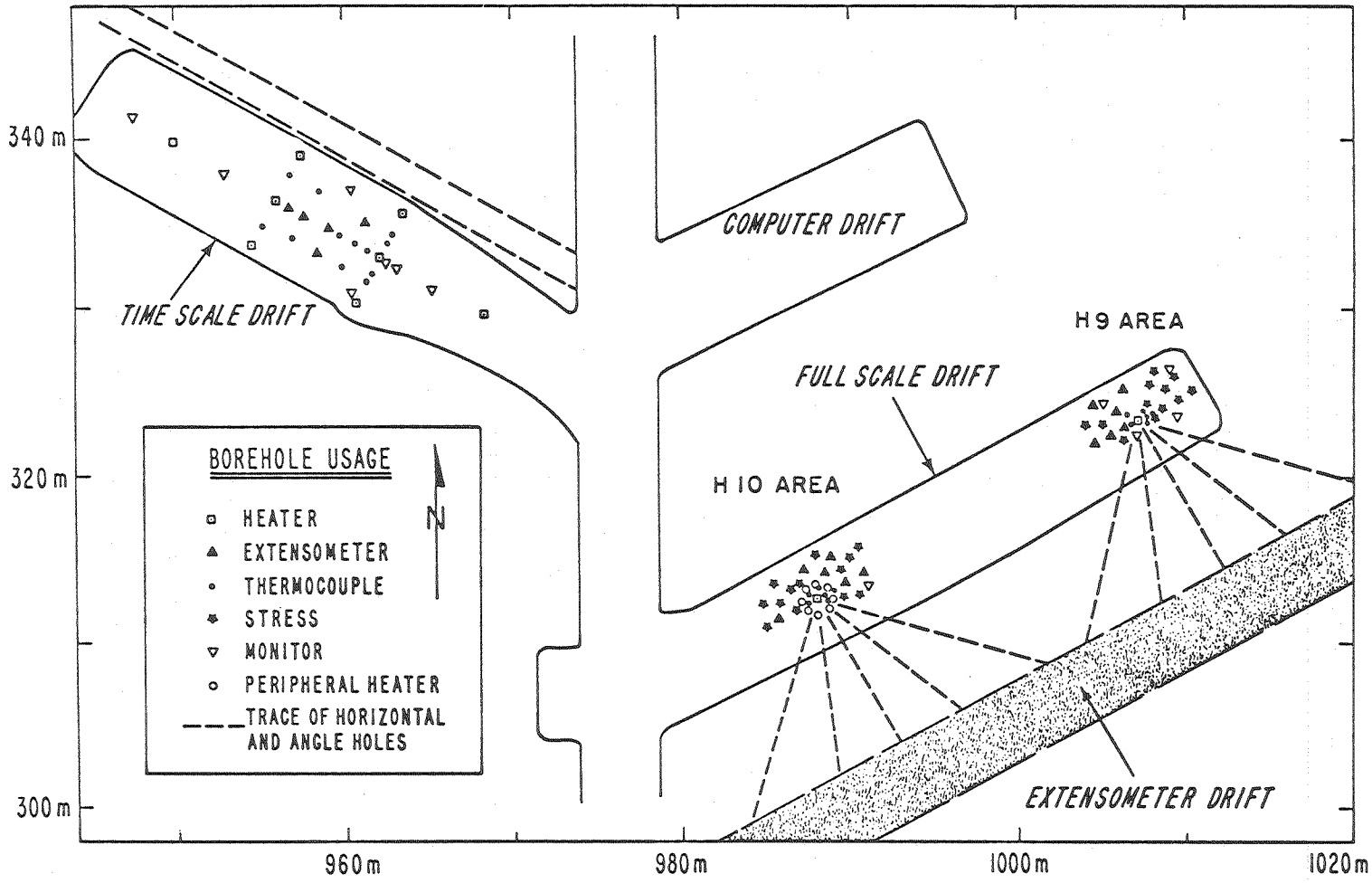

Fig. 1. Plan view of experiment area 340 m underground, showing locations of heater and instrument boreholes (from Schrauf et al., 1979).

circuits, data loggers, computer scanners, analog-to-digital converters, and interfacing electronics were housed in sheds located in the two heater drifts. A 2.5 by 8 m instrumentation shed was located against one wall between the two experiments in the full-scale drift. A 3 by 4 m instrumentation shed was located in the back end of the time-scaled drift. More than 750 sensor signals were digitized and transmitted to a ModComp IV computer housed underground in a climate-controlled room in a drift near the heater experiments.

Thermocouples were used to measure temperature fields in the Stripa granite and to monitor instrument temperatures for thermal compensation. All thermocouples were connected to ice-point temperature references which were connected to Wide-Range Relay Analog-Input Subsystems (WRRAISs) that sampled and digitized data for transmission to the computer system. Parallel outputs from the ice-point references were connected to data loggers located in the experiment areas. Schrauf et al. (1979) describe the original field calibration and installation of the thermocouples.

The Stripa data acquisition system, shown in Fig. 2, used a ModComp IV computer to acquire and digitize data, convert measured values to engineering units, store and randomly access data, provide on-site graphic data displays, and write magnetic tapes used to transfer data to Berkeley for further analysis. Duplicate computer peripherals and back-up data loggers were provided to reduce data losses caused by possible equipment failures during the experiment. McEvoy (1979) provides additional details.

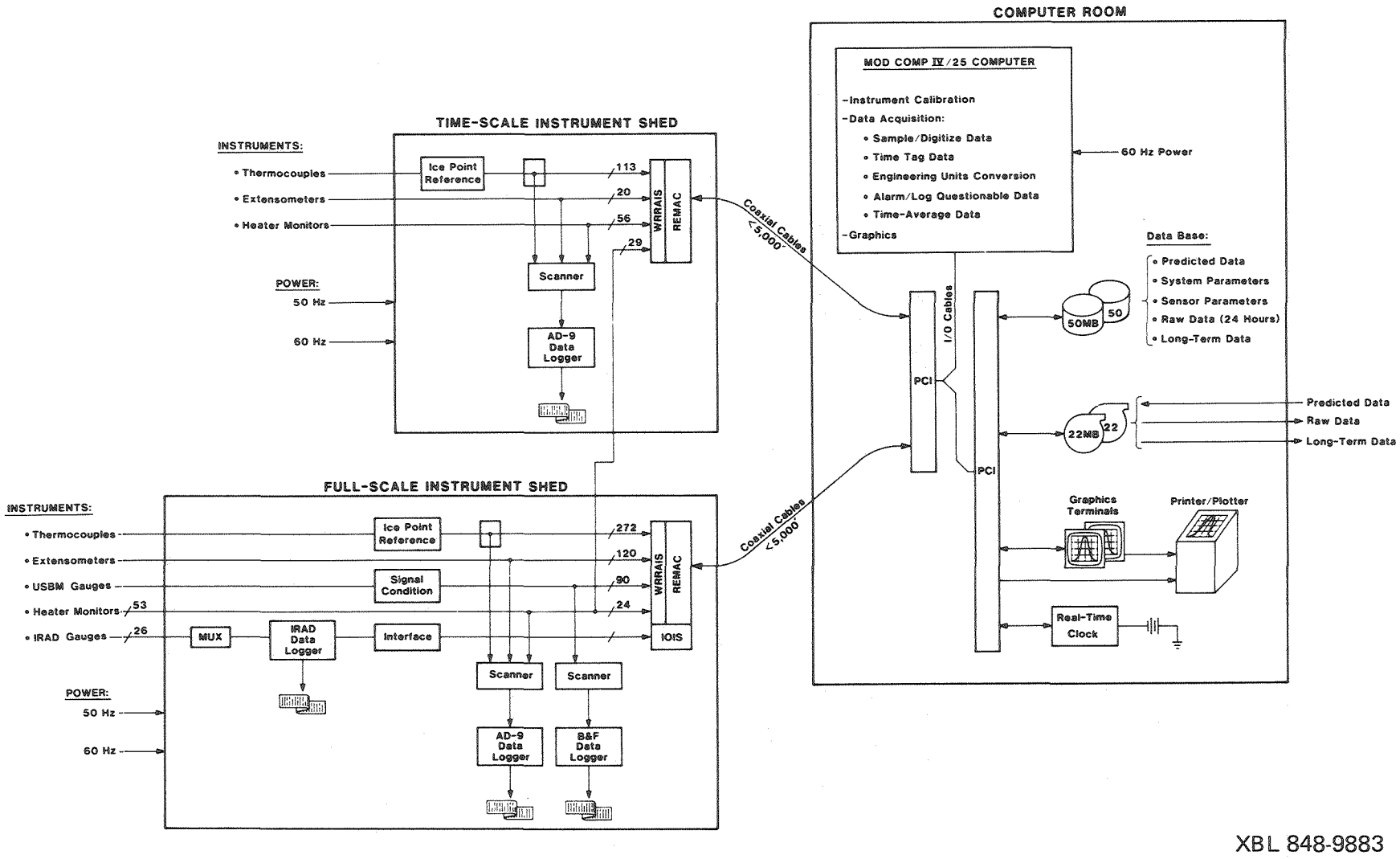

Fig. 2. Block diagram of the Stripa data acquisition system.

Acurex Autodata-Nine and B&F data loggers were used as the back-up data loggers to the computer system. Outputs from these data loggers were printed on paper tape. The data loggers proved quite valuable. They provided cross-checks for the computer's data; aided with instrument calibration, debugging, and maintenance; and provided a convenient means of reading selected sensors while working in the experiment areas where the data loggers were located.

Before the heaters were turned-on, the computer was used interactively to calibrate individual low-temperature thermocouples (i.e., thermocouples that were expected to remain below 200°C). This was done in the mine after the thermocouples were wired in their final operating configuration. During the experiment, all active thermocouple voltages were sampled by the computer at 15-minute intervals. These raw data points were time tagged, converted to temperature, temporarily stored in a 24-hour disc buffer, and logged on magnetic tapes. After raw data points accumulated for one time-averaging interval, their arithmetic mean was computed to obtain a representative mean data value and associated mean time. These less frequent time-averaged points were stored in a long-term disc file which was maintained on-line for the duration of the experiment.

Chan et al. (1980) described the heater power histories and the procedures for data acquisition, handling, verification, processing, and compensating for errors introduced by hardware problems in the computer's data acquisition system.

This report describes the performance of the thermocouples that were used during the heater tests and assesses measurement errors resulting from calibration uncertainties and thermocouple limitations. The performance of the other instruments, with their associated measurement tolerances, are addressed in other SAC reports.

1.1 Thermocouples Used at Stripa

Temperatures were measured at Stripa using Chromel-Alumel (ANSI type K) thermocouples supplied by Omega Engineering, connected to ice-point temperature references manufactured by Kay Instruments. The experiments used five model R170, 100-channel ice-point references (IPRs) with typical stability ±0.01°C and guaranteed stability of ±0.025°C. Thermocouples were attached to one or more points on each in-situ geotechnical instrument to measure temperature and provide data for thermal compensation of instrumentation. Borehole and instrumentation locations are shown in Figs. 3 through 8. Three-dimensional temperature fields in the rock were measured using thermocouples located in the T-boreholes shown in Figs. 3 and 4. A string of five thermocouples was placed in each T-hole as shown in Figs. 7 and 8. In addition, several thermocouples were also mounted to each heater canister.

Type K thermocouples were used exclusively at Stripa: 272 in the full-scale experiments and 113 in the time-scaled experiment. Three types of thermocouple wire coverings were used: Teflon (type TFE) where initial thermal calculations predicted temperatures below 200°C, 304-stainless steel sheaths, where temperatures might exceed 200°C but remain below 400°C, and Inconel-600 sheaths for the heater canisters

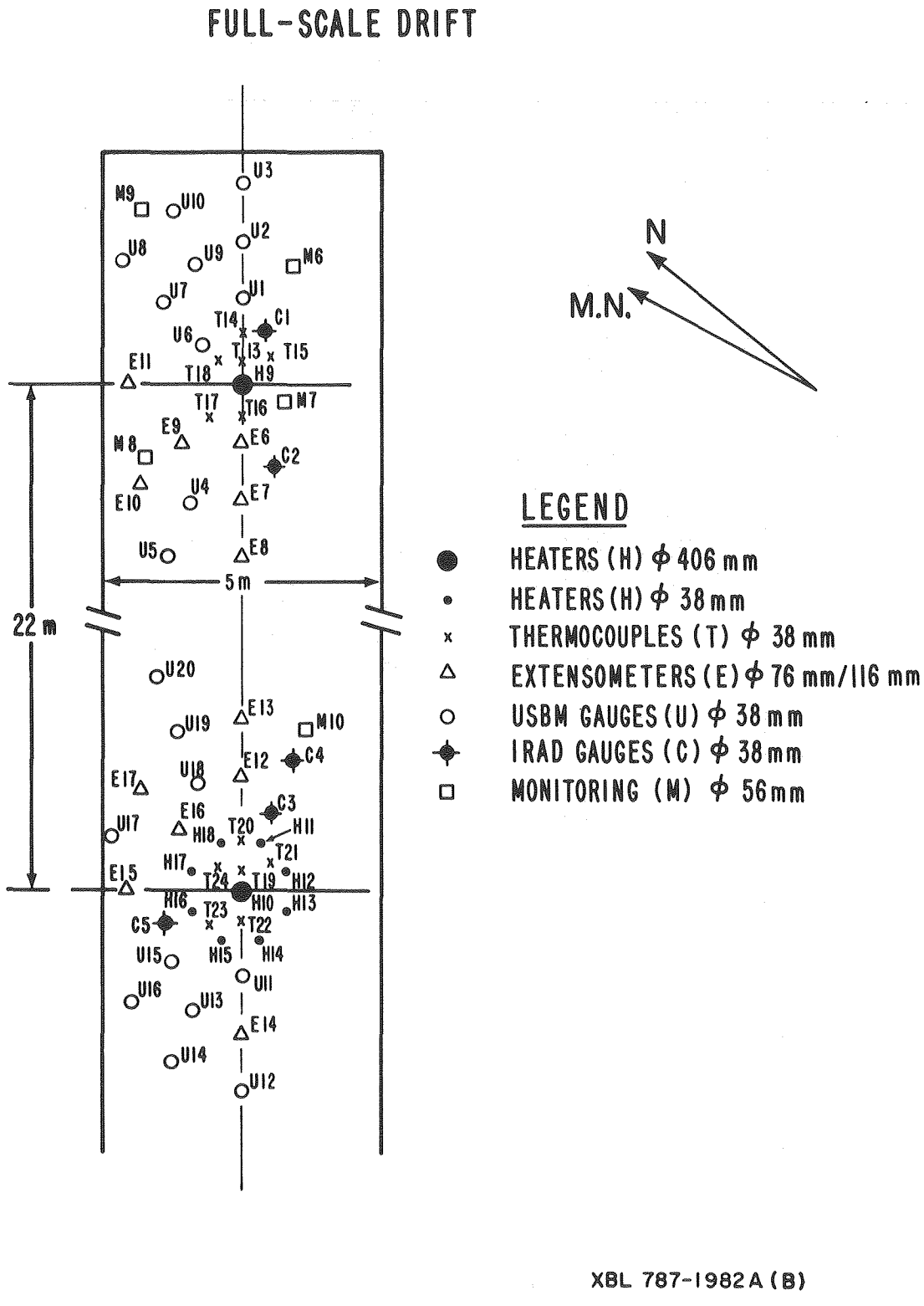

Fig. 3. Borehole layout in the full-scale drift (from Kurfurst et al., 1978).

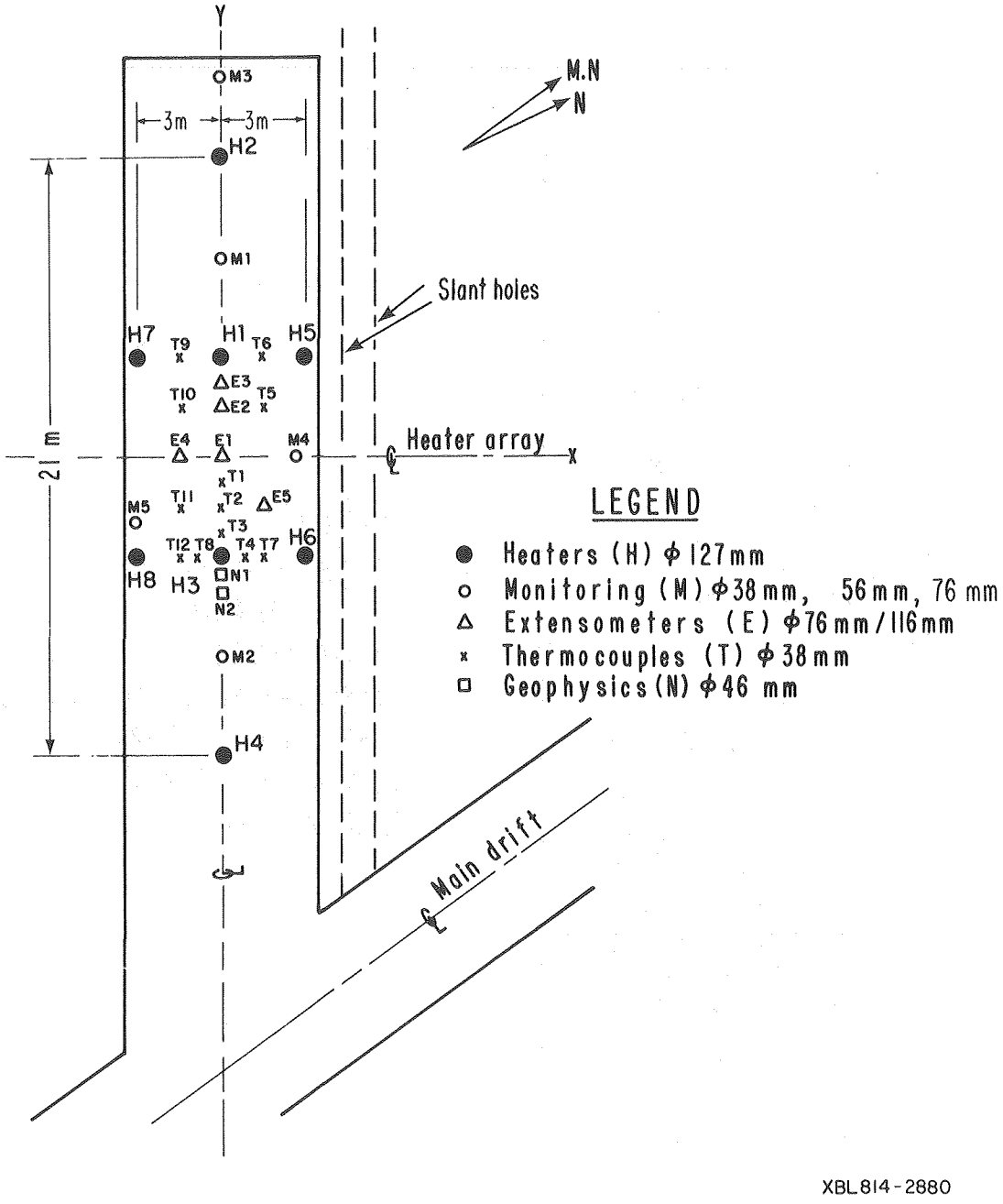

Fig. 4. Borehole layout in the time-scaled drift (from Kurfurst et al., 1978).

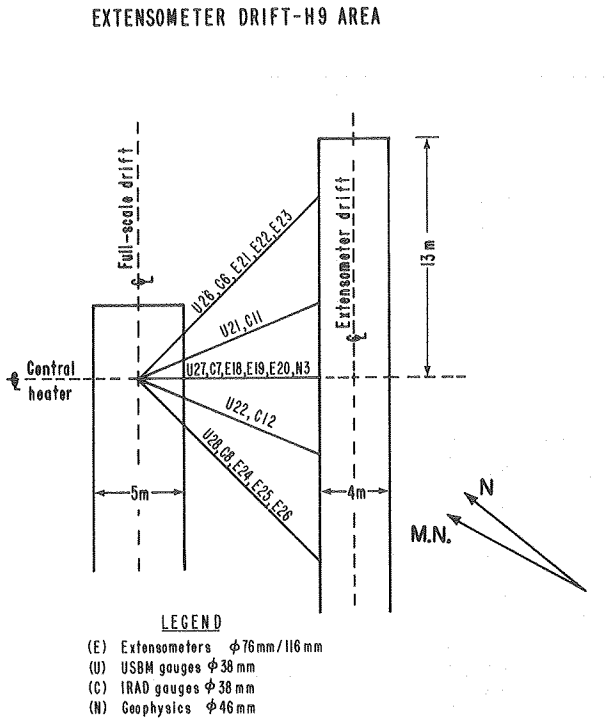

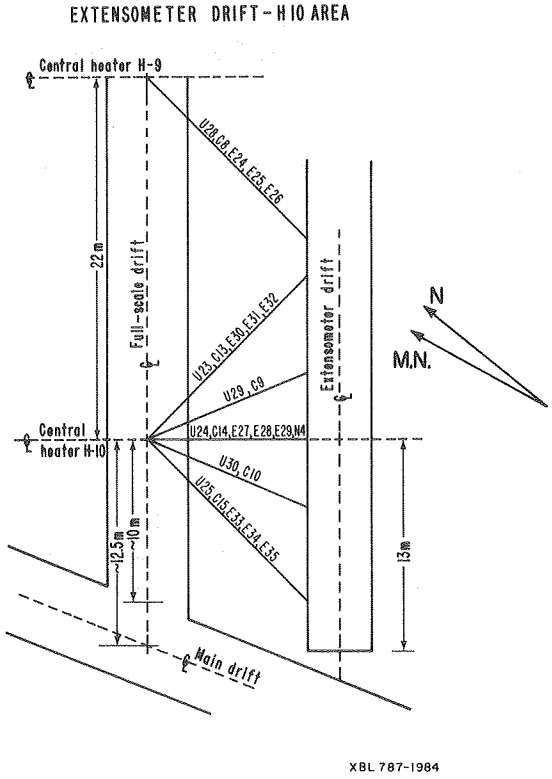

Fig. 5. Borehole layout in the extensometer drift for: (a) H9 heater area and (b) H10 heater area (from Kurfurst et al., 1978).

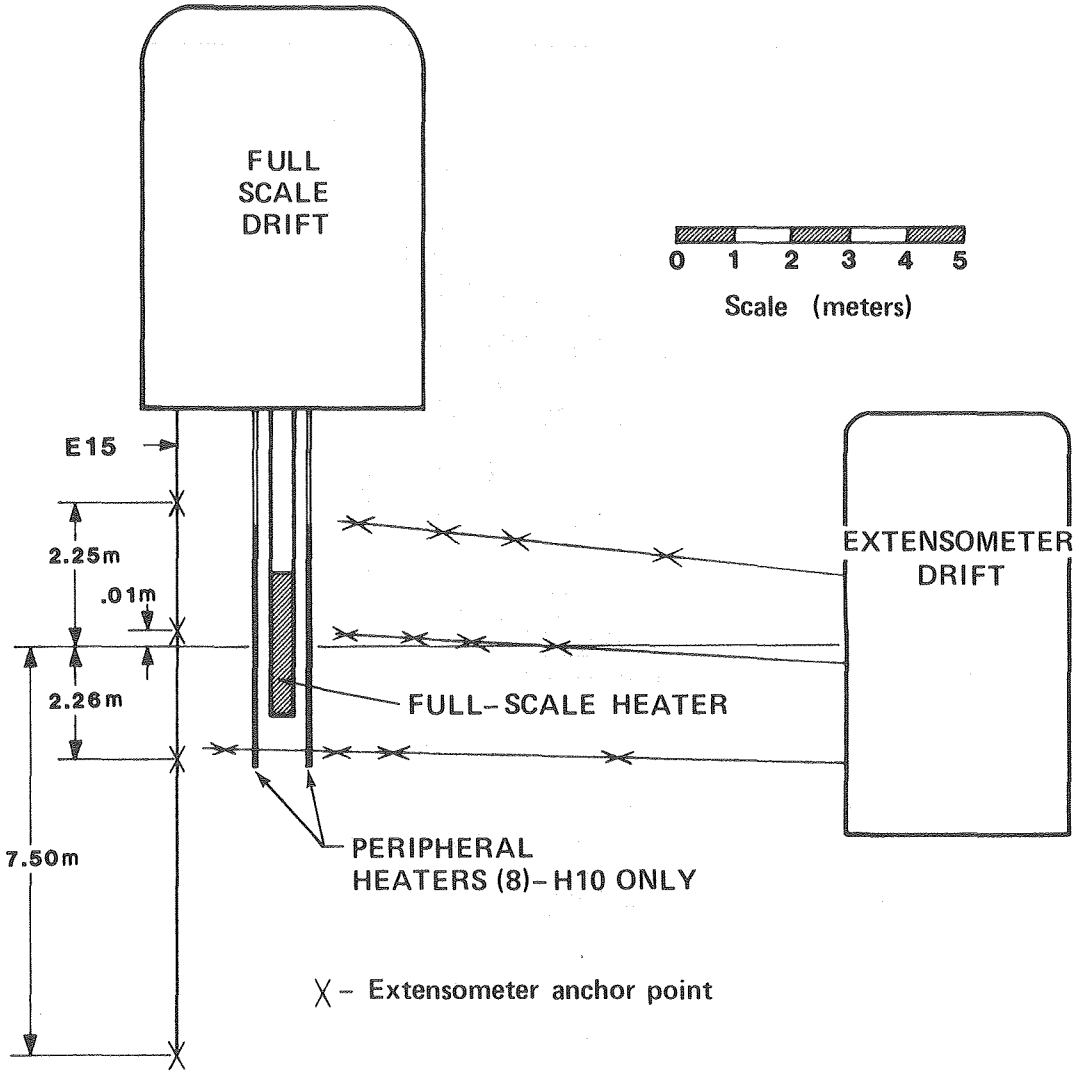

Fig. 6. Elevation view of full-scale experiments 1 and 2 illustrating heater and extensometer locations (from Chan et al., 1980).

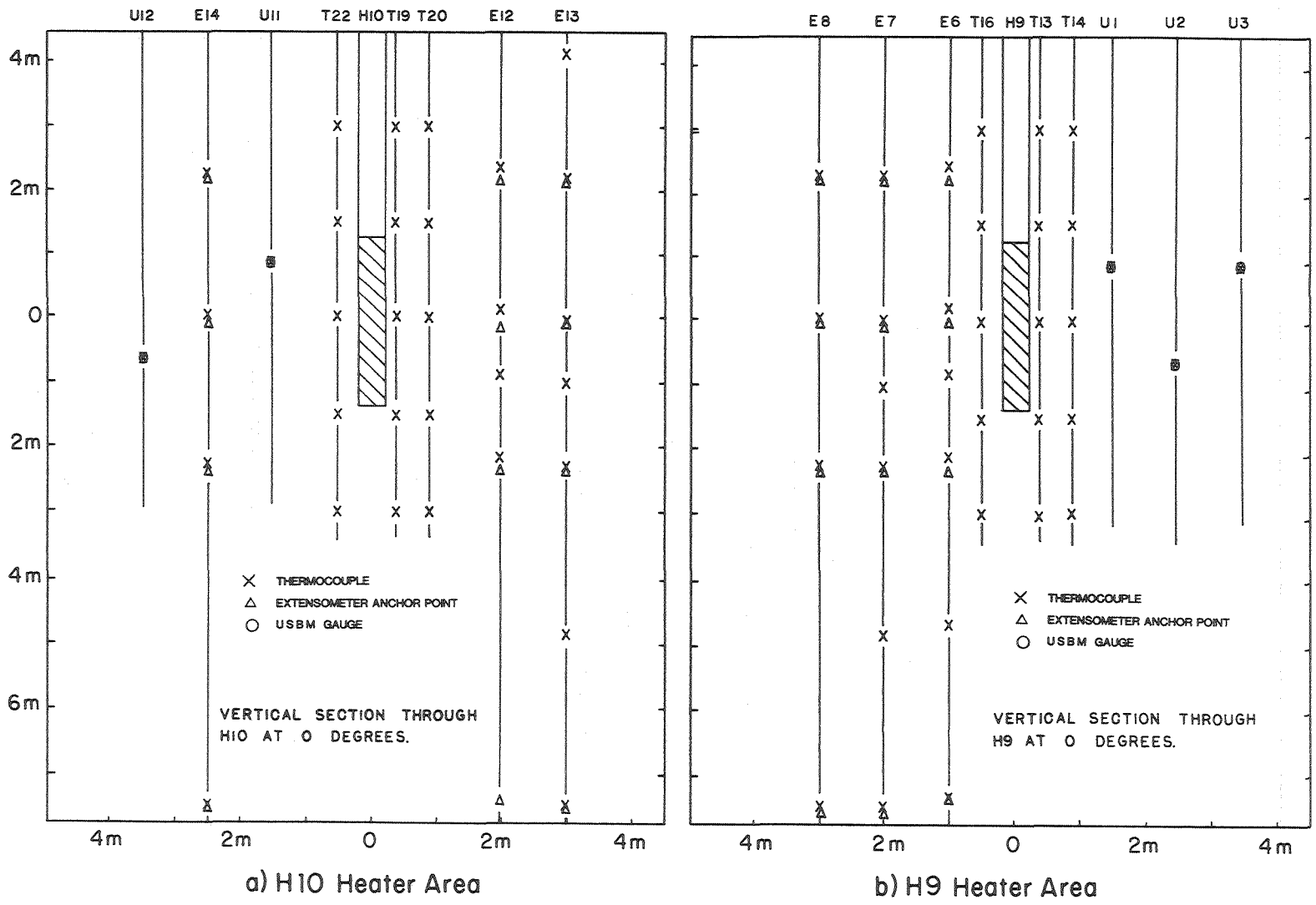

XBL848-9875

Fig. 7. Vertical section along the axis of the full-scale drift. (a) H10 heater area and (b) H9 heater area (from Chan et al., 1980).

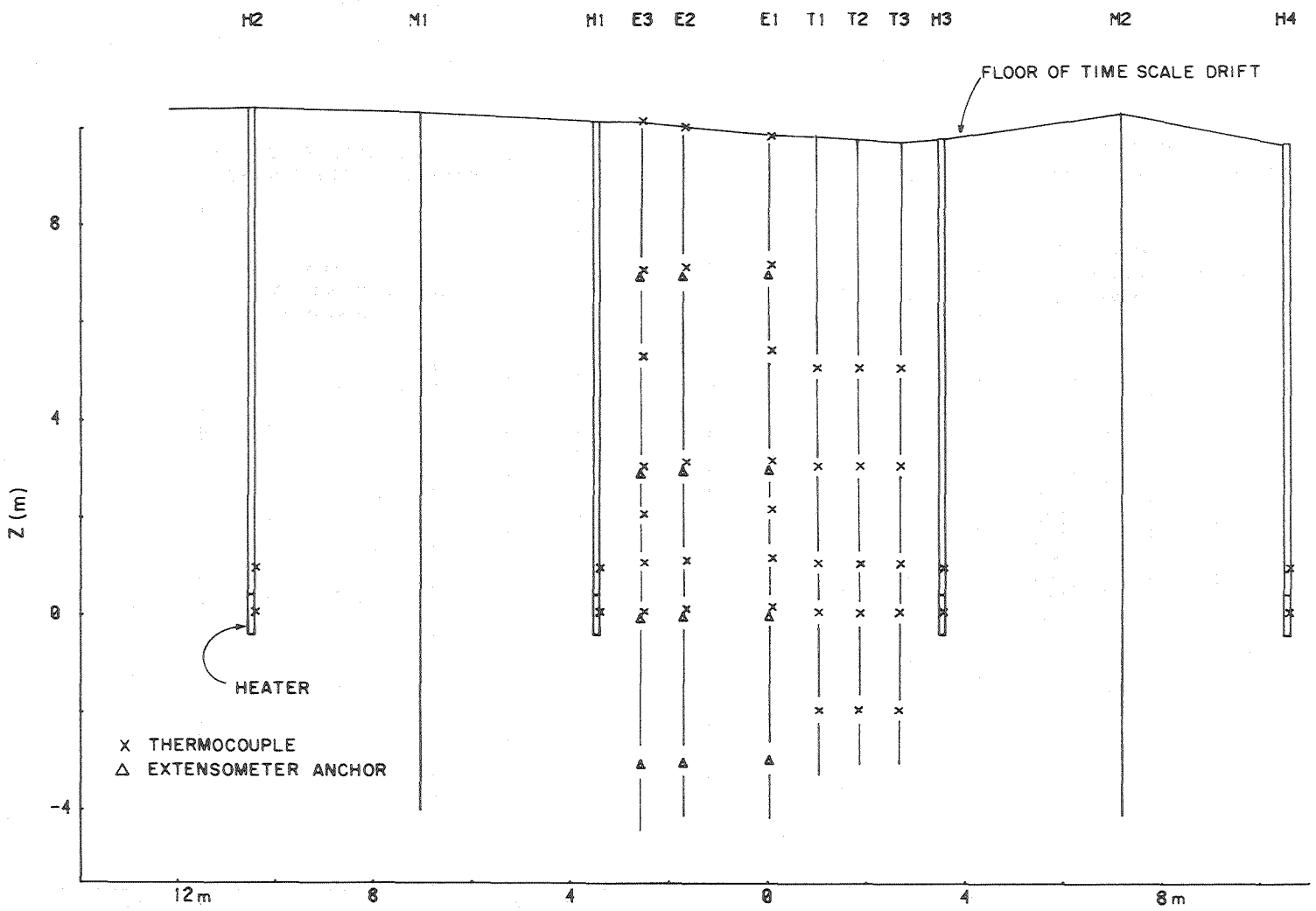

Fig. 8. Vertical section along the axis of the time-scaled drift (from Schrauf et al., 1979).

where some temperatures would exceed 400°C. Initial rock temperature calculations later proved to be high. Table 1 shows the quantities of thermocuples with the three types of wire covering (or sheath material) initially installed before the start of the Stripa experiments and following completion of the experiments after replacements had been made. Where possible, thermocouples were obtained from the same Chromel and Alumel melts and from the same wire lots in order to minimize variability due to differences in metallurgy. All thermocouples used at Stripa were purchased from Omega Engineering, Inc., Stanford, Connecticut.

A temperature measurement accuracy of $\pm$0.5°C, below 200°C, was the original goal. This necessitated individual calibrations in an environment as close as possible to actual operating conditions. During the experiment a fourth-order-polynomial was used to represent each thermocouple's temperature versus voltage calibration profile. Polynomial coefficients derived from NBS tables were used for the higher temperature stainless steel and Inconel sheathed thermocouples. The numerous failures and replacements of thermocouples, along with data acquisition and calibration equipment variables, eventually made the use of individual calibrations impractical without more analysis, and in the end they were abandoned. As described in Chan et al. (1980) and Section 3.0, approximations to the National Bureau of Standards (NBS) voltage-to-temperature conversion for type-K thermocouples are used instead. Table A-1 and Fig. A-1 in the appendix show the NBS data over the temperature range encountered at Stripa.

Table 1. Stripa thermocouple quantities listed by wire covering (insulation or sheath material).

Wire covering (or sheath material)	No. at start of experiments	No. at end of experiments
Teflon (type TFE)	221	279
304-stainless steel	100	32
Inconel-600	64	74
Totals	385	385

1.1.1 Teflon-insulated thermocouples

Teflon-insulated thermocouples were used in regions where peak temperatures less than 200°C were predicted. These thermocouples were manufactured with extruded Teflon insulation over the positive Chromel (nickel-chromium) wire and the negative Alumel (nickel-aluminum) wire, and a Teflon tape, wrapped and fused, over the wire pairs. Junctions were coated with a two component RTV 60 silicone rubber compound. The Teflon (type TFE) was capable of withstanding a maximum continuous-use temperature of 260°C. Since each thermocouple was to be individually calibrated, thermocouples that met ANSI standard-limits-of-error of approximately ±2.2°C over the desired temperature range were purchased rather than thermocouples that met the more accurate ANSI special-limits-of-error.

Some of the RTV-coated junctions on the Teflon thermocouples began leaking water, which caused erroneous readings due to ground currents. This problem was discovered before heater turn-on and solved by removing all electrical ground points other than those that could occur at the thermocouple junctions. In some of the grouted boreholes, head pressure forced water along the thermocouple wire between the two layers of Teflon insulation and into the electronics enclosures. This water was diverted by cutting a short slit in the outer layer of insulation just after the thermocouple wire exited the borehole so that water could escape before reaching the electronics enclosures.

1.1.2 Stainless steel sheathed thermocouples

Type K thermocouples clad in 304-stainless steel sheaths were used where initial calculations predicted that rock temperature might exceed

200°C. These thermocouples were fabricated from 1/16-in. outside diameter thermocouple wire with magnesium oxide (MgO) electrical insulation and with junctions sheathed but ungrounded. Lengths were selected to allow sheathed wire to exit the boreholes into an ambient temperature environment (10 to 20°C) before entering a transition junction, where it was joined to Teflon-insulated, AWG No. 24, type K extension wire that met ANSI standard limits-of-error specifications. The transition junction between sheathed and Teflon-covered wire was welded and strain relieved. The Teflon was sandblasted, and the junction potted with epoxy. The epoxy was then coated with silicone to increase moisture resistance. During manufacture of the sheathed thermocouple wire stock, their Chromel and Alumel thermocouple wires were centered inside a 304-stainless steel tube. The remaining space inside the tube was filled with powered magnesium oxide insulation. The stainless steel tube, insulation and wires were then drawn (or swagged) as a unit to produce a densely packed insulation surrounding the wires inside a stainless steel sheath with an outside diameter of 1/16-in.

All stainless steel clad thermocouples were obtained from a single, special-limits-of-error lot. Sixty stainless steel thermocouples were installed in the twelve close-in temperature boreholes, T13 to T24, which were within a radius of 1 m of either of the two full-scale heaters; four were used with IRAD gauges and thirty-two with extensometer anchor points that were located within 1.5 m of the heaters; and ten were purchased as spares and calibration references. Of the ten spares, four were presumed installed with the initial installation of the four USBM gauges located

within 1.5 m of the heaters, however, documentation fully substantiating this is missing. Table 2 lists boreholes, instruments and sensor numbers associated with the stainless steel sheathed thermocouples. Stainless steel was used rather than Inconel simply because of availability.

1.1.3 Inconel sheathed thermocouple

Type K thermocouples clad in Inconel-600 sheaths and capable of temperatures up to 1150°C were used to monitor heater canister temperatures. Initial calculations indicated that heater temperatures might exceed 500°C. Measured temperatures on the 5-kW full-scale heater (H10) actually approached 500°C. Sixteen thermocouples were used on the two full-scale heaters, twenty-four on the eight peripheral heaters, and twenty-four on the eight time-scaled heaters. Additional units were purchased as spares and for calibration purposes. Ten of these spares were used to replace stainless steel thermocouples in boreholes T-19 and T-20 following some thermocouple failures in these holes.

These thermocouples were fabricated from 1/16-in. diameter Inconel sheathed stock with a transition junction to heavier, AWG No. 20 size, Teflon-insulated extension wire. The Inconel sheathed thermocouples were fabricated to the same general specifications as the stainless steel sheathed thermocouples (see section 1.1.2).

Inconel sheathed thermocouples were inserted down long tubular thermocouple wells attached to the sides of the time-scaled heater borehole casings. These wells were closed at the bottom near the heater elements. The closed bottoms trapped moisture in a number of cases,

Table 2. Initial installation of stainless steel sheathed thermocouples.

Exp.	SPF No.	Borehole	Orientation	Assoc. gauge	Comments**
1(H9)	84-113	T13-T18	Vertical	TC	S/T, Sand
1(H9)	17-20	E6	Vertical	Extens.	G
1(H9)	29-32	E9	Vertical	Extens.	G
1(H9)	44	E18	Horizontal	Extens.	G
1(H9)	48	E19	Horizontal	Extens.	G
1(H9)	51-52	E20	Horizontal	Extens.	G
1(H9)	56	E21	Horizontal	Extens.	G
1(H9)	60	E22	Horizontal	Extens.	G
1(H9)	64	E23	Horizontal	Extens.	G
1(H9)	66	E24	Horizontal	Extens.	G
1(H9)	72	E25	Horizontal	Extens.	G
1(H9)	76	E26	Horizontal	Extens.	G
1(H9)	77	C1	Vertical	C1 (IRAD)	S/T*
1(H9)	78	U6	Vertical	C2 (IRAD)	S/T*
1(H9)	2	U1	Vertical	U1 (USBM)	S*/T*
1(H9)	7	C2	Vertical	U6 (USBM)	S*/T*
2(H10)	510-519	T19-T20	Vertical	TC	S/In, Sand
2(H10)	520-539	T21-T24	Vertical	TC	S/T, Sand
2(H10)	458-461	E16	Vertical	Extens.	G
2(H10)	469	E27	Horizontal	Extens.	G
2(H10)	473	E28	Horizontal	Extens.	G
2(H10)	476-477	E29	Horizontal	Extens.	G
2(H10)	481	E30	Horizontal	Extens.	G
2(H10)	485	E31	Horizontal	Extens.	G
2(H10)	489	E32	Horizontal	Extens.	G
2(H10)	493	E33	Horizontal	Extens.	G
2(H10)	497	E34	Horizontal	Extens.	G
2(H10)	501	E35	Horizontal	Extens.	G, B
2(H10)	502	U15	Vertical	C3 (IRAD)	S/T
2(H10)	504	C5	Vertical	C5 (IRAD)	S/T*
2(H10)	427	U11	Vertical	U11(USBM)	S*/T*
2(H10)	431	C3	Vertical	U15(USBM)	S*/T

**Comments

S/In	Stainless steel sheathed TC initially installed, replaced with Inconel sheathed TC during experiment.
S/T	Stainless steel sheathed TC initially installed, replaced with Teflon insulated TC during experiment.
Sand	Borehole backfilled with sand.
G	Stainless steel sheathed TC in grouted borehole, TC not removable.
B	TC broken during installation, not functional during experiment.
*	Stainless steel sheathed or Teflon insulated TC was presumed installed as indicated, however, substantiating documentation is missing.

which resulted in a boiling and condensing cycle within the tubing that caused erratic temperature readings until the moisture was removed. Holes in the well bottoms would have avoided this problem. Full-scale and peripheral heater thermocouples were not in closed wells and, therefore, did not experience this phenomenon.

1.1.4 Thermocouple heat treatment

As discussed in Schrauf et al. (1979), thermocouples can exhibit a shift in their voltage-temperature characteristics following exposure to high temperature. If Chromel-Alumel is subjected to temperatures between 500 to 600°C for periods of 5 to 10 hours, chromium in the Chromel precipitates out along the grain boundaries as chromium carbide, causing a permanent increase in thermocouple output voltages and, consequently, increased temperature readings. This precipitation is complete after about 30 hours. In an attempt to minimize these drift effects, all stainless steel and Inconel sheathed thermocouples were heat treated at LBL before to shipment to Sweden. They were baked at just below 600°C for about 50 hours and then slowly cooled. Selected thermocouple samples were calibrated before and after this heat treating process, confirming an upward but nonreoccurring shift in output voltage equivalent to about 0.5°C per 100°C of operating temperature above 0°C.

A sample of five of the stainless steel sheathed thermocouples were calibrated from 0 to 300°C both before and after the heat treatment. Before heat treatment they matched the NBS curves within -0.5°C at 0°C and +1.0°C at 300°C. After heat treatment they showed negligible shift

at 0°C, with a linearly increasing shift to +2 to +2.5°C above the NBS curve at 300°C. A second heat-treatment cycle of two of these samples caused no further shift.

The Inconel sheathed thermocouples exhibited nearly identical results. Five samples, calibrated from 0 to 300°C before heat treatment, matched the NBS tables within -0.5°C at 0°C and +1.0°C at 300°C. After heat treatment there was no measurable shift at 0°C, with an increasing shift (proportional to temperature) to between +2 and +3°C above the NBS tables at 300°C.

An unforeseen side effect of this heat treatment was that the stainless steel sheaths became sensitized to corrosion (see Section 2.1). Subsequent corrosion required the replacement of 60 thermocouples (see Section 2.2). The Inconel sheaths remained trouble-free throughout the experiment even though corrosion was evident in some of the 10 thermocouples used as replacements in the T-19 and T-20 boreholes. None of the Inconel sheathed thermocouples used directly on the heaters showed signs of corrosion.

2.0 OPERATING HISTORY

Present thermocouple evaluations indicate that more than 80% functioned without serious problems or replacement for the duration of the heater experiments. However, two types of thermocouple catastrophic failures led to a number of replacements in the full-scale experiments.

The most serious type of failure occurred in the six thermocouple boreholes (T-holes) surrounding each of the two full-scale heaters. A string containing five thermocouples (see Fig. 7) was installed in each of the twelve boreholes. Removal and examination of failed thermocouples in these holes revealed that their 304-stainless steel sheath had failed due to intergranular corrosion, as discussed in detail in Sections 2.1 and 2.2. The first failure was observed in borehole T-19 on August 18, just 46 days following turn-on of H10. Similar failures followed in succession over the next 3 months. As a result, all (60) full-scale T-hole thermocouples were replaced by Teflon insulated or Inconel sheathed thermocouples during this period, though only 23 of the stainless steel sheathed thermocouples actually failed. We have estimated that had these 60 thermocouples not been replaced, the lower four thermocouples in each string of five would likely have failed (a total of 48) before the end of the experiments. No thermocouple catastrophic failures were observed in the time-scaled experiment T-holes where Teflon insulated thermocouples had been initially installed. Morever, the time-scaled thermocouples had been grouted in place, whereas, the full-scale T-holes had been backfilled with sand as described by Schrauf et al. (1979).

The second type of failure requiring replacement was simply due to mechanical breakage of thermocouples during removal of USBM and IRAD gauges for replacement or recalibration. These thermocouple failures are discussed in Section 2.3. The USBM and IRAD gauges were used only in the full-scale experiments, confining this problem to that area. One stainless steel sheathed thermocouple was also destroyed during initial installation of the extensometers, but was not replaced (SPF No. 501 on extensometer E35). Temperature data from a thermocouple on extensometer E32 (SPF No. 489), similarly located in the temperature field and theoretically representative of the damaged thermocouple, has been used to replace the lost data from the thermocouple on E35 (Chan et al., 1980).

The Inconel sheathed thermocouples used with the heaters, totaling 64, proved reliable and rugged. Teflon and stainless steel sheathed thermocouples used with extensometers in the full-scale experiments also gave no indication of failure during the experiments. There may have been intergranular corrosion in the stainless steel sheathes of these thermocouples, but it was not obvious from the data. These thermocouples had been grouted in place along with the extensometers, consequently, eliminating visual inspection. Only Teflon insulated thermocouples had been used with extensometers in the time-scaled experiment and these also gave no indication of catastrophic failure.

2.1 Corrosion of Sheathed Thermocouples

An overlooked side effect of the heat treatment described in section 1.1.4 was that the stainless steel sheaths became susceptible to intergranular corrosion. The phenomenon of formation of chromium carbide

and its precipitation into the grain boundaries is a well-known result of holding 304-stainless steel at temperatures between 425 and 850°C, then cooling slowly. The cause of intergranular corrosion is summarized in the section on corrosion failures in the Metals Handbook of the American Society for Metals (1975). Chromium carbide precipitation depletes adjacent areas of corrosion-preventing chromium, and develops electropotentials within the material. This leaves the regions at grain boundaries highly susceptible to corrosion. The degree of sensitization depends upon the time and temperature history of the heat treatment. The time and temperature scenario used to stabilize the Stripa thermocouples caused their sheaths to become extremely sensitive to intergranular corrosion. This type of corrosion results in brittle failure along the grain boundaries. A portion of the sheath from a failed thermocouple removed from borehole T-20 was photomicrographed, and showed an extreme case of intergranular corrosion.

Several mechanisms could have been responsible for the corrosion. Dissolved oxygen in solution could have accelerated the corrosion since there was a continual supply during borehole dewatering. A dewatering system, described by Schrauf et al. (1979) and Nelson et al. (1981), was used to remove water from the T-holes at intervals of two to eight days for durations of ten to sixty minutes, providing a source of fresh oxygen into the boreholes. Corrosion could also have been increased by carbonic acid produced by the equilibrium shift from carbonate at elevated temperatures. This would be especially prevalent in recondensation where the CO_2 driven out of solution would lack cations necessary to pull the

equilibrium away from acid when redissolved. Both of these dissolved gas corrosions are analogous to the problems commonly associated with boiler corrosion. Chloride ions and sulfur, which are notoriously corrosive, could be a third cause of corrosion. No specific ion analysis was performed in the full-scale experiment room. The closest areas that were analyzed were the time-scaled room and the 410 m level (see Fritz et al., 1979). Both of these areas were low in sulfur. They showed conflicting Cl^- levels of roughly 60 ppm and 300 ppm, respectively. At 200°C, chloride levels as low as 200 ppm can cause destruction to 304-stainless steel. Heat treatment sensitized the stainless steel sheaths to corrosion and could have greatly increased the effect.

Selecting materials for long-term service in an environment such as Stripa requires careful consideration. The 304-stainless steel alloy is resistant to some corrosive environments when it leaves the mill, however, its corrosion resistance depends on maintaining at least 12 percent chromium at the surface to form a passive oxide, and maintaining its austenitic crystal structure. An uncorroded portion of stainless steel sheath material from T-20 was shown to be highly martensitic (a less resistant crystal) probably from both the work hardening that resulted from the drawing process and the carbon repletion within the grains caused by the heat treatment. Even minute concentrations of elements can greatly affect the kinetics of corrosion, and the long-term effects of an environment cannot be understood without complete chemical analysis with an emphasis on corrosion factors. Chromium carbide precipitation in stainless alloys that will be subjected to high

temperatures can be reduced by using noble materials and a lower carbon content. Increased nickel content, such as used in Inconel, is the most effective means of maintaining crystal integrity. This of course increases the expense of the material. Retempering should be considered after any forming processes (e.g., working, or welding). Boiler techniques such as de-oxygenation and carbonate buffering could be applied. The ion content of the water, particularly chloride, should also be considered.

Inconel clad thermocouples proved to be reliable and rugged, and experienced few corrosion problems. However, solid-solution nickel-base alloys such as Inconel-600 are subject to grain-boundary carbide precipitation if held at or slowly cooled through the temperature range of 540 to 760°C (American Society for Metals, 1975). If thus sensitized, they are susceptible to intergranular corrosion in hot caustic solutions and in high-temperature water containing low concentrations of chlorides or other salts. Inconel clad thermocouples used on the heaters were subjected to temperatures approaching 500°C (H10), while others were immersed in hot or boiling mine water, or covered with condensation for periods during the experiments. None of these failed due to Inconel intergranular corrosion. However, there were signs of intergranular corrosion in most of the ten Inconel sheathed thermocouples used as replacements in boreholes T-19 and T-20. These thermocouples functioned properly during the experiment but six broke due to brittleness of the Inconel during removal from the sand backfilled boreholes for recalibration at the conclusion of the experiment.

It may be significant that all thermocouples where intergranular corrosion was detected, whether in stainless steel or Inconal sheath material, were in boreholes that had been backfilled with sand.

Future use of stainless steel sheathed thermocouples in a repository or test facility should probably be avoided, or the type of stainless steel should be carefully matched to the environment and operating conditions.

2.2 Replacement of Stainless Steel Sheathed Thermocouples in T-Hole

The large number of thermocouple failures made it necessary to replace all T-hole thermocouples in the full-scale experiments. Each T-hole contained a string of five thermocouples spaced at 1.5-m intervals. The center thermocouple in the string was located at a depth coplanar with the mid-plane of the heater. Ten Inconel-600 sheathed replacement thermocouples were installed in boreholes T-19 and T-20, and 50 Teflon insulated replacement thermocouples were installed in the other full-scale T-holes. None of these replacement thermocouples were calibrated prior to installation, however, most were calibrated at the conclusion of the experiment. The following three sections discuss the initial installation procedure for the T-hole thermocouples, their failures, and the replacement procedure.

2.2.1 Initial installation procedure

A general description of T-hole thermocouple and dewatering system installation is provided by Schrauf et al. (1979). The installation procedure is reviewed here with some details elaborated.

Thermocouple wires were partially unrolled from their packaging coils so that the open-ended leads could be laid along the cabling trays into the instrumentation sheds and connected to ice-point references in the electronics racks. At the thermocouple junction end, enough length was uncoiled to reach inside the calibration oven.

After calibration, the five thermocouples for one T-hole installation were uncoiled along the catwalk. Thermocouple spacing was established by laying the wires along a measured and marked catwalk rail, then taping the wires together with teflon tape at a number of points along the length while maintaining proper spacing. The thermocouple string was then attached to the T-hole dewatering assembly, as shown in Fig. 9, for installation as a unit. The bottom thermocouple was secured with Teflon tape to a steel wire attached to a steel washer on the bottom plug of the dewatering system. The steel washer was soldered to the 1/8-in. o.d. copper vacuum and pressure tubes used for dewatering. A final check and adjustment of thermocouple spacing was made using a tape measure just prior to installation into the borehole. The thermocouple string was not taped to either of the dewatering tubes and the two tubes were not taped together. This complete assembly, including bottom washers and plug was pushed down the borehole with an installation rod assembly and positioned according to a depth mark. It should be noted that the thermocouple string could lie to any side of the hole or any place laterally within the hole. The hole was then backfilled with sand. Depth measurements were recorded in a field notebook and later transferred to the Master Instrumentation Listing book.

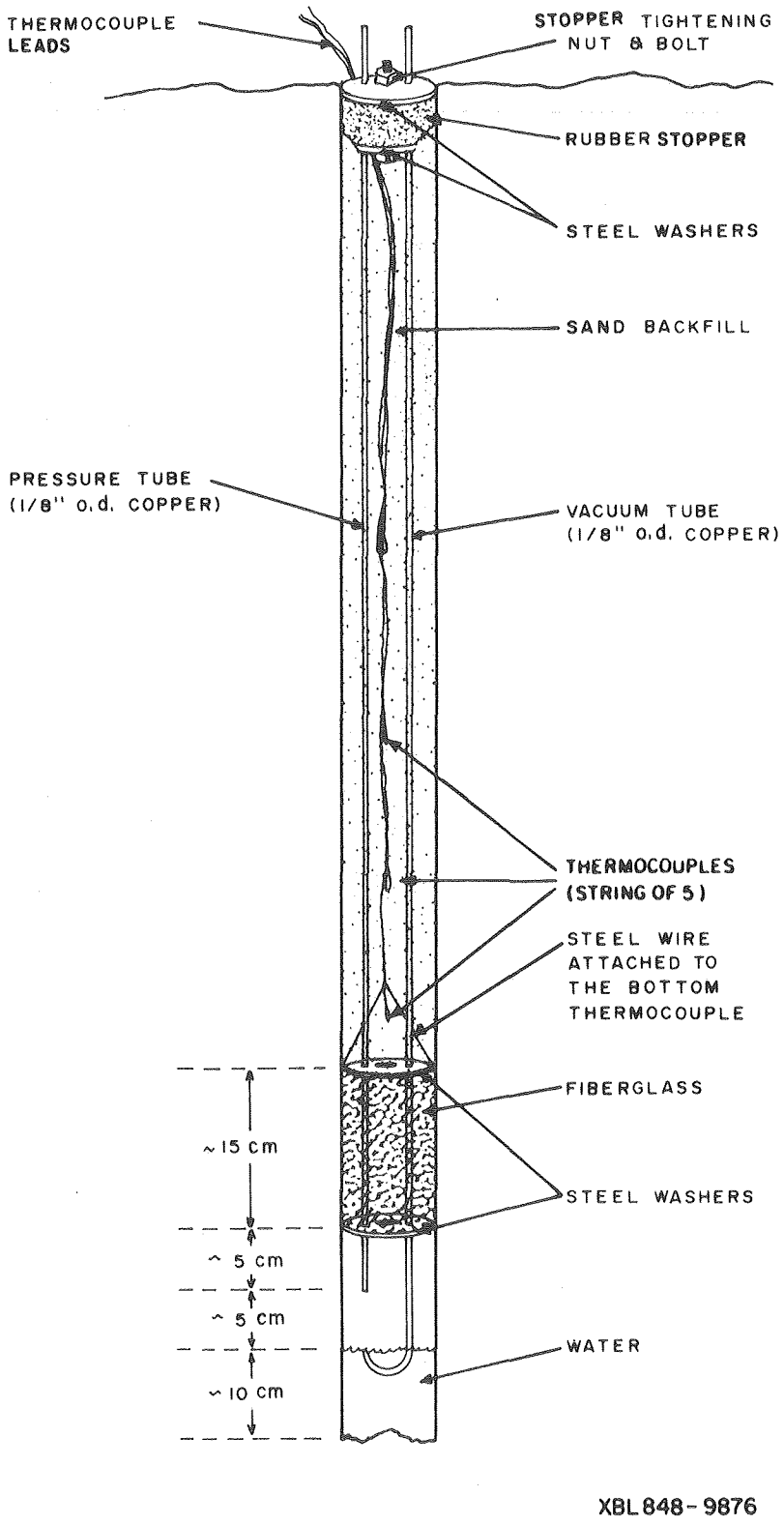

Fig. 9. T-hole thermocouple string and dewatering system (from Schrauf et al., 1979).

2.2.2 T-hole thermocouple failures

Stainless steel sheathed thermocouples, located in T-holes, began to malfunction in August 1978. When the malfunctioning thermocouples were removed, the sheath material was found to be corroded and very brittle.

Table 3 lists the thermocouples that were determined by field operations personnel to have failed. The table lists thermocouple depths with respect to the heater midplane ($z = 0$), experiment day and date of failure, thermocouple temperature reading just prior to failure, and average measured water inflow into the T-hole on the day of failure. Of the 25 thermocouples listed, ten were tentatively confirmed to have failed catastrophically by open ohmmeter readings or analysis of data from the experiments. A catastrophic failure (CF in comments column) indicates that not only did the stainless steel sheath corrode, but one or both of the thermocouple wires also opened (i.e., corroded or broke). Other failures were indicated by erratic readings, many of which stabilized with time or after a common electrical ground was removed from the thermocouple inputs at the ice point references. The latter phenomenon indicates that the sheath probably corroded allowing moisture to reach the thermocouple wires and establish a second ground, and, hence, a ground loop, or that moisture established a resistive connection between the two thermocouple wires forming a parallel, relatively high resistance thermocouple, but in a higher and hotter location of the borehole. The ground loop scenario is more likely because stability occurred simultaneously with removal of the electrical grounds at the ice point references. It may have been only a matter of time before that

Table 3. T-hole thermocouple failure and replacement history

Hole	Sensor	Z(1) [m]	Failure: Exp. day	Failure: Date [1978]	Failure: Temp. [°C]	Failure: Water inflow [ml/day]	Replacement Dates: Removed	Replacement Dates: Installed and activated	Replacement Dates: Backfilled	Comments (2)
Experiment 2 (H10) Turned-on July 3, 1978										
T19	514	-3	46	Aug. 18	93	28.0	Sep. 27	Sep. 28		CF
	513	-1.5	66	Sep. 7	77	28.5				CF
T20	519	-3	57	Aug. 29	27	22.5	Oct. 2	Oct. 4		
"	518	-1.5	86	Sep. 27	85	7.0				CF
"	517	0	89	Sep. 30	93	15.0				
T21	522	0	119	Oct. 30	117	31.0	Nov. 17	Nov. 17	Nov. 17	
"	521	+1.5	119	Oct. 30	77	31.0				
T22	528	-1.5	79	Sep. 20	75	13.0	Nov. 2	Nov. 2		
T23	532	0	102	Oct. 13	106	3.3	Nov. 14	Nov. 15		
T24	539	-3	57	Aug. 29	28	19.0	Oct. 12	Oct. 24	Oct. 25	CF
	536	+1.5	89	Sep. 30	79	18.3				CF
Experiment 1 (H9) Turned-on Aug. 24, 1978										
T13	88	-3	15	Sep. 8	15	0	Oct. 31	Nov. 1	Nov. 2	CF
T14	91	0	46	Oct. 9	67	0.8	Oct. 21	Oct. 24	Oct. 25	CF
"	93	-3	46	Oct. 9	22	0.8				
T15	96	0	19	Sep. 12	72	3.0	Oct. 10	Oct. 11	Oct. 12	
"	97	-1.5	34	Sep. 27	42	2.5				CF
"	98	-3	37	Sep. 30	21	1.2				
T16	102	-1.5	25	Sep. 18	44	7.7	Oct. 12	Oct. 13	Oct. 16	
"	103	-3	25	Sep. 18	18	7.7				
"	101	0	28	Sep. 21	96	7.0				
T17	107	-1.5	44	Oct. 7	44	11.0	Nov. 13	Nov. 14	Nov. 15	CF
"	106	0	75	Nov. 7	77	1.7				
T18	111	0	14	Sep. 7	70	13.5	Oct. 6	Oct. 9	Oct. 10	CF
"	112	-1.5	32	Sep. 25	41	5.0				
"	113	-3	39	Oct. 2	21	5.0				

(1) (-) indicates below heater mid-plane
(+) indicates above heater mid-plane

(2) CF = Catastrophic Failure of thermocouple as confirmed by ohmmeter (open), or reviewing data.

type of failure became catastrophic. Other erratic temperature readings that jumped to temperatures near 100°C but stabilized with time (as with T-21 sensors 521 and 522) may have been due to thermal cycling within the T-holes caused by small amounts of water boiling and recondensing.

Additional analysis of the T-hole temperature data following the conclusion of the experiments indicates that field operations personnel may not have detected all the catastrophic thermocouple failures during the confusion and urgency of the replacement operations. As many as 23 of the stainless steel sheathed thermocouples in full-scale experiment T-holes may have catastrophically failed before replacement, and three others originally thought to have catastrophically failed may have stabilized after removal of the electrical ground loops. The 23 potential catastrophic failures found by analyzing the temperature data are listed in Table 4 along with their depths in the boreholes. It has been estimated that 48 of the 60 thermocouples, the bottom four in each string of five, would probably have failed if replacements had not been made.

Table 3 shows that all failed thermocouples, except in T-21 and T-24, were located at or below the heater mid-plane, and Table 4 shows that 22 of the 23 potential catastrophically failed thermocouples were at or below the heater mid-plane. Visual inspection of failed thermocouples located below the mid-plane, showed that most corrosion occurred in sheathed sections closest to the heater midplane. This indicates that heat was a major contributing factor to the thermocouple corrosion.

Table 4. T-hole thermocouple catastrophic failures as indicated from temperature data.

Experiment 1 (H9)			Experiment 2 (H10)		
Hole	SPF No.	Z* [m]	Hole	SPF No.	Z* [m]
T13	88	-3	T19	511	+1.5
T15	97	-1.5		512	0
T16	103	-3		514	-3
T17	107	-1.5	T20	517	0
T18	111	0		518	-1.5
				519	-3
			T21	522	0
				523	-1.5
				524	-3
			T22	527	0
				528	-1.5
				529	-3
			T23	532	0
				533	-1.5
				534	-3
			T24	537	0
				538	-1.5
				539	-3

* (-) indicates below heater mid-plane
(+) indicates above heater mid-plane

2.2.3 T-hole thermocouple replacement procedure

All of the stainless steel sheathed thermocouples originally installed in the T-holes were replaced by the middle of November 1978. Inconel sheathed replacement thermocouples were installed in boreholes T-19 and T-20 and Teflon thermocouple replacements were installed in all other T-holes. The lengths of the copper dewatering tubes extending out the top of each T-hole were accurately measured prior to removal of the dewatering system and original thermocouple string from the borehole. The top rubber stopper was then removed. Occasionally, the rubber stopper used to seal the top of each T-hole had been pressed too far down into the borehole and was difficult to remove. The fiberglass plug near the bottom of the T-holes also occasionally became stuck due to sand between the plug and the borehole wall. After removal of the assembly from the borehole, the distance was accurately measured between the top washer of the bottom plug and the bottom thermocouple of the string, which had been attached to a steel wire connected to the bottom plug (see Fig. 9).

Replacement thermocouple lengths and spacing were measured with a tape measure and assembled into a string of five thermocouples equally spaced at 1.5-m intervals. The thermocouples were taped together at a number of points with Teflon tape. The bottom thermocouple was then attached, using Teflon tape, to the steel wire on the bottom plug at the same distance from the plug as the original thermocouple. In some cases the top of the string was taped to one of the dewatering tubes near the borehole opening to keep the string reasonably tight during

installation. The remainder of the string could lie to either side of the hole or any place between. The assembly was then reinstalled to its original depth as determined by the length of copper dewatering tube protruding from the T-hole. Thermocouple depths were checked during reinstallation using original depth measurement data derived from Viak survey data. No measurement inconsistancies were found (telephone communication with Gunnar Ramqvist, Stripa, Sweden, June 2, 1981).

The boreholes were backfilled with sand after allowing an adequate period to confirm proper thermocouple operation, usually one day.

A temperature offset sometimes occurred between apparently legitimate readings from the original stainless steel sheathed thermocouples and their replacements. None of the replacement thermocouples were calibrated at the site, so the NBS temperature versus voltage relationship was used. This offset was usually small but a maximum of 10°C occurred for T-19 sensor 512. Temperatures measured by the new Teflon insulated thermocouples were generally closer to the predicted data, which one hopes indicated that the new readings were more accurate. Javandel and Witherspoon (1981) analyzed these shifts.

2.3 Replacement of Thermocouples Associated with USBM and IRAD Gauges

When IRAD or USBM gauges failed, they were removed from their boreholes and repaired. Sometimes removal of a gauge was difficult and resulted in damage to the associated thermocouple, requiring it to be replaced. Table 5 lists the dates of ten of these thermocouple replacements that were documented in field notebooks or logbooks. There

Table 5. Replacement history of thermocouples associated with IRAD and USBM gauges.

Exp.	TC SPF No.	Borehole	Associated gauge	TC replacement dates	Comments**
1(H9)	4	U3	U3 C9	9/13/79	T/T
1(H9)	6	U5	U5	9/11/79	T/T
1(H9)	7	C2	U6	8/10/79	S*/T
1(H9)	10	U9	U9	8/22/79	T/T
2(H10)	429	U13	U13	1/20/79	T/T
2(H10)	431	C3	U15	6/27/79	S*/T
2(H10)	433	C4	U17	1/20/79	T/T
2(H10)	434	U18	U18	2/20/79	T/T
				7/02/79	T/T
2(H10)	504	C5	C5	7/11/79	S/T*
Possible replacements not recorded in field documentation					
1(H9)	2	U1	U1		S*/T*
1(H9)	77	C1	C1		S/T*
1(H9)	78	U6	C2		S/T*
2(H10)	427	U11	U11		S*/T*
2(H10)	502	U15	C3		S/T

** Comments
T/T Teflon insulated TC replaced with another Teflon insulated TC.
S/T Stainless steel sheathed TC replaced with Teflon insulated TC.
* Stainless steel sheathed or Teflon insulated TC was presumed to be installed as indicated, however, substantiating documentation is missing for these cases.

are indications that other IRAD and USBM gauge thermocouples replacements were also made during the experiment, but not documented. This is evident by the fact that stainless steel sheathed thermocouples were initially installed with certain IRAD and USBM gauges and Teflon insulated thermocouples were with these gauges at the conclusions of the experiments as indicated in Table 2. These possible replacements are also listed in Table 5, but should not be considered as including all replacements that may have been made.

2.4 Ice-Point Reference Changes

Each thermocouple was connected to one of five ice-point reference units as discussed in Sections 1.0 and 1.1. Each unit provided ice-point reference junctions for 100 thermocouples. As indicated in Table 6, ice-point references failed and were replaced on several occasions. Several hours were required to change the references due to the numerous wire connections. Each case of total ice-point reference failure was due to failure of one or more of the transistors in the driver circuits for the ice bath thermoelectric coolers (Peltier effect devices). The first two failures were caused by small pieces of styrofoam packing material used during shipment to Sweden that finally circulated into cooling fan blades and jammed them. Power transistors then overheated and failed. The units were easily repaired in the field.

DuBois et al. (1981) report that thermocouple number 126 on extensometer E13 indicated too low a temperature when checked at the conclusion of the heater cool-down period (about 700 days after heater turn-on). This negative temperature error resulted from a 7.5°C positive temperature error at one or both of the ice-point reference junctions for

Table 6. Failure history of ice-point references.

Date	Description of Failure
29 Aug. 78	Ice point reference chassis No. 4 in the full-scale experiment failed at 7:45, was replaced by a spare unit, and was back in operation at 11:30. Data from thermocouples 77-83, 114-128, and 520-574 were affected.
28 Nov. 78	Ice point reference chassis No. 2 failed at 10:30. The spare ice-point reference chassis was installed and the thermocouple wires were reconnected at 15:00. Data from thermocouples 2-11, 17-72, 427-431, and 442-465 were affected.
29 July 79	A faulty connection between the ice-point reference and the data logger caused time-scaled alarms around 14:00.
9 Aug. 79	An electrical storm caused several power failures between 5:00 and 9:00. All of the transistors in full-scale ice-point reference chasses No. 4 were blown. The ice-point reference was replaced by 12:00.
13 Aug. 79	A cold solder joint was discovered in ice-point reference chassis No. 4. Surface thermocouple 572 was affected.
24 Oct. 79	Ice point reference chassis No. 0 in the time-scaled experiment failed at 9:00 and was replaced by 21:30. Data from thermocouples 902-949 and 982-1013 were affected.

that particular thermocouple. This can occur if a reference junction is pulled slightly from its ice bath. The ice-point reference unit (IPR Chassis No. 4) with the faulty reference junction had been installed as a replacement on day 402 (9 August 1979) of the experiment (eight days following turn-off of full-scale heater H10 and the peripheral heaters) and thermocouple number 126 appears to have given valid temperature readings at that time. It seems evident by inspection of the output data that the 7.5°C offset occurred gradually between days 402 and 700 of the experiment. This has been the only case detected of this particular type of ice-point reference failure during the Stripa experiments.

Total lost operating time of the five ice-point references in the three Stripa experiments due to catastrophic failures amounted to less than 28 hours over a total operating time of about 72,000 unit hours. This amounts to a down time of less than 0.04%. Down time was minimized by keeping a spare unit in good repair to serve as a replacement.

2.5 Data Logger Reliability and Stability History

The data acquisition system (DAS) is discussed in detail by McEvoy (1979) and Chan et al. (1980). Data loggers were a part of the DAS, acquiring data independently but in parallel with the computer and printing it on paper tape as computer backup.

One Acurex Autodata-Nine (AD-9) data logger was located in the time-scaled experiment drift and another was located in the full-scale experiment drift. Cabling was installed between the two so that either AD-9 could be connected to take over for the other in the event that one

should fail. This feature was used only once, during a seven day period from August 7 to August 14, 1978, when a problem developed and the full-scale AD-9 was disassembled for repair. For that period all full-scale AD-9 data appears on the time-scaled AD-9 data printout. There were several other minor failures resulting in lost data over shorter periods, typically one-half to two days. These periods of short term data loss have not been found significant enough to warrant tabulation.

Long term stability of the AD-9s is discussed in Appendix B of Chan et al. (1980). Each AD-9 continuously recorded a voltage from a dedicated reference voltage source, and zero-volt references from short-circuited input terminals. Figure 10 shows the reference voltages recorded by the data loggers, which indicate that drift occurred. Full-scale drift amounts to about 40 μV and time-scaled drift about 60 μV. The same reference voltages recorded in parallel on other data logger channels agreed to within one or two microvolts. The stability of the reference source voltages, shown in Table 7, indicates that the AD-9 data loggers drifted rather than the source voltage with the exception of a negative 10-μV drift in the reference voltage source used with the full-scale AD-9. For a reference voltage of approximately 0.112 V, this brings the total drift in the full scale AD-9 up to 50 μV, nearly equivalent to the 60-μV drift monitored in the time-scaled AD-9. Drift on the shorted inputs was essentially zero. Calibrations discussed in Section 3.4.2 furnish additional information on the AD-9s, and how their accuracies affect temperature data.

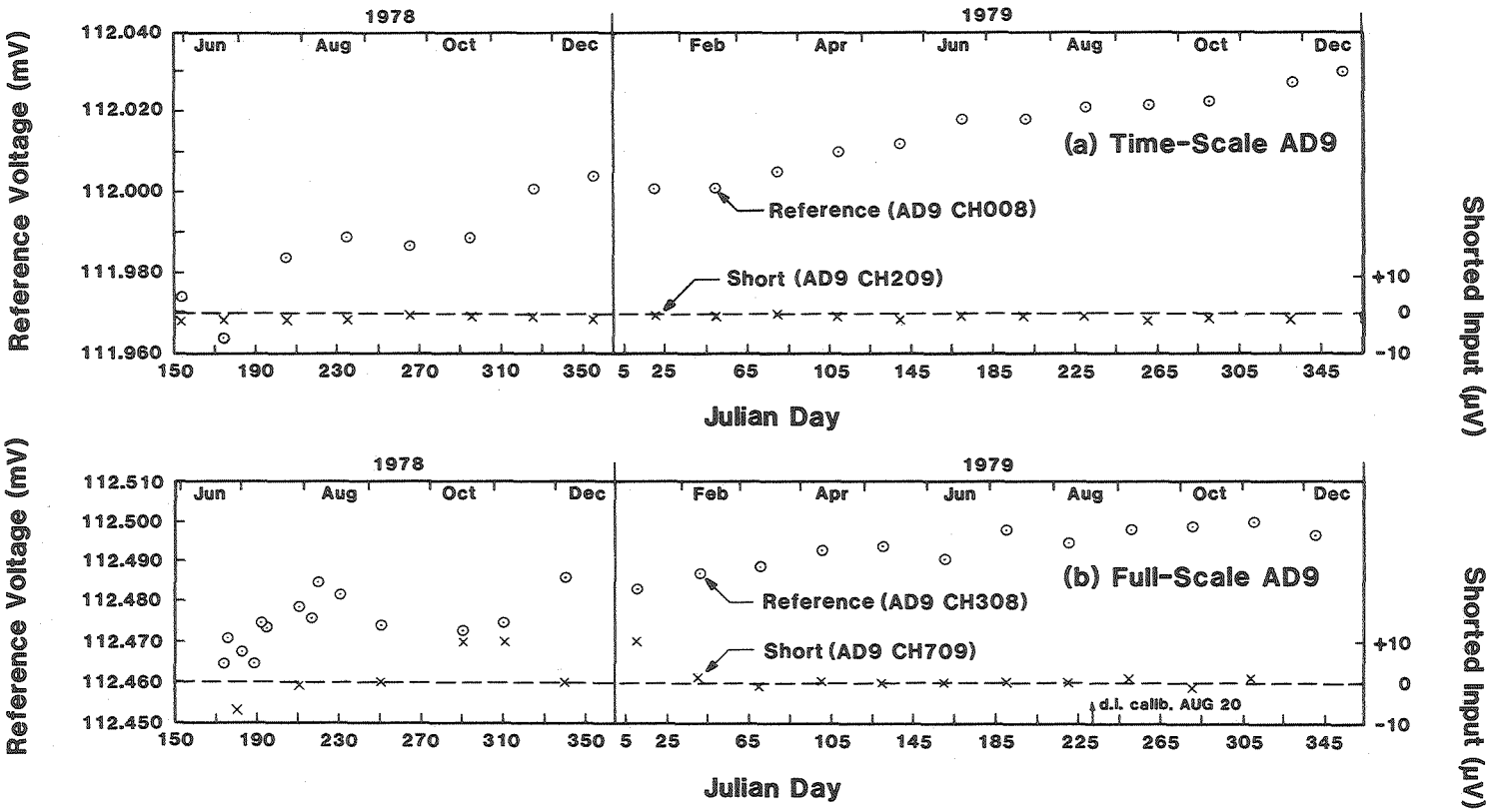

XBL 8011-7439

Fig. 10. Reference voltage and shorted input measurements for: (a) Time-scaled AD-9 and (b) Full-scale AD-9 (from Chan et al., 1980).

Table 7. AD-9 reference voltages measured with the Fluke 8500A DVM (S/N 805003).

Reference voltage unit No.	Location	Pre-burn-in 4 Jan 78 at LBL (mV)	Post-burn-in 18 Jan 78 (mV)	Final 24 Apr 80 at Stripa (mV)	Final(-) initial (μV)	Final(-) post-burn-in (μV)
-1	Time-scaled	111.962	111.978	111.979	17	1
-2	Full-scale	112.408	112.424	112.414	6	-10
-3	Stored in Lulea drift	114.086	114.100	114.100	14	0

A B&F data logger located in the full-scale drift monitored USBM gauges, all thermocouples associated with USBM and IRAD gauges, and six of the extensometer thermocouples (SPF Nos. 122-127). Long term stability and reliability of the B&F data logger is questionable, consequently, B&F data should not be considered a reliable source of back-up data for the computer without further analysis. Detailed comparisons between carefully selected B&F data channels and computer data could possibly alleviate doubts, or at least quantify them.

3.0 THERMOCOUPLE CALIBRATIONS

The initial goal of measuring temperatures to a precision of ±0.5°C below 200°C required individual thermocouple calibrations. Calibrations of these low-temperature thermocouples were done after they had been connected to the data acquisition system (computer and data loggers) in their final wired configuration, but before borehole installation. Thus, calibration was done as a complete operational temperature measuring system. Thermocouples for the full-scale and time-scaled experiments were calibrated separately in the proximity of their instrumentation sheds.

The block diagram in Fig. 11 represents the Stripa temperature measuring system including thermocouples, data acquisition equipment, signal and data flow paths, and conversion and correction algorithms. The effects of the various components of the system on the signals and data are also listed in the figure. Some of the operators and algorithms were generated from results of the in-situ thermocouple system calibrations that encompassed the associated data acquisition hardware, and others were generated from standards and calibration tables and other calibrations of the computer's analog-to-digital conversion hardware (Chan et al., 1980).

The thermocouple system calibration procedures (Sections 3.1 and 3.2) were performed using a well regulated oven and a temperature reference system composed of a calibrated platinum resistance thermometer RTD and a

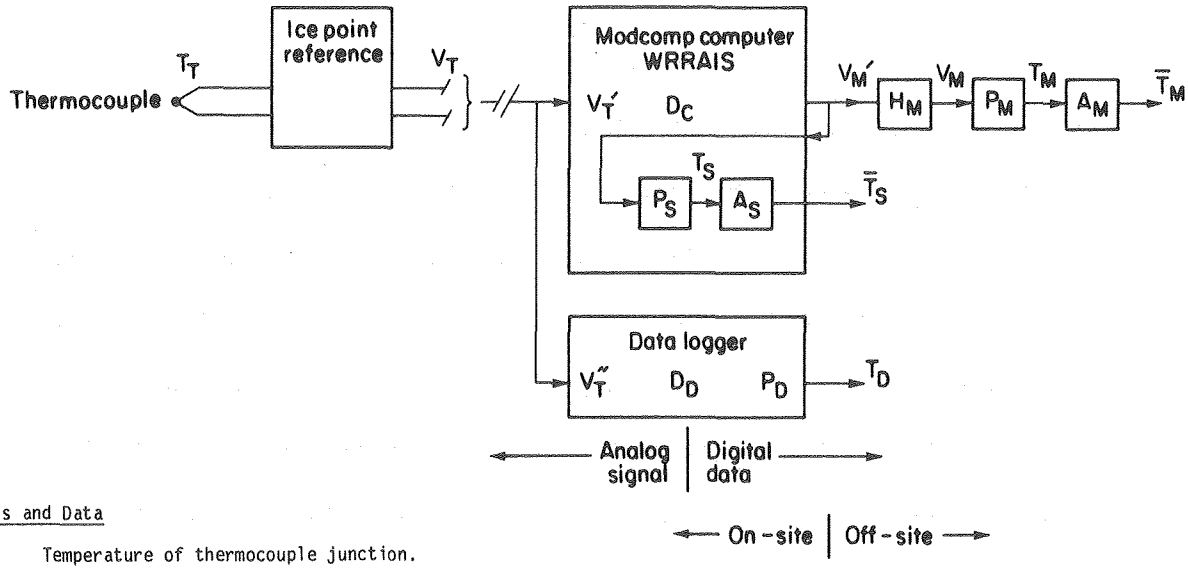

Signals and Data

T_T Temperature of thermocouple junction.

V_T Voltage generated by thermocouple at temperature T_T.

V_T' V_T plus noise voltage sensed by computer's analog circuitry (e.g., from ground loop currents, common-mode and normal-mode noise pickup, etc.). Common-mode noise was not rejected well by computer input circuits.

V_T'' VT plus noise voltage sensed by data logger circuits: Common-mode noise was well rejected by data logger input circuits.

V_M' Computer digitized and recorded voltages

$$V_{M'} = GV_{T'} + V_{OS} + f(V_{cm})$$

where: G = 1.0 ideally, but in practice differed from 1.0 and varied with time.

V_{OS} = 0.0 ideal offset voltage, but in practice was generally non-zero and varied with time.

V_{cm} = Common-mode noise voltage picked-up on thermocouple wires. Affected output in a nonlinear fashion.

V_M Corrected voltages (computer data, $V_{M'}$, corrected for known errors with time that were introduced by computer system).

T_M Temperature conversion from V_M using polynomial operator P_M. Stored on Stripa data base magnetic tapes.

$\overline{T_M}$ Time averaged equivalent of T_M. Also stored on Stripa data base magnetic tapes.

T_S On-line temperature conversions at Stripa using polynomial operator P_S.

$\overline{T_S}$ Time averaged equivalent of T_S.

T_D Data logger digitized and converted temperatures, printed on paper tape. Data are free of computer errors and common-mode noise problems.

Devices

D_C Computer system. Introduced gain and offset voltage errors. Common-mode noise rejection was poor for small signals (see $V_{M'}$). Because separate gain-ranging amplifiers were used in the time-scaled and full-scale experiment drifts, data have different gain and offset errors between the two drifts.

D_D Data loggers. Introduced some long-term drift, judged to be quite low in Autodata-Nines.

Algorithms

H_M Removes many of the time-dependent errors introduced by D_C (SAC-29, Chan et al., 1980).

P_M Polynomial operators (Table 9, Section 3.0) based on NBS thermocouple voltage-to-temperature conversion tables (Table A-1).

P_S Polynomial operators based on individual thermocouple initial calibrations (SAC-25, Appendix G, Schrauf et al., 1979).

P_D Interpolation algorithm used in Autodata-Nine loggers for voltage-to-temperature conversion (Table 14, Section 3.4.2).

A_M Computer arithmetic mean of T_M over specified time spans.

A_S Same algorithm as A_M; used with T_S.

Fig. 11. Stripa temperature measuring system.

high resolution ohmmeter. The temperature reference system as used in calibrating the thermocouple system is shown in Fig. 12 along with a list of parameters measured during calibration routines, including potential sources of errors and uncertainties.

In any calibration procedure the reference system can introduce its own errors and uncertainties to the calibration data. Sources of these errors and uncertainties for the Stripa thermocouple calibrations are summerized below and discussed in detail in later sections of this report. These include:

- o Errors and uncertainties introduced by RTD self-heating. This type of error is equivalent to the difference between the RTD temperature and the thermocouple temperature, $T_R - T_T$, in Fig. 12; and corrections for it must be made by adding the equivalent values for $T_R - T_T$ to the computer and AD-9 outputs obtained during calibrations, and to any NBS deviation plots similar to those in Sections 4.1, 4.2, and 4.3. Those particular plots, however, have already been corrected to some extent for RTD self-heating as discussed in Section 4.0. RTD self-heating is discussed in more detail in Section 3.3.1.
- o Errors and uncertainties associated with the Fluke ohmmeter used to measure RTD resistance, which include 1) calibration uncertainties of the ohmmeter itself, and 2) the failure to properly zero the ohmmeter during the first series of thermocouple recalibrations following the conclusion of the Stripa experiments. The

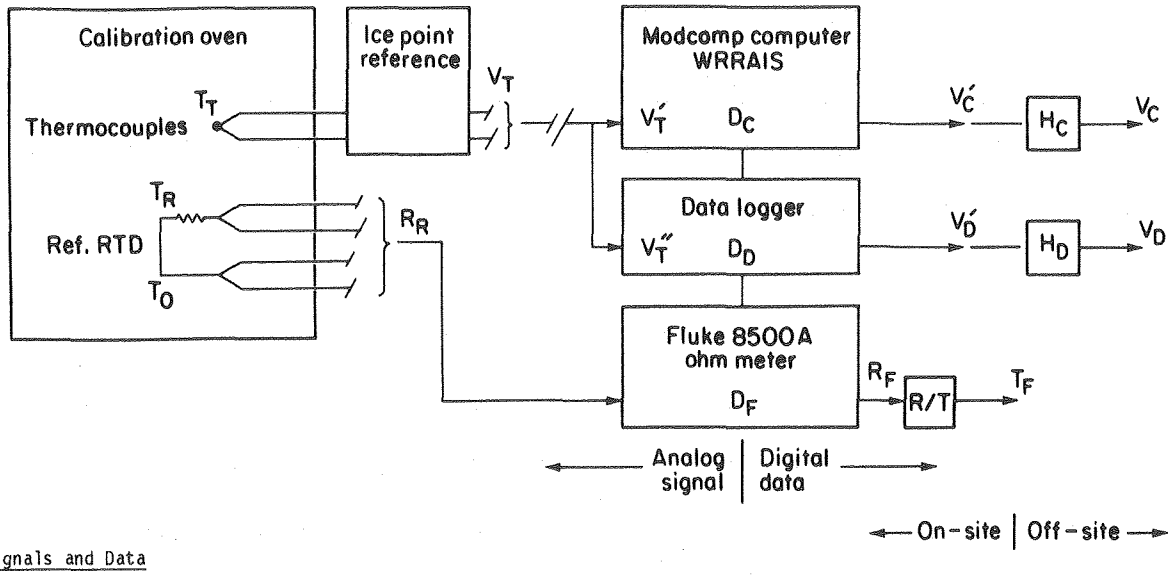

XBL 842-9605

Signals and Data

T_O	Oven temperature.
T_R	Temperature of RTD's Platinum resistance wire (T_O plus temperature offset due to RTD self-heating).
T_T	Temperature of thermocouple junction (T_O plus temperature increase at thermocouple junction from close proximity to self-heated RTD).
V_T	Voltage generated by thermocouple at temperature T_T.
V_T'	V_T plus noise voltage sensed by computer's analog circuitry (e.g., from ground loop currents, common-mode and normal-mode noise pickup, etc.). Common-mode noise was not rejected well by computer input circuits.
V_T''	V_T plus noise voltage sensed by data logger circuits. Common-mode noise was well rejected by data logger input circuits.
V_C'	Computer digitized and recorded voltages.
V_C	Corrected voltages (computer data corrected for known system and calibration errors).
T_D'	Data logger digitized and recorded voltages.
T_D	Corrected voltages (data logger recorded voltages corrected for known system and calibration errors).
R_R	Resistance of RTD at temperature T_R.
R_F	Resistance measured by Fluke digital ohmmeter (including Fluke calibration and non-zero offset errors).
T_F	Temperature conversion of R_F using Swedish Bureau of Standards tables for the RTD.

Devices

D_C	Computer system. Introduced gain and offset voltage errors. Common-mode noise rejection was poor.
D_D	Data loggers. Introduced some long-term drift, judged to be quite low in Autodata-Nines.
D_F	Digital ohmmeter. Induced self-heating of RTD in initial calibrations and first recalibration series. Ohmmeter was not properly zeroed during first recalibration series.

Algorithms

H_C	Algorithm to remove errors introduced by D_C, D_F and RTD self-heating during calibrations.
H_D	Algorithm to remove errors introduced by ohmmeter zero-offset and RTD self-heating.
R/T	Field conversion of R_F to temperature T_F using RTD calibration by Swedish Bureau of Standards.

Fig. 12. Thermocouple system calibrations.

ohmmeter calibration uncertainties are discussed in Section 3.3 and proved to be negligible for all practical purposes. Corrections for ohmmeter non-zero offsets have been made to thermocouple calibration data as discussed in Section 4.0.

- Combined uncertainties associated with the complete RTD reference system composed of the RTD, Fluke ohmmeter, and Swedish Bureau of Standards RTD calibration table (R/T in Fig. 12). These uncertainties are generally less than 0.1% of the calibration temperature and are discussed in Section 3.3.

Calibration of the thermocouples and data acquisition hardware as a complete temperature measuring system should provide data adequate to compensate for errors introduced by individual components at the time of the calibration. However, the calibrations in themselves do not provide adequate data to correct for time-varying errors and uncertainties. Some of these errors have been tabulated from other sources and corrections have been made to the Stripa data on the public domain data tapes (PDTs) as described by Chan et al. (1980). Causes of known time varying errors and uncertainties in the temperature measuring system are shown in Fig. 11 and listed below:

- Offset and noise due to ground loop currents in thermocouple wires (Section 2.2.2).
- Noise in computer data due to poor common-mode noise rejection capabilities (Sections 4.2, 4.3, and 5.0).
- Changes due to thermocouple failures and replacements (Sections 2.0 - 2.3).

- Changes in the computer's analog-to-digital conversion hardware (WRRAIS) characteristics with time (Sections 4.0, 5.0, and Chan et al., 1980).
- Drifts and uncertainties associated with Autodata-Nine data loggers. These were generally less than 0.1% (Sections 2.5 and 3.4.2).
- Erratic data due to water boiling and condensation cycles in thermocouple wells or boreholes (Sections 1.1.3 and 2.2.2). These data, however, constitute valid temperature readings at the thermocouple junction locations.

During the experiment, the computer used a fourth-order polynomial voltage-to-temperature conversion routine to reduce on-line storage requirements. Five polynomial coefficients were determined for each thermocouple using a least-squares criterion for best fit. The curve fit used data from the individual thermocouple calibrations whenever available. A curve fit to the NBS temperature versus voltage data (listed in appendix Table A-1) was used for uncalibrated thermocouples. The AD-9 data loggers did not use data from these individual calibrations since they were programmed to convert measured thermocouple voltages to temperature as explained in Section 3.4.2.

Laboratory measurements of several samples of heat-treated thermocouples showed that these thermocouples differed slightly from the NBS data. Sample measurements indicated maximum deviations of -0.4°C near ambient increasing linearly to +3°C at 300°C. Typical deviations from

NBS data were approximately -0.2°C near ambient, increasing linearly to approximately +2°C at 300°C.

At the conclusion of the experiment, removable thermocouples (i.e., those not grouted in place) were recalibrated during a series of four calibration runs. Immediately after completion of the last of these runs, two problems affecting RTD reference temperature readings were discovered (see Section 3.2). As a result, a second single-run recalibration was done in the full-scale drift, repeating measurements made during two of the first recalibration runs. Table 8 summarizes which thermocouples were included in the original calibration and the two recalibrations, and whether computer or data logger data are available for the respective calibrations. It should be noted that medium- and high-temperature thermocouples could not be calibrated in the mine beyond 220°C due to temperature limitations of the oven.

Uncertainties in thermocouple calibration data caused by RTD self-heating, computer WRRAIS offset and gain variations during calibrations, and replacement of numerous thermocouples made it impractical to continue use of the individually derived polynomial coefficients without considerable additional work. Individual thermocouple calibrations were therefore abandoned and it was decided to use a polynomial representation of the NBS voltage-to-temperature table (Table A-1) to convert thermocouple voltages to temperature for computer-acquired data on the public domain data tapes. Three sets of coefficients have been computed from curve fits to data taken from the NBS table. There is a set for thermocouples within each of the following maximum temperature ranges:

Table 8. Thermocouple (TC) calibration summary.

Experiment	Holes	No. of TCs	Pre-exp. calib.	First recalib.	Second recalib.	Comments
1(H9)	T13-T18	30	M,D(1)	M,D	M,D	1) TCs replaced after pre-exp. calib.
1	H9	8	NC	M,D	M,D	
2(H10)	T19-T24	30	M,D(1)	M,D(2)	M,D(2)	2) 24 calibrated, 6 broken during removal
2	H10	8	NC	M,D	M,D	
2	H11-H18	24	NC	M,D	M,D	
1 & 2	E6-E35	129	M,D	NC	NC	TCs grouted in place
1 & 2	U,C	43	M	M,D_{BF}	M,D_{BF}(3)	3) Vertical holes only
3(TS)	H1-H8	24	M,D(4)	M,D	NC	4) Only 4 heater and 1 spare TC calibrated
3	E1-E5	29	NC	M,D(5)	NC	5) Only 5 surface TCs calibrated, others grouted in place
3	T1-T12	60	M,D	NC	NC	TCs grouted in place

M = ModComp calibration data available
D = Data logger calibration data available
NC = Not calibrated

1) Below 200°C maximum temperature. This set of coefficients provides a maximum deviation from the NBS tables of less than 0.05°C for temperature to 200°C.
2) From 200-300°C maximum temperature. Maximum deviation from the NBS tables is less than 0.18°C for temperatures to 295°C.
3) From 300-500°C maximum temperature. Maximum deviation from the NBS tables is less than 0.63°C for temperatures to 500°C, and less than 0.28°C for temperatures from 275 to 500°C, where these thermocouples typically operated.

Table 9 lists the polynomial coefficients that were obtained for these selected temperature ranges. Thermocouple temperatures on the public domain data tapes were obtained using the coefficients for the temperature range that corresponded to the maximum temperature that the thermocouple experienced during the experiment. Table 10 lists each thermocouple by temperature group. As described in Chan et al. (1980), additional adjustments were made to the computer-acquired voltages before they were converted to temperature.

3.1 Original On-Site Calibrations

Thermocouple calibrations were performed in a well regulated oven capable of temperature up to about 220°C. The calibration oven (Blue M, model OV-560A-2) was moved from area to area, so that thermocouple output leads could be wired directly into ice-point reference units located in the two instrumentation sheds.

For each calibration, the thermocouples were partially unrolled from their packaging coils until their open-ended leads could be laid along

Table 9. Polynomial coefficients used to convert thermocouple voltages to temperatures on the Public Domain Data Tapes (Chan et al., 1980).

$$T = C_0 + C_1V + C_2V^2 + C_3V^3 + C_4V^4$$

where: C_0, C_1, C_2, C_3, C_4 are the polynomial coefficients,

T is temperature in degrees Celsius [°C], and

V is thermocouple output voltage in millivolts [mV]

Thermocouple Max. temp. range [°C]	C_0	C_1	C_2	C_3	C_4
0-200	-.0544334	25.5679392	-.5652087	.08611938	-.00385947
200-300	.1139723	25.1789712	-.3857018	.05892778	-.0025899223
300-500	1.1004193	23.4824814	.2231085	-.015158225	.0002885662

Table 10. Thermocouples grouped by peak temperature (Chan et al., 1980).

Peak temp.	SPF number	Sensor label
300-500°C	540, 541, 542	TH10A, TH10B, TH10C
	543, 544, 545	TH10D, TH10E, TH10F
	548, 549, 551, 552	TH11A, TH11B, TH12A, TH12B
	554, 555, 557, 558	TH13A, TH13B, TH14A, TH14B
	560, 561, 563, 564	TH15A, TH15B, TH16A, TH16B
	566, 567, 569, 570	TH17A, TH17B, TH18A, TH18B
	982, 983, 986, 987	TH1A, TH1B, TH2A, TH2B
	990, 991, 994, 995	TH3A, TH3B, TH4A, TH4B
	998, 999, 1002, 1003	TH5A, TH5B, TH6A, TH6B
	1005, 1006, 1007	PROBE, TH7A, TH7B
	1009, 1010, 1011	RACK, TH8A, TH8B
200-300°C	114, 115, 116	TH9A, TH9B, TH9C
	117, 118, 119	TH9D, TH9E, TH9F
	512, 522, 527	T19C, T21C, T22C
	532, 537	T23C, T24C
0-200°C	ALL REMAINING THERMOCOUPLES	

the cabling trays into the instrumentation sheds and connected to the ice-point references. The thermocouple ends were then uncoiled, tied together in a single bundle around a platinum RTD (resistance temperature device) reference thermometer, and the complete bundle was inserted inside a thick-walled aluminum cylinder designed to stabilize small temperature variations inside the oven. The oven temperature uniformity is rated at ±0.2°C. The RTD (Omega Engineering Model, PR-11-3-100-1/4-18 inches E) was calibrated at the Swedish Bureau of Standards to a stated accuracy of ±0.05°C (see Appendix A) and provided the temperature reference during testing. The aluminum cylinder was filled with silicone oil during calibration of the first bundle. The hot oil had a tendency to free the protective potting compound covering the junction ends of the Teflon insulated thermocouples, so use of the oil was discontinued. After the aluminum cylinder and enclosed thermocouples were placed in the oven for 2-1/2 to 4 hours and allowed to reach thermal equilibrium, the first calibration data point was recorded. The oven was then turned up and permitted to stabilize for an additional 2-1/2 to 4 hours, then calibration voltages were recorded for that temperature. This procedure was repeated over a temperature range of 15 to 215°C at nineteen or twenty discrete temperatures. At each temperature the computer sampled and recorded the voltage of each thermocouple. The resistance reading of the RTD was measured by a Fluke 8500A digital ohmmeter (S/N 805003), manually recorded, converted to temperature using the Swedish Bureau of Standards calibration table (Table A-3), and entered into the computer. The calibration of each thermocouple was thus recorded by the computer as a series of incoming voltages and corresponding temperatures.

The coefficients for a fourth order polynomial were obtained individually for each low temperature thermocouple that was calibrated. Polynomial coefficients that fit the NBS voltage-to-temperature conversion were used in the computer for all other thermocouples. These field derived coefficients were eventually abandoned because of difficulties described in Chan et al. (1980). Section 3.0 described the voltage-to-temperature conversion used for temperature data on the public domain data tapes.

3.2 Recalibrations

After the heater turn-off and rock cool-down periods, all recoverable thermocouples were recalibrated during four separate runs in the following order:

1) Time-scaled drift: Heater thermocouples and the five extensometer surface thermocouples.
2) H10 experiment area: Most H10 vertical borehole IRAD, USBM and T-hole thermocouples and the extensometer surface thermocouples. The ten Inconel sheathed thermocouples used to replace corroded stainless steel thermocouples in T-19 and T-20 had also experienced some corrosion and, consequently, six of them broke during removal from the sand back-filled holes. However, they apparently gave valid readings before removal.
3) H9 experiment area: H9 vertical borehole IRAD, USBM, T-hole, extensometer surface, H9 heater, H10 heater, peripheral heater and a few remaining H10 vertical borehole thermocouples.
4) Extensometer drift: Horizontal borehole IRAD, USBM, and extensometer surface thermocouples.

Thermocouples in the time-scaled T-holes and the down-hole extensometer thermocouples were grouted in place and could not be removed for recalibration.

Two sources of calibration error were discovered at the conclusion of the first recalibration runs:

1) The Fluke 8500A digital multimeter, used to measure resistance of the RTD reference thermometer, had not been reset to zero. The equivalent error in the extensometer drift recalibration was about 0.6°C, and probably applied to recalibrations in the other drifts as well.
2) The RTD was also self-heating due to a continuously applied current (about 9.35 mA) from the Fluke multimeter. A series of tests showed this to cause an increase in RTD temperature of 0.55 to 1.2°C above actual oven temperature for all calibrations up to this time. The amount of increase depended on the thermal conductivity around the RTD and temperature of the RTD (the higher the temperature, and greater the self-heating). Errors due to this self-heating are discussed in Section 3.3.1.

These errors were discovered immediately after completion of the first recalibration series and while the calibration equipment was still set up in the extensometer drift. The two individual effects were each larger than indicated by calibration data, since the two errors were somewhat self-compensating. The original calibration, prior to the start of the experiment, was also affected by self-heating of the RTD but probably not affected by an ohmmeter reset problem. The effect of RTD self-heating

can be seen in the figures in Section 4 as a spread in temperature at the lowest temperatures in the original calibration and the first recalibration. The plots show similar effects on the data logger and the computer outputs.

As a result of the discovery of these sources of error, all recoverable thermocouples from the H9 and H10 vertical boreholes and heaters were again recalibrated, with the Fluke ohmmeter properly zeroed, and the RTD readings taken immediately after applying current through the RTD to avoid self-heating. This second recalibration did not include thermocouples in the time-scaled drift and extensometer drift, but did provide enough characteristic information so that the first recalibrations of thermocouples in these locations can be analytically corrected if so desired.

3.3 Temperature Reference System for Thermocouple Calibrations

The basic thermocouple calibration reference system consisted of a platinum RTD (100 ohms at 0°C) four-wire reference thermometer, purchased from Omega Engineering (S/N 1116), and a Fluke 8500A multimeter (S/N 805003) used to measure the RTD resistance. Detailed results of RTD calibrations by Omega Engineering and the Swedish Bureau of Standards are given in Appendix A. Results of a third calibration by LBL personnel after completion of the Swedish experiments are also shown in Fig. A-4.

The RTD was connected to the Fluke 8500A ohmmeter in a four-wire configuration to eliminate errors due to RTD lead-wire resistance. Table 11 gives pertinent ohmmeter specifications covering the resistance range

Table 11. Fluke 8500A ohmmeter specifications over equivalent RTD range of 0 to 240°C.

		Fluke 8500A ohmmeter					
		Resolution		Accuracy (1 yr) 18°C to 28°C		Temp. coeff.	
RTD temp. [°C]	RTD res. [ohms]	[ohms]	Eq. RTD temp. [°C]	[ohms]	Eq. RTD temp. [°C]	[ohms/°C]	Eq. RTD temp. [°C/°C]
0	100.010	0.001	0.00256	0.008	0.020	0.0009	0.0023
100	138.472	0.001	0.00264	0.010	0.027	0.0012	0.0031
200	175.722	0.001	0.00273	0.012	0.034	0.0014	0.0039
240	190.287	0.001	0.00276	0.013	0.037	0.0015	0.0042

equivalent to an RTD temperature range of 0 to 240°C. The accuracy specifications apply only to room ambient operating temperatures between 18 and 28°C, and the ohmmeter performed considerably better than these specifications. Since ambient temperatures in the extensometer drift were below 10°C, and also to confirm ohmmeter accuracies when used within the specified room operating temperature range, the ohmmeter was calibrated under a number of conditions in the Stripa work areas where it was used. A resistance reference, covering the range from 0 to 200 ohms in 10 ohm increments, was fabricated and calibrated at LBL for this purpose. When necessary the resistance reference was maintained at laboratory environment temperatures inside the thermocouple calibration oven during on-site ohmmeter calibrations. The "worst-case" valid calibration occurred in the extensometer drift with the Fluke ohmmeter located in a 9°C environment. The error was 0 at 0 ohms increasing approximately linearly to negative (-) 0.025 ohms error at 200 ohms. This translates to an equivalent RTD reading error of negative (-) 0.04°C at 0°C increasing to negative (-) 0.064°C at 240°C; a very small error relative to thermocouple variances.

Ohmmeter calibrations in the full-scale and time-scaled drifts, where ambient temperatures were near laboratory conditions, gave even better results; less than 0.01°C equivalent RTD error in some cases. Uncertainty bounds for these latter calibrations are within ±0.05°C total error over the range of 0 to 240°C. The Fluke ohmmeter was also calibrated in a laboratory environment after its return to LBL at the conclusion of the experiments. The equivalent RTD temperature error for that calibration

was negative (-) 0.010°C at 0°C increasing to negative (-) 0.014°C at 240°C; a negligible error contribution.

The RTD and Fluke ohmmeter were also calibrated as a complete system at the University of California's Richmond field Station (RFS) in August 1980. This calibration was done at five temperatures using a heated oil bath. Two highly accurate reference temperature measuring systems were used: A Hewlett-Packard 2801A quartz thermometer system (instrument No. 1248-28) provided by LLNL, and an RTD standard (Thermohm L&N S/N 633113) connected to a L&N Mueller bridge (S/N 734195) provided by RFS. The Fluke 8500A ohmmeter was carefully zeroed and a shorting plug was used to short the ohmmeter current source so that RTD self-heating would not occur. Readings were taken, after allowing the oil bath to stabilize at each temperature, by removing the shorting plug from the Fluke ohmmeter and taking the first or second reading to flash on the ohmmeter digital display. Four to six readings were taken at each of the five temperatures.

The results of this calibration are plotted in Fig. A-4 in Appendix A. Average temperature variations using the quartz reference thermometer as a reference are plotted using both the Omega Engineering and the Swedish Bureau of Standards conversion tables. Maximum and minimum readings are also shown. It is interesting to note that the two temperature references used for this calibration compared within 0.02°C of each other over the entire calibration to 200°C.

Figure 13 is a piece-wise linearization of the RTD/Fluke ohmmeter calibration done at the Richmond Field Station. The plot shows average RTD deviations from the Hewlett-Packard quartz temperature reference along with upper and lower boundaries indicating calibration uncertainties. Only temperature deviations for the Swedish Bureau of Standards conversion table are shown because this table was used exclusively during thermocouple calibrations at Stripa. Uncertainty levels were determined from the two worst-case readings with respect to both temperature references used during the RFS calibration. They are taken from a total of 25 valid readings at five calibration temperatures. The upper worst-case reading is 0.082°C above the average deviation and the lower worst-case reading is 0.091°C below the average deviation. In drawing the uncertainty boundaries, it is assumed that these worst-case readings could have occurred at any temperature.

A second lower uncertainty level is also shown in Fig. 13 to account for the ohmmeter calibration error found when operating in the 9°C environment of the extensometer drift. This, however, affects only eighteen thermocouples calibrated in the extensometer drift during the first recalibration.

3.3.1 RTD self-heating

As explained in Section 3.2, it was discovered that the temperature reference RTD had been self-heating during the original thermocouple calibrations and first recalibrations. Self-heating is caused by I^2R electrical power dissipation in the RTD resistance element. This was significant during the Stripa calibrations due to the relatively high

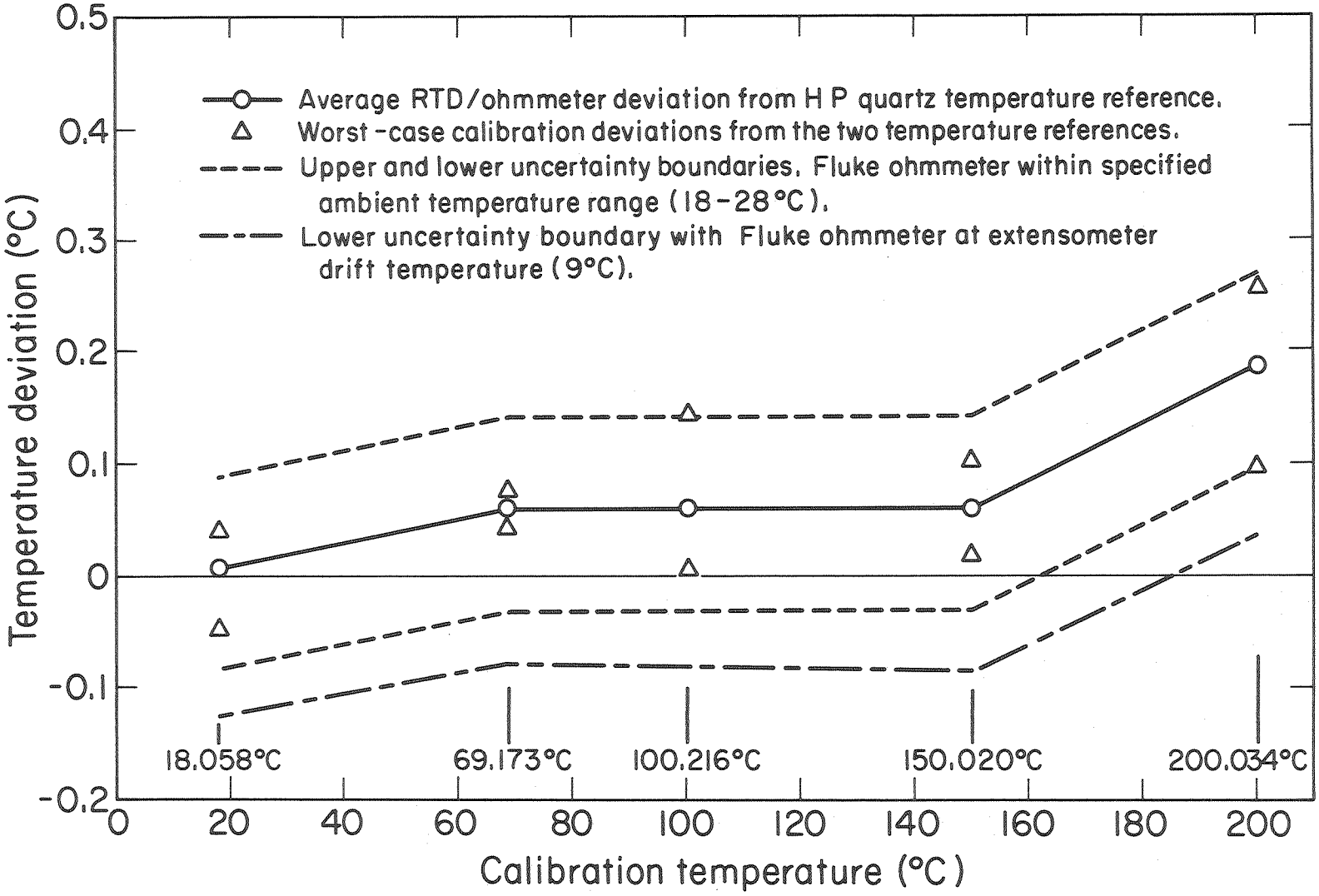

XBL848-9868

Fig. 13. Temperature reference system (RTD and Fluke ohmmeter) calibration summary with uncertainty boundaries.

constant current (I) from the Fluke 8500A ohmmeter in the range selected for greatest RTD resolution. The Swedish Bureau of Standards calibration of the RTD was done at a current of 1.0 mA and caused no significant self-heating. At any given temperature the 9.35 mA constant current from the Fluke ohmmeter resulted in a power dissipation nearly 90 times greater than the dissipation at 1.0 mA. It should also be noted that the electrical resistance (R) of the RTD increased from 100 ohms at 0°C to over 175 ohms at 200°C, thus the greatest self-heating occurred at the highest calibration temperature.

After discovery of the RTD self-heating, a number of tests were performed at Stripa in an attempt to determine the influence on the thermocouple calibrations. The first series of tests were done at the conclusion of the last run of the first recalibration. Thermocouples were taped in a bundle around the RTD with the thermocouple junctions in approximately the same plane as the RTD element. The bundle was placed inside the cylindrical aluminum mass in the calibration oven, simulating a thermocouple calibration run. The oven, RTD and thermocouples were then allowed to stabilize at a preselected oven temperature. An electrical shorting plug was used at the ohmmeter current source terminals to keep it from supplying current to the RTD. The shorting plug was removed at some convenient starting time, and RTD and randomly selected thermocouple readings were monitored with respect to time until the RTD self-heating reached stability; usually about 1-1/2 hr. RTD self-heating was determined from the difference between the first reading after shorting plug removal and the final reading after RTD temperature stability had been reached.

The amount of RTD self-heating was a function of variations in thermocouple bundling around the RTD, placement in the aluminum cylinder, the amount of insulation and method used to close the cylinder opening, and the selected oven temperature. As a result RTD self-heating varied from a low of 0.55°C with the RTD and thermocouple bundle in contact with the aluminum cylinder and the oven at 13.5°C, to a high of 1.2°C with the bundled RTD centered in the cylinder and the oven at 200°C.

The RTD self-heating also caused a rise in temperature in the thermocouples bundled around it. The effect on any thermocouple in the bundle was dependent on its proximity to the RTD; the closer to the RTD, the greater the heating, and, consequently, the less the calibration error. Figure 14 shows the results of the best behaved series of self-heating tests at five oven temperatures from 13 to 212°C. Each test was done at a fixed oven (ambient test) temperature. Test temperatures are shown on the figure. The bundle configuration and placement in the oven were the same for all five temperatures. RTD self-heating (A) and the resulting average temperature increase of four randomly picked thermocouples (B) in the bundle are plotted. The third plot (A minus B) shows the average error that should have been introduced between the four thermocouples and the RTD due to self-heating during a thermocouple calibration run. This error is approximately 0.5°C at low temperature, increasing to about 0.6°C at higher temperatures for tests in the full-scale experiment drift. The low values on curves A and B at 13°C are probably due to a slight change in the oven temperature during that test run. This should have negligible effect on the A minus B point at 13°C.

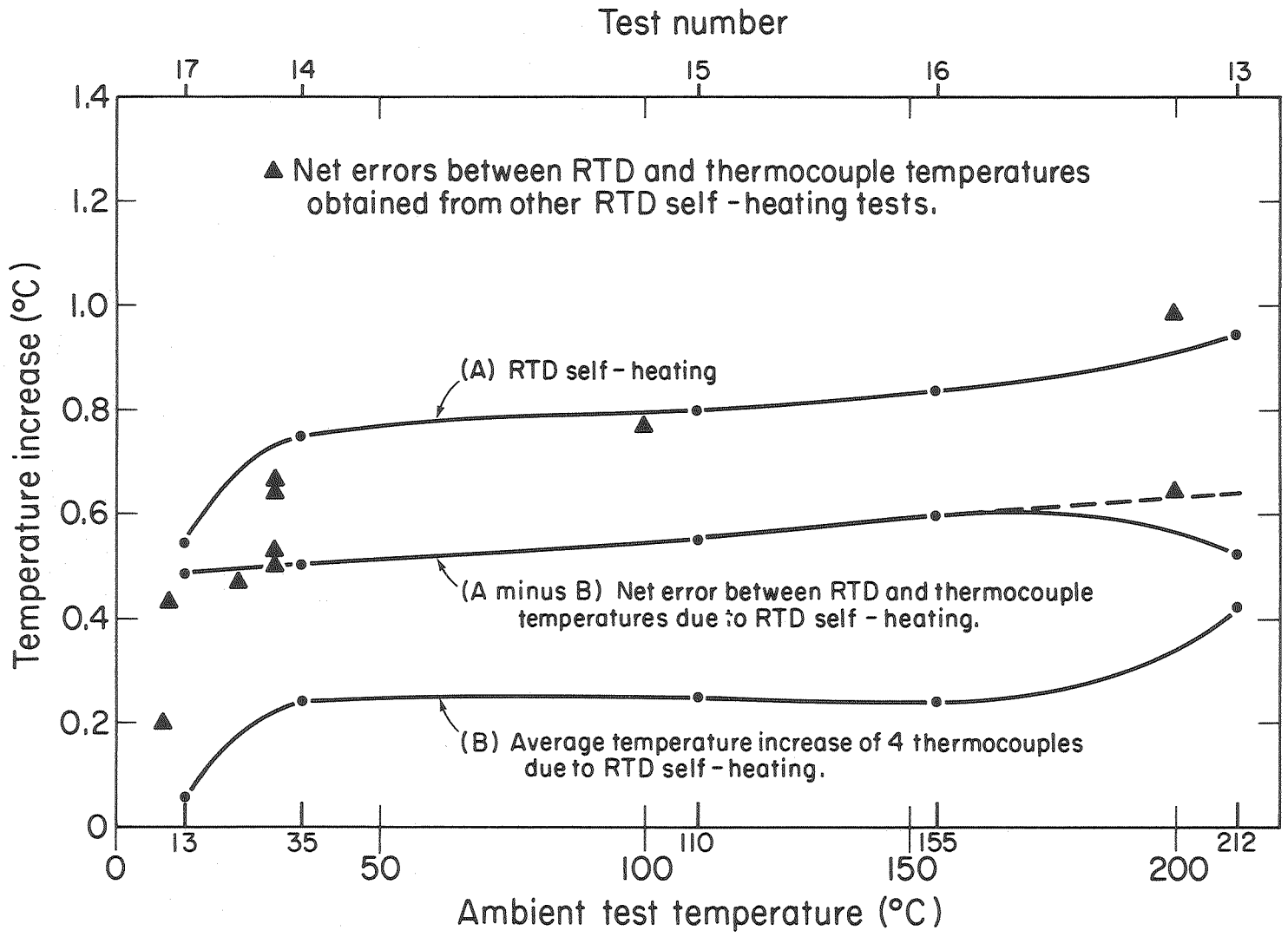

Fig. 14. Results of RTD self-heating tests.

Self-heating tests under other conditions that could have existed during thermocouple calibrations resulted in net thermocouple calibration errors ranging from 0.2 to nearly 1.0°C. Ten points representing net error results from these other self-heating tests are also shown in Fig. 14.

As explained above, RTD self-heating induced a temperature gradient through the thermocouple bundle surrounding it, resulting in a thermocouple temperature spread during calibrations. This is apparent in the original calibration and first recalibration deviations plotted from AD-9 data, shown in Section 4 (Figs. 16, 18, and 20), as a spread in temperature deviation at the lowest calibration temperature. Temperature spreading from this effect was eliminated during the second recalibration when RTD self-heating was avoided.

It should be reiterated that during the first recalibration the Fluke ohmmeter had not been properly zeroed, causing an offset in RTD readings that compensated for RTD self-heating to some extent. Further corrections to the thermocouple calibration data are discussed in Section 4.

3.4 Data Acquisition Equipment Deviations

Errors introduced in computer acquired data by the data acquisition hardware, and compensating corrections made to these data are covered in detail by Chan et al. (1980). Back-up data from the AD-9 data loggers were used as reference data in quantifying the computer errors as a function of time. The AD-9s were also heavily relied on for their stability and accuracy during thermocouple calibrations. This section covers the

influence of AD-9 accuracy and stability deviations on thermocouple data and calibrations. Calibration results for the Fluke 343A dc voltage calibrator and the Fluke 8500A DVM, used as references during computer and AD-9 calibrations, are also included here.

3.4.1 Fluke voltage reference calibrations

The Fluke 343A dc voltage calibrator (S/N 825010) and the dc voltmeter function of the Fluke 8500A digital multimeter (S/N 805003) were calibrated in the Stripa work areas where they had been used as references. These calibrations were done after conclusion of the heater experiments using a voltage reference fabricated and calibrated at LBL. The field calibrations indicated that the two Fluke instruments were generally accurate to ±1 microvolt (equivalent to ±0.025°C) over the Stripa thermocouple temperature range (equivalent to 0-20 mV). Later calibrations at LBL confirmed the two Fluke Instrument accuracies to be at least comparable with the accuracy of the voltage reference taken to Stripa for their calibration. The LBL calibrations are summarized in Tables 12 and 13. The Fluke 343A dc calibrator was calibrated in LBL's Meter Shop Standards Laboratory using a Guildline 9144L potentiometer (AEC No. 12112) and a Certavolt voltage standard (S/N 3318) accurate to better than 10 ppm. The Fluke 8500A DVM was compared against the Fluke 343A at the time of this calibration.

Any contributions to errors in thermocouple data due to computer or AD-9 calibration errors introduced by inaccuracies from the Fluke 343A dc voltage calibrator or the Fluke 8500A DVM are negligible.

Table 12. Fluke 343A DC Voltage Calibrator (S/N 825010) calibration summary.

Voltage	Maximum deviation from LBL lab standard
0.000 to 10.000 mV	0.000 mV
10.000 to 900.000 mV	±0.001 mV
1 to 10 V	±0.002%

Table 13. Fluke 8500A DVM (S/N 805003) calibration summary.

Voltage	Maximum deviation
0.000 to 1.000 mV	0.000 mV
1.000 to 100.000 mV	±0.001 mV
100.000 to 300.000 mV	+0.000 to -0.002 mV
0.4 to 10 V	$\leq$ +0.01%

3.4.2 Acurex Autodata-Nine deviation effects on thermocouple data

Autodata-Nine (AD-9) data loggers use a piece-wise linear approximation to convert measured thermocouple voltages to temperatures. The algorithm uses linear interpolation between 53 points selected from the NBS reference table for type K thermocouples (Table A-1) to make these conversions to a resolution of 0.1°C. The selected points that fall within the temperature range encountered in the Stripa experiments are given in Table 14. They identically match points in the NBS table and are closely distributed over a nearly linear portion of the thermocouple voltage-to-temperature characteristic curve. It is reasonable, therefore, to expect AD-9 conversion errors to be within plus or minus one least-significant digit after conversion (i.e., within ±0.1°C). Actual voltage-to-temperature conversions made during AD-9 calibrations generally confirm this tolerance with a small percentage of random samples slightly exceeding ±0.1°C, but falling within ±0.2°C.

Calibrations of the AD-9s and their stabilities are discussed in Chan et al. (1980), and the stability history is briefly reiterated in Section 2.5 of this report. Worst case values found during these calibrations and stability evaluations have been linearly interpolated to arrive at maximum and minimum thermocouple temperature errors reasonably expected to have been introduced by the time-scaled and full-scale AD-9s for temperatures up to 500°C. The results are summarized in Table 15. The minimum error values occurred in June 1978, and the maximums in April 1980. They, however, can be considered as reasonable minimum and maximum

Table 14. Temperature versus voltage points used by Autodata-Nine interpolation algorithm.

Voltage [mV]	Temperature [°C]
0.0	0
0.557	14
1.081	27
2.022	50
3.266	80
4.095	100
5.124	125
5.733	140
6.939	170
7.538	185
8.137	200
9.745	240
11.793	290
13.039	320
16.395	400
18.513	450
22.346	540

Table 15. Temperature uncertainties introduced by Autodata-Nine data loggers.

Temp. [°C]	Time-scaled AD-9 Min.* [°C]	Time-scaled AD-9 Max.* [°C]	Full-scale AD-9 Min.* [°C]	Full-scale AD-9 Max.* [°C]
0	-0.00	0.00	0.00	0.00
10	-0.00	0.00	0.00	+0.01
50	-0.01	+0.02	+0.02	+0.05
100	-0.01	+0.05	+0.04	+0.09
150	-0.02	+0.07	+0.05	+0.14
200	-0.03	+0.09	+0.07	+0.18
250	-0.03	+0.11	+0.09	+0.23
300	-0.04	+0.14	+0.11	+0.27
400	-0.05	+0.18	+0.15	+0.37
500	-0.07	+0.23	+0.18	+0.46

*Note: +0.1°C should be added to max. values, and -0.1°C to min. values for voltages that were converted to temperatures by the AD-9s (see Section 3.4.2).

uncertainties for AD-9 voltage readings over the full time of the experiments. An additional uncertainty of +0.1°C should be added to the maximum values and -0.1°C added to the minimum values for data converted to temperature by the AD-9s to include the interpolation and rounding errors discussed in the preceding paragraph.

4.0 THERMOCOUPLE VARIABILITY BY CLASS

The characteristics of the thermocouples used at Stripa varied by class as discussed in Schrauf et al. (1979). The stainless steel and Inconel sheathed thermocouples were heat treated before installation in order to force a one-time shift in characteristics that occurs at elevated temperatures. This heat treatment accounts for much of the difference between the sheathed and Teflon insulated thermocouple characteristics.

Comparison of the thermocouple calibrations with the NBS voltage-to-temperature conversion table for type K thermocouples is of interest because both the computer data released on the public domain data tapes (PDTs) and the AD-9 data logger's printed paper tapes used the NBS conversion.

Figure 15 illustrates how the thermocouple calibration data, the RTD reference temperatures, and the NBS voltage-to-temperature conversion were combined to show the deviation from NBS conversion tables of the Stripa thermocouples. Deviation values were computed by converting the RTD measured temperatures (T_F in Fig. 12) to equivalent type K thermocouple voltages using the NBS tables, then subtracting these voltages from the appropriate computer or data logger voltages (V_C' or V_D', respectively) read from the thermocouple during calibration. These deviations generally increase with increasing temperature. At 200°C, average deviations are as large as +2°C and some individual thermocouples deviated by as much as 3.5°C.

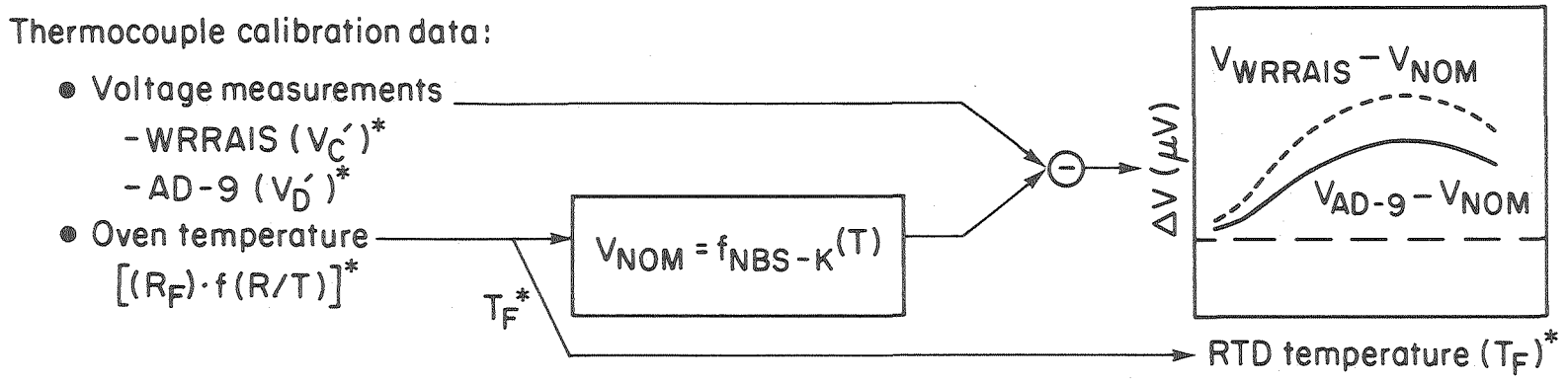

* V_C' Computer digitized and recorded voltages
V_D' Data logger digitized and recorded voltages
R_F RTD resistance measured by Fluke ohmmeter
T_F Temperature converted from R_F using Swedish Bureau of Standards tables

XBL 842-9606

Fig. 15. Comparison of thermocouple calibration voltages with NBS equivalent voltages.

Errors from several sources have been removed from the calibration data. The plots shown in Figs. 16-21 have been corrected for the error values given below. Chan et al. (1980) described errors that occurred in the computer's wide-range relay analog-input subsystem (WRRAIS). During the original calibration, the full-scale WRRAIS had a voltage offset of 22.8 μV and a gain of 0.99775, and the time-scaled WRRAIS had a voltage offset of 32.5 μV and a gain of 0.99637. During the first and second recalibrations, the full-scale WRRAIS had a voltage offset of 81 μV and a gain of 0.9945, and the time-scaled WRRAIS had a voltage offset of -1.8 μV and a gain of 0.9982. The effects of the RTD self-heating and ohmmeter zeroing problem were estimated using the AD-9 data logger calibration data at the lowest calibration temperature readings. The RTD self-heating and non-zeroing of the ohmmeter caused an offset in the deviation of the thermocouple calibration voltages from the NBS values. This is most obvious at the lowest calibration temperatures where that deviation should approach zero in the deviation plots. RTD self-heating also causes a spreading in the thermocouple calibration voltage deviations from NBS values due to varying degrees of thermal coupling from the RTD to the thermocouples bundled around it during calibrations. This spreading is also most obvious at the lowest calibration temperature since the thermocouples should approach a common voltage output when near the cold junction reference temperature. Offset voltages for corrections to the deviation plots were determined by computing average offset at the lowest calibration temperatures for each class of thermocouples. These voltage offsets were -22.5 μV during the original calibration, 8.8 μV

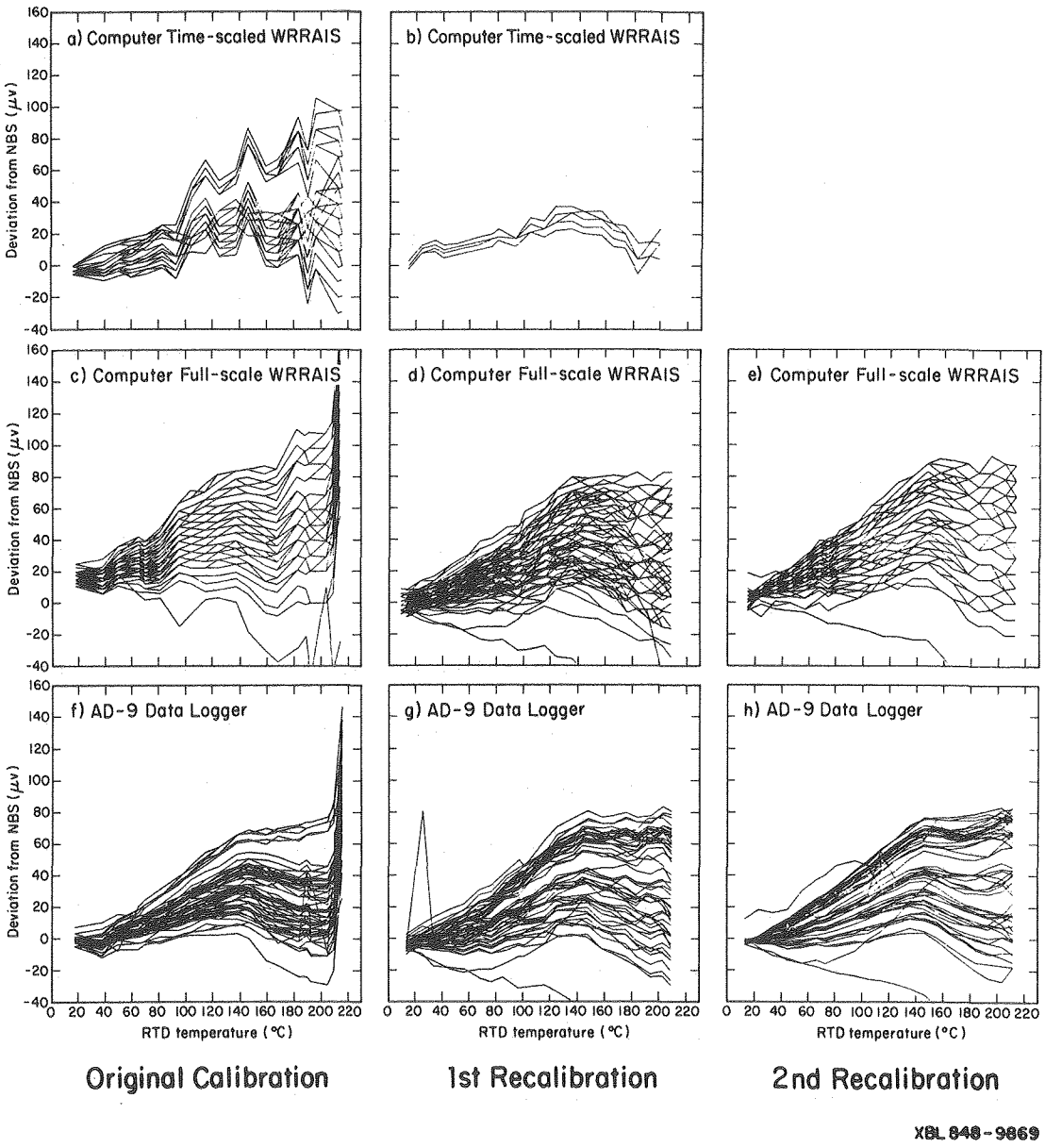

Fig. 16. Deviations of the Teflon thermocouple calibrations from the NBS reference.

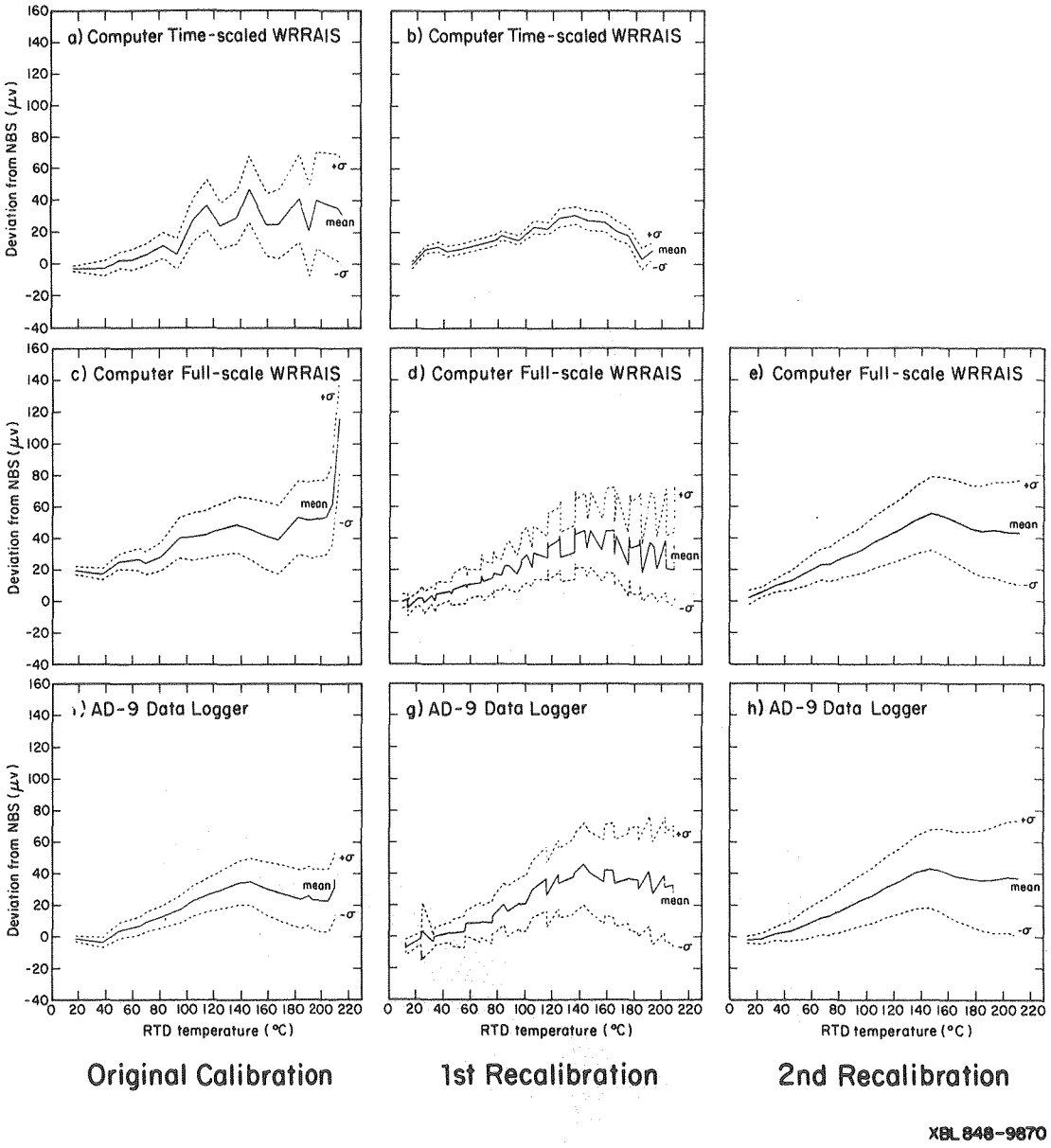

Fig. 17. Statistical deviations of the Teflon thermocouple calibrations from the NBS reference.

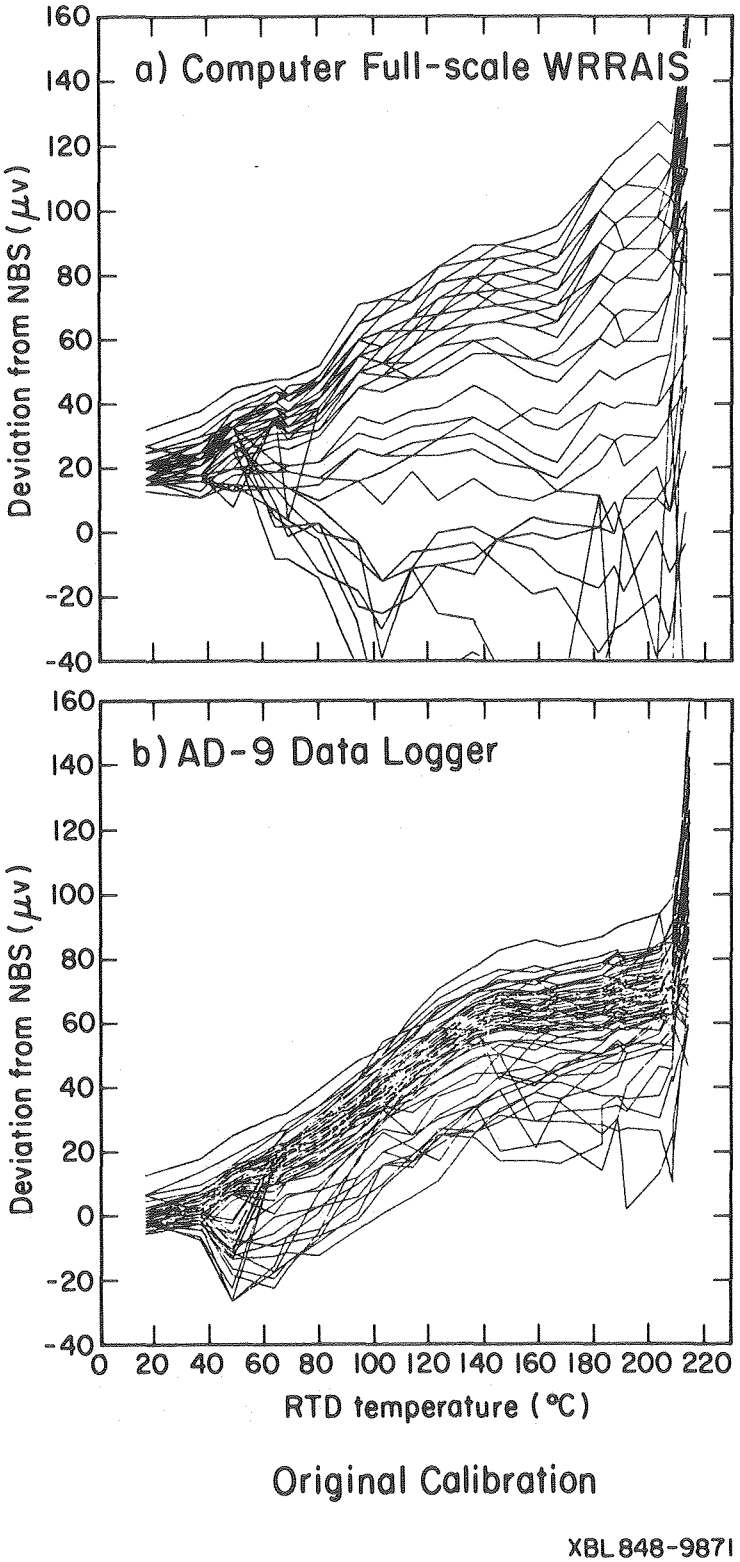

Fig. 18. Deviations of the stainless steel sheathed thermocouple calibrations from the NBS reference.

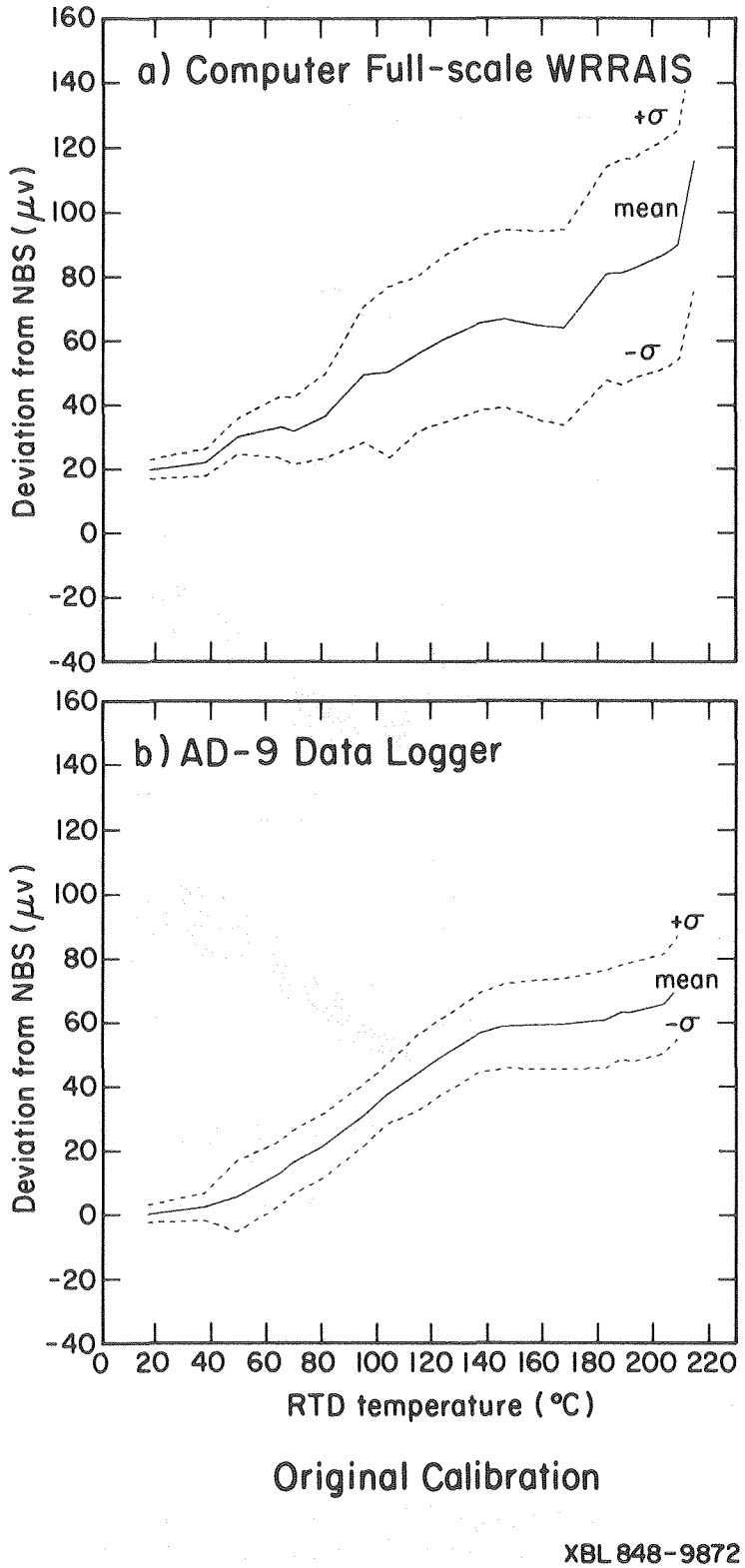

Fig. 19. Statistical deviations of the stainless steel sheathed thermocouple calibrations from the NBS reference.

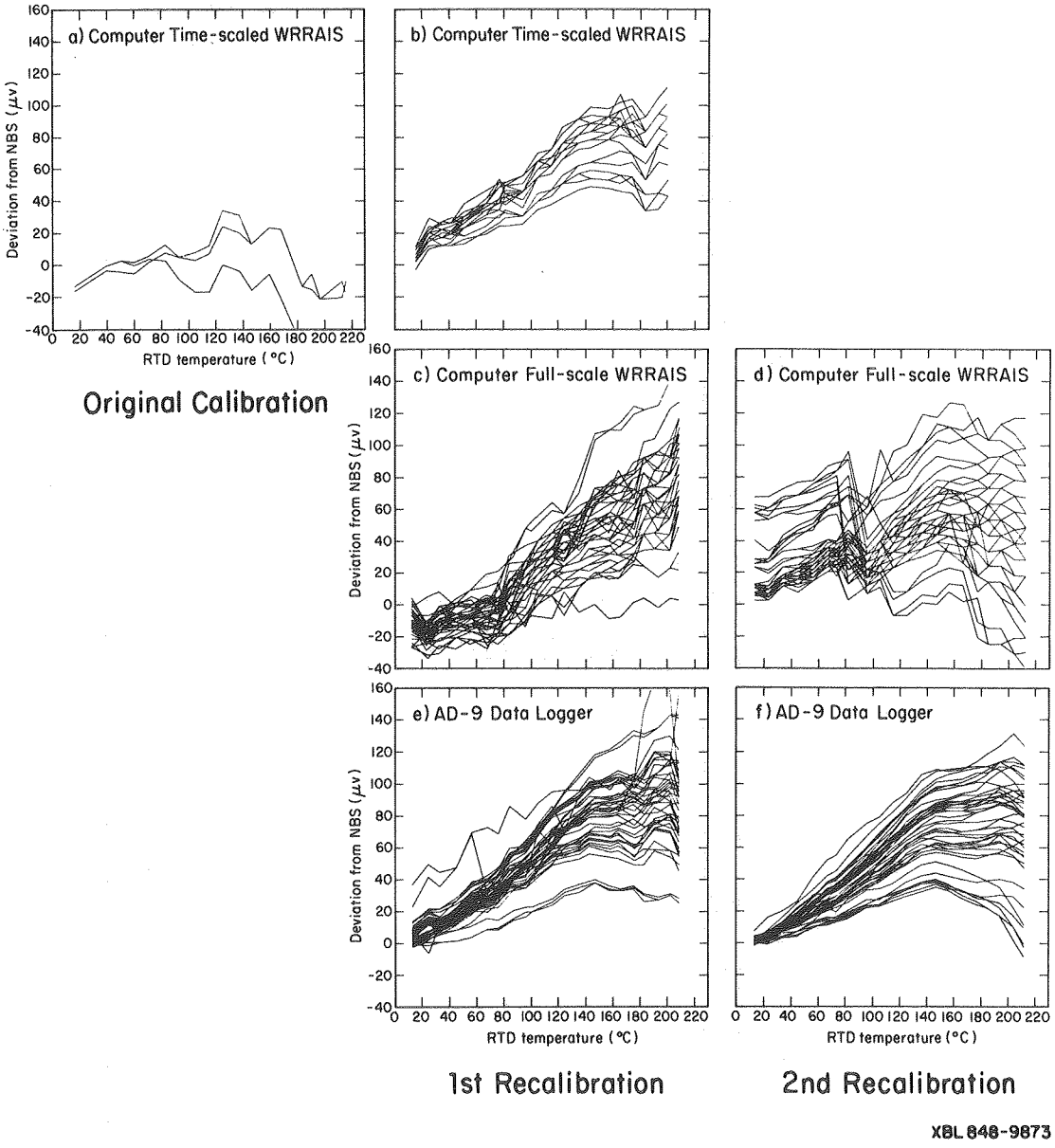

Fig. 20. Deviations of the Inconel sheathed thermocouple calibrations from the NBS reference.

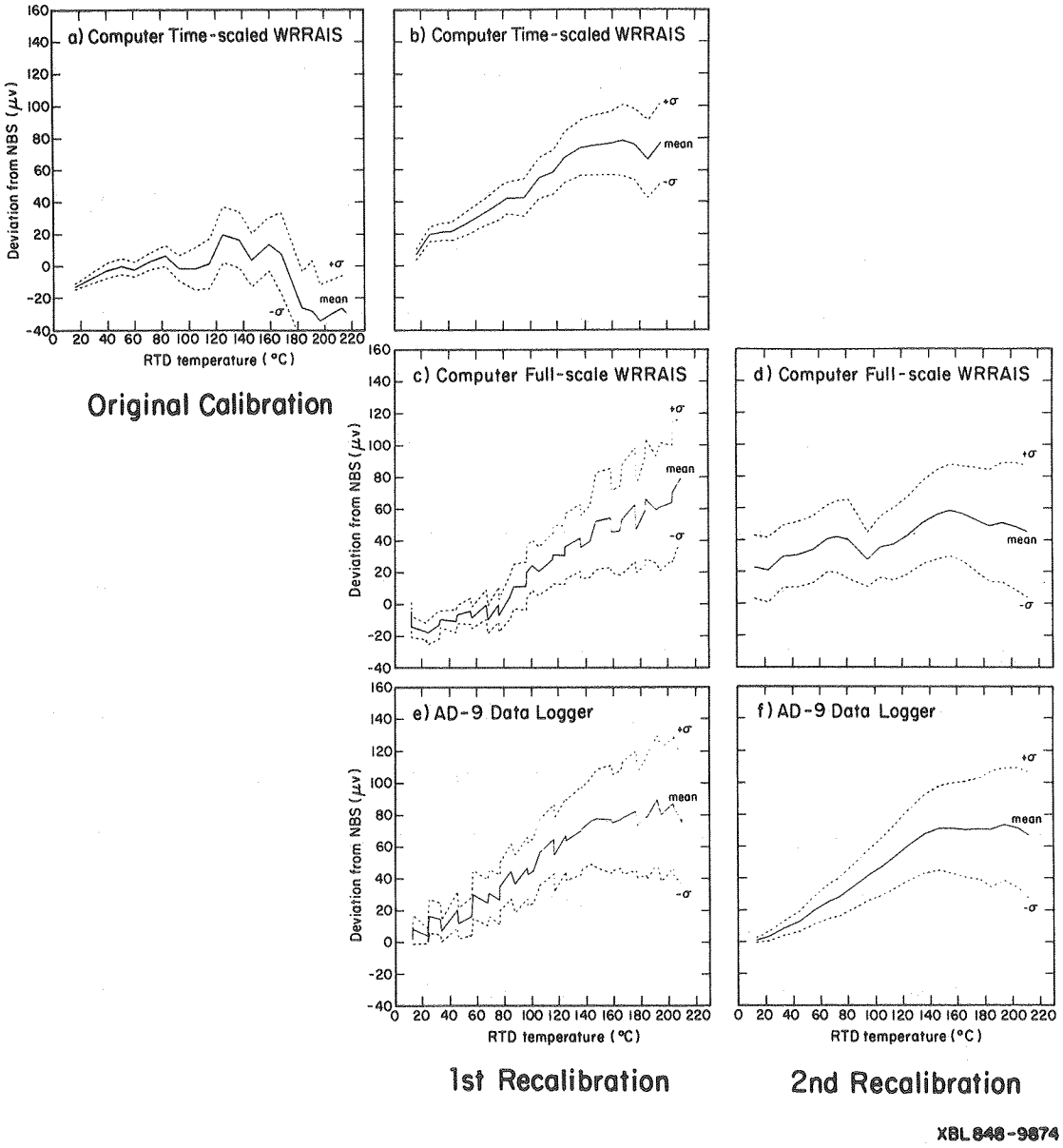

Fig. 21. Statistical deviations of the Inconel sheathed thermocouple calibrations from the NBS reference.

during the first recalibration and -0.5 μV during the second recalibration. Deviation corrections are given in μV, where 40 μV is approximately equivalent to 1°C for type K thermocouples.

The deviation plots for the AD-9 data loggers are generally quite smooth except for a few remaining data entry errors. The deviation plots of the computer-acquired calibration data are less smooth due, primarily, to the resolution of the analog-to-digital converter in the wide-range relay analog-input subsystem (WRRAIS). Three gain ranges are apparent on the plots: 0 to 3.75 mV, 3.75 to 7.50 mV, and 7.50 to 15.0 mV. Changes between these gain ranges occur at approximately 92 and 184°C.

The calibration results indicate how the thermocouples behaved on the three calibration occasions, but that does not ensure similar behavior at other times. The family characteristics of the three thermocouple types does appear, however, to have changed little from before the experiments to after the experiments. Figure 16 shows calibration data for Teflon thermocouples, Fig. 18 for stainless steel sheathed thermocouples, and Fig. 20 for Inconel sheathed thermocouples.

A measure of the statistical variability was obtained by computing the sample variance

$$s^2 = E[X^2] - E[X]^2$$

where:

$$E[X^2] = \frac{1}{n} \sum_{i=1}^{n} X_i^2$$

is the second moment, and

$$E[X] = \frac{1}{n} \sum_{i=1}^{n} X_i$$

An unbiased estimate of the variance is then

$$\sigma^2 = \frac{n}{n-1} s^2$$

The statistical plots (Figs. 17, 19, and 21) show the mean and the ±1 standard deviation (σ) bounds.

Section 5 provides additional indications of the magnitude of time varying errors.

4.1 Teflon Insulated Thermocouples

The Teflon insulated thermocouples were generally well behaved as shown in Fig. 16. There were no apparent aging affects and they were not as susceptible to common-mode noise as sheathed thermocouples. Residual effects of the RTD self-heating can be seen as the deviation spread at the lowest temperature for the data logger data in Fig. 16f. Figure 16h illustrates by the close grouping at the lowest temperature, that self-heating had been avoided during the second recalibration.

All of the statistical deviation plots in Fig. 17 show similar results. In some cases calibration results from more than one calibration run were combined. The ragged appearance of Figs. 17d and 17g

occurs because the oven temperature settings differed during separate calibration runs.

4.2 Stainless Steel Sheathed Thermocouples

Calibration deviations for stainless steel sheathed thermocouples are shown in Fig. 18. The results from the computer and data logger for the original calibration differ considerably. A likely reason for these differences is due to electrical noise pick-up by the sheathed thermocouples and the inability of the computer's analog-to-digital conversion electronics to reject that noise. The AD-9 data loggers had considerably better common-mode noise rejection capabilities.

The statistical deviations of the stainless steel sheathed thermocouples in Fig. 19 show a similar mean, but a larger variance between computer and data logger plots. The distribution of deviations in Fig. 18a is skewed considerably. The stainless steel thermocouples were either grouted in place, thus were not removable, or were replaced by Inconel sheathed or Teflon insulated thermocouples during the experiment because of the sheath corrosion problems discussed in section 2.0, therefore, post-experiment calibration data are not available.

4.3 Inconel Sheathed Thermocouples

Calibration deviations for Inconel sheathed thermocouples are shown in Fig. 20. Few were calibrated before the experiment because they were used in high temperature applications such as on heater canisters where accuracy was not as critical as lower rock and instrument temperatures. Common-mode noise effects are quite pronounced in the computer-acquired

data shown in Fig. 20d. The effect is greatest at low temperatures that correspond to the highest gain range in the WRRAIS. The data logger results shown in Fig. 20f were obtained simultaneously with those data in Fig. 20d and illustrate excellent rejection of the common-mode noise. The computer data shown in Fig. 20d was acquired one month after the data shown in Fig. 20c. Common-mode noise effects are not apparent in the earlier calibration. Too few Inconel sheathed thermocouples were calibrated before the experiment to be statistically significant (Fig. 20a).

4.4 Additional Improvements to Thermocouple Calibration and Temperature Data

There are a number of additional corrections that can be made to improve the thermocouple calibration data and reduce uncertainties. Some of these and other approaches in using data acquired during the experiments are briefly discussed in the following paragraphs.

Additional thermocouple calibration corrections can be made for RTD self-heating by individually correcting each thermocouple by its offset at the lowest calibration temperature. These corrections can be further refined by compensating for the increased RTD self-heating offset at higher temperatures by adding a slope of up to 0.2°C per 100°C to the low temperature offset correction (see Fig. 14). These corrections, however, will probably contribute maximum improvements of 0.25°C at ambient temperatures, to 0.5°C near 200°C; and these improvements will benefit only those thermocouple calibrations affected by RTD self-heating. Additional corrections can also be made to further correct computer WRRAIS-generated

offset voltages. In some cases the corrections to WRRAIS data can provide more significant results, up to 0.7°C in a few cases.

The most significant improvements to temperature accuracies could be made by returning to individual thermocouple polynomials generated from the available thermocouple calibrations after a thorough analysis of all the variables that influenced the calibrations. This would be time consuming but, by inspection of the plots in Figs. 16, 18 and 20, could improve average thermocouple temperature accuracies to within 0.5%. An alternative would be to generate polynomial coefficients from the calibration mean plots (Figs. 17, 19, and 21) for various classes of thermocouples. This too could provide significant improvements in average temperature accuracies.

It should be reiterated here that the best temperature data obtained during the experiments and the thermocouple calibrations were obtained by the Autodata-Nine data loggers. Unfortunately these data are on printed paper tapes and computer entry is time consuming. However, in the cases where more accurate and stable temperature data are needed, it is worth the inconvenience of using the data logger printed outputs.

5.0 TIME VARYING ERRORS

The computer's WRRAISs in both the full-scale and time-scaled experiments malfunctioned on several occasions during the experiment. Chan et al. (1980) described these failures and compensations that were applied to improve the computer acquired data. Fortunately, the AD-9 data loggers provided an independent data source that was free from these errors and maintained good accuracies (see Section 3.4.2) throughout the experiment. Table 16 illustrates the residual deviations between the computer data and the AD-9 data for thermocouple sensor number 160 after the voltage correction procedure described by Chan et al. (1980) had been applied. Good correlation generally exists between temperatures recorded by the data loggers and those obtained by reprocessing the computer's corrected raw data.

Table 17 summarizes the residual root-mean-square (rms) deviations between corrected computer voltages and corresponding data logger voltages for several thermocouples. These residual errors are much smaller for the full-scale experiments (1 and 2) than for the time-scaled experiment (3). Many thermocouples in the time-scaled experiment were grouted in place and were not removable, therefore, they were neither replaced nor recalibrated at the conclusion of the experiment. Signals from many of the time-scaled thermocouples were noisy throughout the experiment.

Comprehensive comparisons between computer and data logger data were not practical since the data logger values were printed on paper tape and required manual entry and verification. In addition, during periods when temperatures were not expected to vary rapidly the data loggers were

programmed to acquire data at intervals as great as 6 hours while the computer acquired data at 15-minute intervals. Figures 22-24 are provided as examples comparing plots from data logger and computer-acquired data as a function of time.

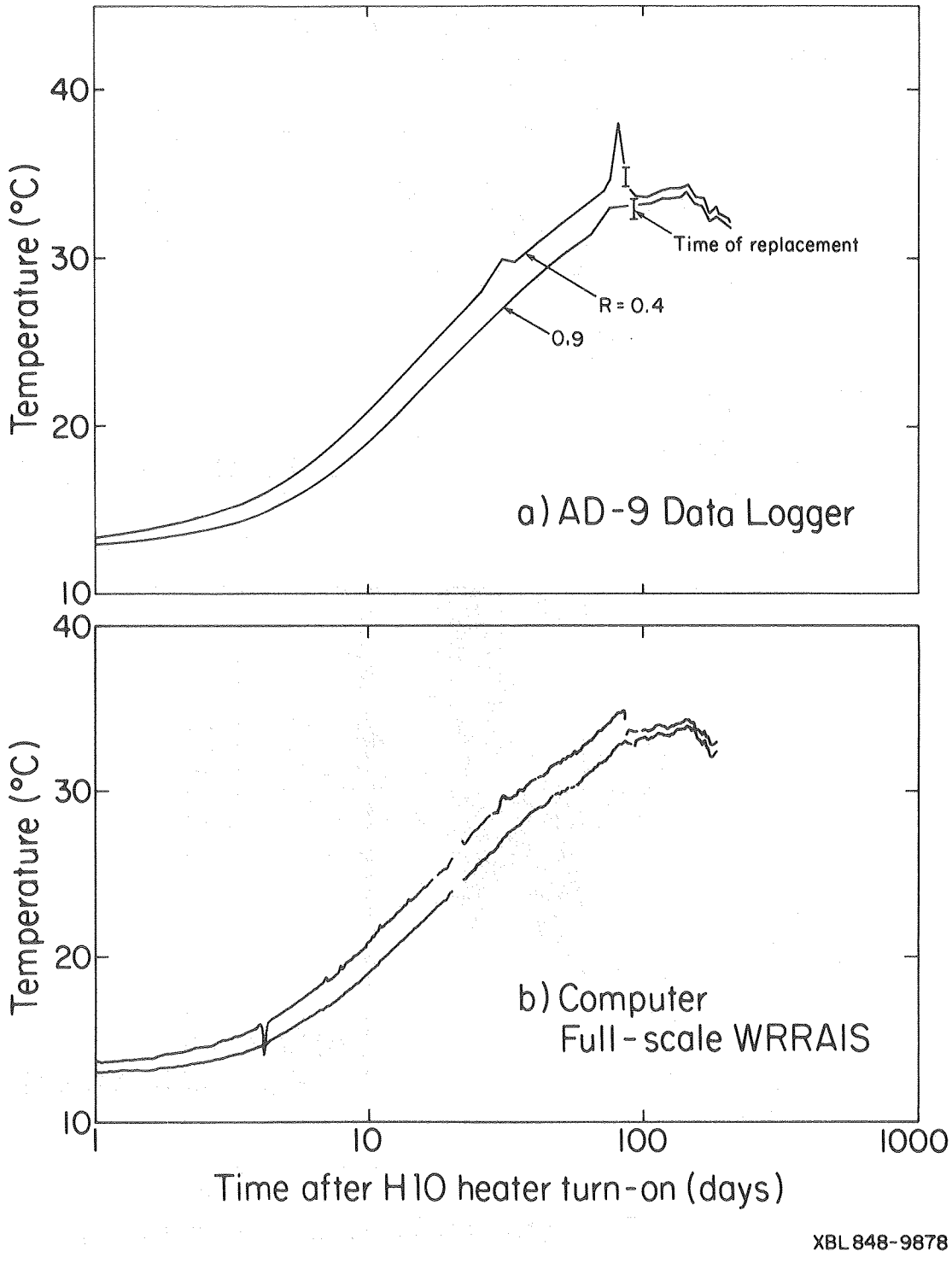

Fig. 22. Temperature after H10 heater turn-on, measured at z = +3m by: (a) AD-9 data logger (from Javandel and Witherspoon, 1981) and (b) full-scale WRRAIS.

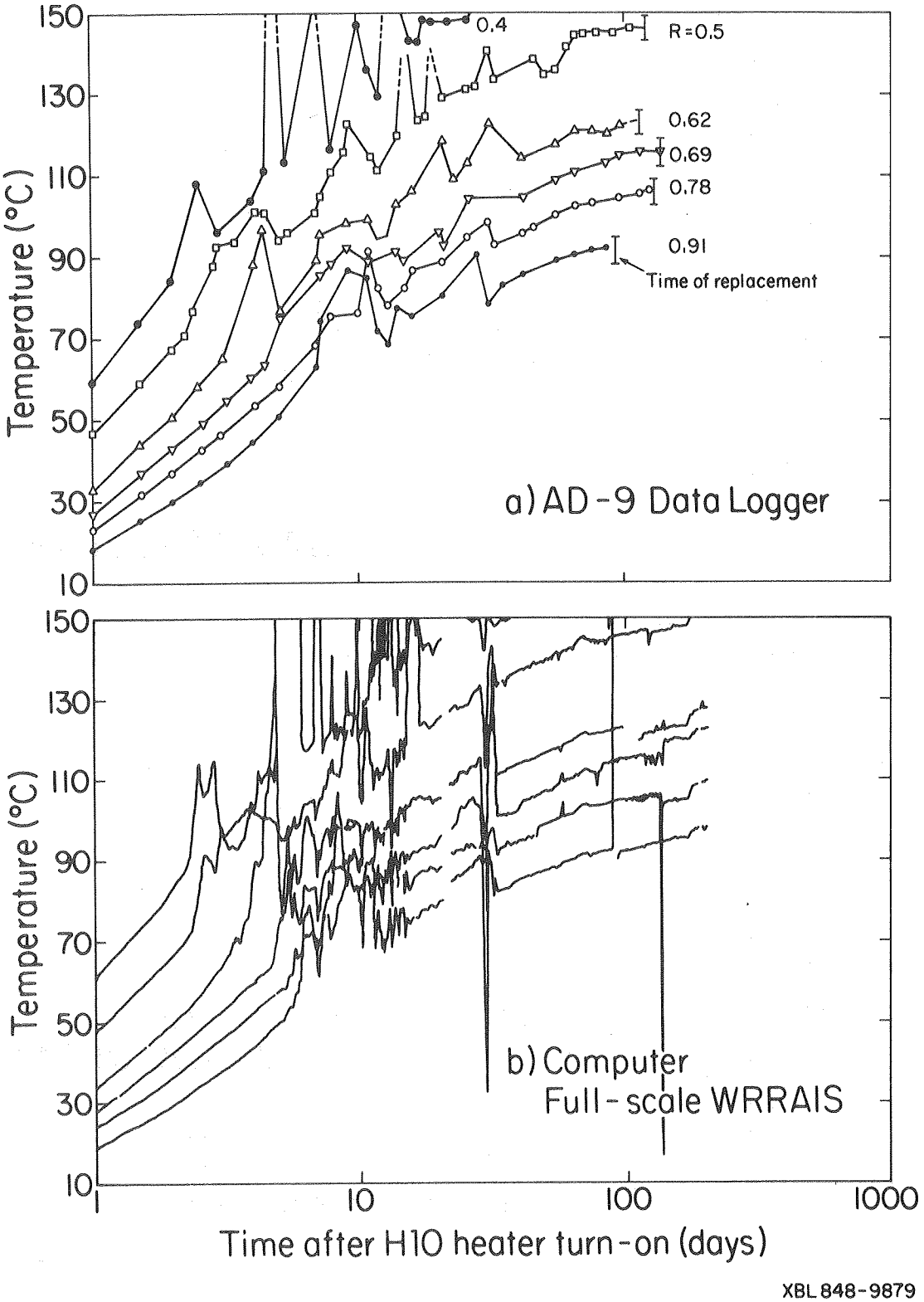

Fig. 23. Temperature after H10 heater turn-on, measured at heater midplane (z = 0.0) by: (a) AD-9 data logger (from Javandel and Witherspoon, 1981) and (b) full-scale WRRAIS.

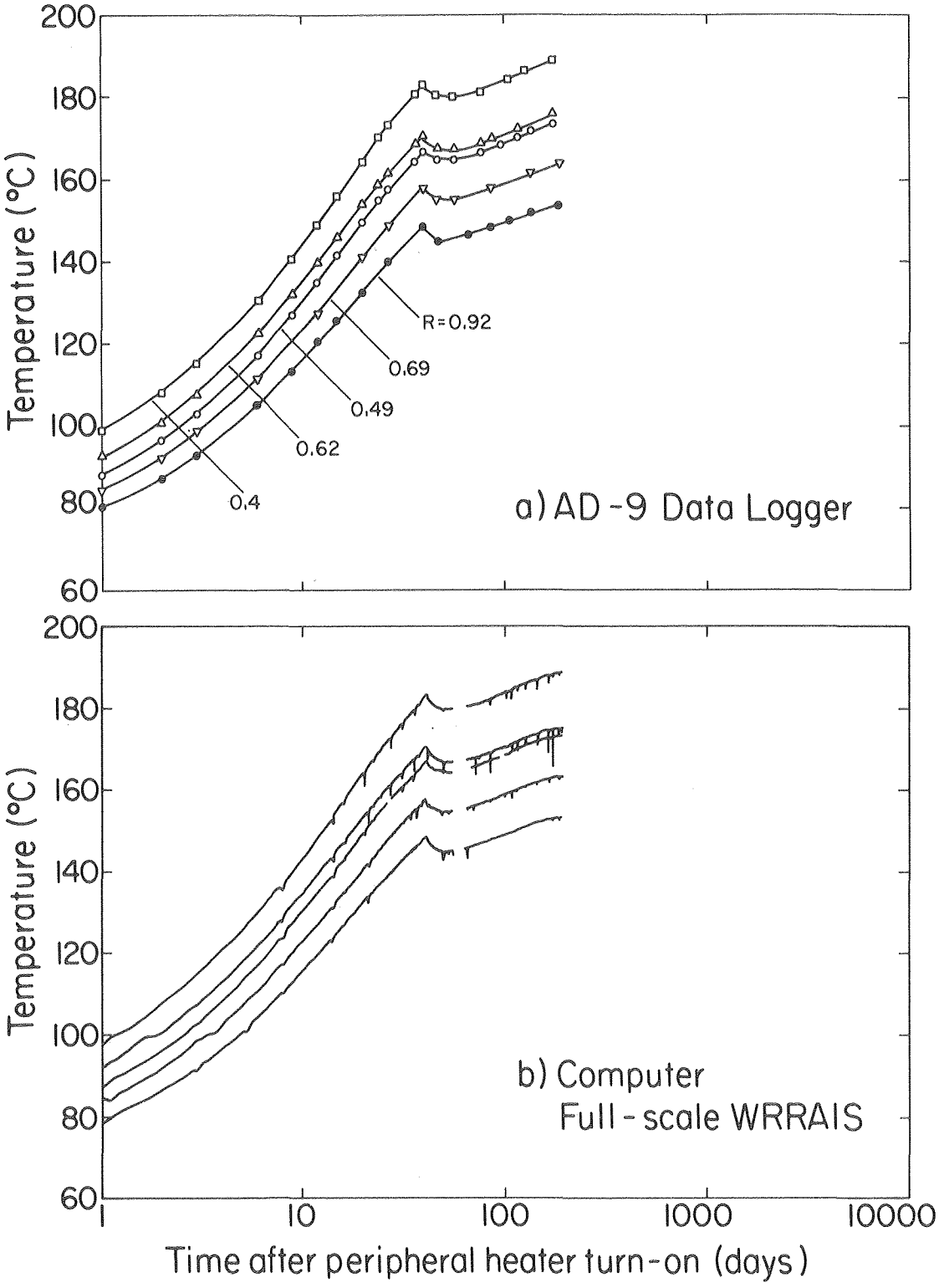

XBL848-9880

Fig. 24. Temperature after peripheral heater turn-on, measured at z = -1.5 m by: (a) AD-9 data logger (from Javandel and Witherspoon, 1981) and (b) full-scale WRRAIS.

6.0 SUMMARY AND RECOMMENDATIONS

Chromel-Alumel (ANSI type K) thermocouples were used to measure temperature fields at Stripa. Computer-acquired temperature measurements provide the primary data record. These data have been compensated for malfunctions that occurred to the computer's data acquisition system, and are available on 9-track digital computer tape (Chan et al., 1980). More accurate data were acquired by the backup data loggers, but those data are printed on paper tape and are not machine readable. It would be possible, although time consuming and error prone, to manually enter the data-logger data for computer compatibility. Such an effort does not appear warranted at this time, though certain detailed data analysis has already required the transfer of selected data-logger data into a computer readable form and future analysis may require the transfer of additional data.

Two types of catastrophic failures occurred with the thermocouples, one due to corrosion of the protective sheath material on certain stainless steel sheathed thermocouples, and the other due to mechanical breakage of thermocouple leads during removal and installation of other instruments in the same boreholes as the thermocouples. The failures due to corrosion were of most concern. These affected 60 thermocouples in 12 sand-backfilled boreholes. Analysis of the temperature data following the experiments indicated that only 23 of these 60 thermocouples actually failed, however all 60 were replaced, using 50 Teflon insulated and 10 Inconel sheathed thermocouples. It has been estimated that if these thermocouples had not been replaced, up to 48 of them, located in the

most severe environments, would probably have failed catastrophically before the end of the experiments. This would have amounted to a 12.5% failure rate for the complete operational time (approximately two years) of the 385 thermocouples in the experiments. Thermocouples destroyed by breakage are not included in the 12.5% since breakage was strictly a function of handling. None of the grouted thermocouples gave indications of catastrophic failure with the exception of one destroyed during installation.

Erratic temperatures were observed in a few cases when small quantities of water were captured in vertical closed-bottom tubes in which thermocouples were installed. This resulted in a boiling and condensing cycle within the tubing, which caused thermocouple readings to oscillate erratically between 100°C and the valid temperature. This continued until the tubes were cleared of moisture. Several similar but less dramatic oscillations were also observed in other boreholes indicating the presence of boiling water or circulating vapor.

The Stripa thermocouples were calibrated at the site on three occasions. Data acquired during the first two of these calibrations were biased due to self-heating of the RTD used as a temperature reference. In addition, the Fluke ohmmeter used to measure RTD resistance was not properly zeroed before one calibration series. Most of these effects have been removed from the thermocouple calibration data. Comparisons showing deviations of these corrected calibrations from the NBS voltage-to-temperature relationship were made and are plotted in Figs. 16, 18,

and 20. These plots illustrate both the variability between thermocouples and differences between classes such as Teflon insulated or sheathed thermocouples. Plots of mean deviations, of thermocouple calibrations from NBS reference data, indicate the statistical errors that exist for data on the public domain data tapes, which used approximations to the NBS thermocouple reference tables. These mean deviation plots along with plus and minus one standard deviation (sigma) error-bands provide a measure of the statistical variability between thermocouples (Figs. 17, 19, and 21). The average values of these deviations are up to ±0.5°C at ambient temperatures (about 20°C) and are as large as +2°C at 200°C

Individual thermocouple calibration data were originally used in the computer to convert measured voltages to temperatures for the low temperature thermocouples. The numerous thermocouple replacements, uncertainties in calibration data, and computer conversion offset and gain variations made it impractical to continue this approach without considerable additional work. The NBS voltage-to-temperature conversion had been used in the Autodata-Nine data loggers for all thermocouples and in the computer for thermocouples with peak temperature above 200°C. The Stripa public domain data tapes (PDTs) also used an approximation of the NBS conversion. Data in this report provides statistical error deviations for both the computer data on the PDTs and the more accurate data-logger data. With additional effort these error deviations can be used to make more refined corrections to PDT and data logger temperatures.

Accurate thermocouple responses are available for the times of the three field calibrations. The data loggers used as computer backup

proved stable throughout the experiments. Drifts and uncertainties were less than 10 μV (or 0.25°C) for temperatures less that 250°C. The computer's data acquisition system was much less stable over time. Malfunctions in the computer's data acquisition system, its sensitivity to common-mode noise, and a thermal emf effect caused by mercury-wetted relays in its multiplexers greatly reduce confidence in the magnitude and stability of its error estimates over time. An extensive effort would be required to increase confidence in these error estimates, which is not currently planned. Spot checks suggest that agreement between the computer and data logger acquired data is acceptable enough to warrant use of computer data for most analysis purposes. The more laborious approach of extracting data logger acquired temperatures from the printed output may be required in some cases where more accurate temperature data are necessary.

Thermocouple aging effects appear to be small, however, very few of the thermocouples were calibrated both before and after the experiments. Those that were calibrated on both occasions were mostly calibrated using the computer only, hence apparent differences are likely due to changes in the computer's data acquisition system. Statistical data from the three thermocouple calibrations (Figs. 16-21) indicate that thermocouple characteristics were generally stable over the periods of the experiments.

Experience using thermocouples in the heated rock and wet underground environment at Stripa have resulted in the following recommendations for future systems (Binnall et al., 1979):

1) Use Inconel sheathed thermocouples exclusively for high temperature environments. At least avoid stainless steel sheaths and heat treatment that may sensitize materials to corrosion or decomposition. Materials must be carefully selected for the environment.
2) Use grounded junctions in enclosed sheaths.
3) Obtain all thermocouple wire from a common batch manufactured from single material melts.
4) Retain control samples of thermocouples and test their long-term stability.
5) Install tubing whenever possible for the insertions of movable thermocouples. Take care that this tubing does not collapse during installation or grouting.
6) Thermocouples should be removable for recalibration and/or replacement.
7) Provide a means to drain or remove moisture from thermocouple wells (tubes).
8) Data from backup data acquisition systems should be recorded on a machine readable data archiving medium.
9) Provide periodic loop resistance measurements to verify that thermocouples have not electrically opened or shorted somewhere along their wire length.

7.0 REFERENCES

American Society for Metals, 1975. Metals Handbook--8th Edition, Vol. I "Properties and Selection of Metals," ASM, Metals Park, Ohio.

American Society for Metals, 1975. Metals Handbook--8th Edition, Vol. 10, "Failure Analysis and Prevention," Section on Corrosion Failures, ASM, Metals Park, Ohio.

ANSI, 1976. American National Standard for Temperature Measurement Thermocouples, ANSI-MC 96.1-1975; Pittsburgh: Instrument Society of America.

ASME, 1974. Temperature Measurement : Performance Test Codes Supplement on Instruments and Apparatus, Part 3, ASME/ANSI PTC 19.3-1974, American Society of Mechanical Engineers.

ASTM, 1972. Standard Methods for Calibration of Thermocouples by Comparison Techniques, ASTM E220-72, American Society for Testing and Materials.

Binnall, E., A. DuBois, and R. Lingle, 1979. "Rock Instrumentation Problems Experienced during In Situ Heater Tests," Proceedings of the International Symposium on the Scientific Basis for Nuclear Waste Management, Materials Research Society (1980); and Lawrence Berkeley Laboratory, LBL-9952 (1979).

Chan, T., E. Binnall, P. Nelson, R. Stolzman, O. Wan, C. Weaver, K. Ang, J. Braley and M. McEvoy, 1980. Thermal and Thermomechanical Data from In Situ Heater Experiments at Stripa, Sweden, LBL-11477, SAC-29, Lawrence Berkeley Laboratory, Berkeley, California.

DuBois, A. O., M. Hood, E. P. Binnall and L. Andersson, 1981. Extensometer Performance during Heater Experiments at Stripa, LBL-13531, SAC-50 Lawrence Berkeley Laboratory, Berkeley, California.

Fritz, P., J. F. Barker and J. E. Gale, 1979. Geochemistry and Isotope Hydrology of Groundwaters in the Stripa Granite, Results and Preliminary Interpretation, LBL-8285, SAC-12, Lawrence Berkeley Laboratory, Berkeley, California.

Javandel, I., and P. A. Witherspoon, 1981. Thermal Analysis of the Stripa Heater Test Data Full Scale Drift, LBL-13217, SAC-43, Lawrence Berkeley Laboratory, Berkeley, California.

Kurfurst, P. J., T. Hugo-Persson and G. Rudolph, 1978. Borehole Drilling and Related Activities at th Stripa Mine, LBL-7080, SAC-05, Lawrence Berkeley Laboratory, Berkeley, California.

McEvoy, M. B., 1979. Data Acquisition, Handling, and Display for the Heater Experiments at Stripa, LBL-7062, SAC-14, Lawrence Berkeley Laboratory, Berkeley, California.

Nelson, P. H., R. Rachiele, J. S., Remer, 1981. Water Inflow into Boreholes During the Stripa Heater Experiments, LBL-12574, SAC-35, Lawrence Berkeley Laboratory, Berkeley, California.

Schrauf, T., H. Pratt, E. Simonson, W. Hustrulid, P. Nelson, A. DuBois, E. Binnall, R. Haught, 1979. Instrumentation Evaluation, Calibration and Installation for the Heater Experiments at Stripa, LBL-8313, SAC-25, Lawrence Berkeley Laboratory, Berkeley, California.

Witherspoon, P. A., N. G. W. Cook and J. E. Gale, 1980. Progress with Field Investigations at Stripa, LBL-10559, SAC-27, Lawrence Berkeley Laboratory, Berkeley, California.

Witherspoon, P. A., and O. Degerman, 1978. Swedish-American Cooperative Program on Radioactive Waste Storage in Mined Caverns: Program Summary, LBL-7049, SAC-01, Lawrence Berkeley Laboratory, Berkeley, California.

APPENDIX A: CALIBRATION REFERENCE DATA

A.1 NBS Type K Thermocouple Reference Table

Reference tables that relate thermocouple voltages and temperatures for standard thermocouple types are produced by the United States National Bureau of Standards (NBS). Values in these tables are ensemble averages of results from calibrating a sample of thermocouples of the specified type. These NBS tables are representative of what a user would except to encounter from a randomly selected thermocouple of that type. Table A-1 is a portion of the NBS reference table for Chromel-Alumel (ANSI type K) thermocouples for the range of temperatures encountered at Stripa. Data in this table supersedes NBS circular No. 561. Figure A-1 shows type K thermocouple voltage-versus-temperature characteristics in graphical form, and illustrates that these characteristics are nearly linear between 0 and 500°C.

A.2 RTD Calibrations

A platinum resistance temperature device (RTD), model number PR-11-3-100-1/4-18"E (serial number 1116) purchased from Omega Engineering Inc., was used as a temperature reference for the field calibrations of thermocouples used at Stripa. This RTD was calibrated on three occasions.

The RTD manufacturer originally calibrated the RTD on 12 August 1977 using an L&N model 8167-25 B (S/N 1821338) platinum resistance thermometer, an L&N G2 Mueller bridge (S/N 1169-36), and an ESI model 300 bridge (S/N 80846). This calibration equipment was traceable to NBS standards and had a stated temperature measurement accuracy of ±0.1°F. Calibrations were performed at 32, 211, and 502.237°F, which resulted in sensor

Table A-1. NBS table for Chromel-Alumel (ANSI type-K) thermocouples with reference junction at 0°C. (Note: this table supercedes NBS Circular No. 561.)

Thermoelectric voltage (in absolute millivolts)

DEG C	0	1	2	3	4	5	6	7	8	9	10	DEG C
0	0.000	0.039	0.079	0.119	0.158	0.198	0.238	0.277	0.317	0.357	0.397	0
10	0.397	0.437	0.477	0.517	0.557	0.597	0.637	0.677	0.718	0.758	0.798	10
20	0.798	0.838	0.879	0.919	0.960	1.000	1.041	1.081	1.122	1.162	1.203	20
30	1.203	1.244	1.285	1.325	1.366	1.407	1.448	1.489	1.529	1.570	1.611	30
40	1.611	1.652	1.693	1.734	1.776	1.817	1.858	1.899	1.940	1.981	2.022	40
50	2.022	2.064	2.105	2.146	2.188	2.229	2.270	2.312	2.353	2.394	2.436	50
60	2.436	2.477	2.519	2.560	2.601	2.643	2.684	2.726	2.767	2.809	2.850	60
70	2.850	2.892	2.933	2.975	3.016	3.058	3.100	3.141	3.183	3.224	3.266	70
80	3.266	3.307	3.349	3.390	3.432	3.473	3.515	3.556	3.598	3.639	3.681	80
90	3.681	3.722	3.764	3.805	3.847	3.888	3.930	3.971	4.012	4.054	4.095	90
100	4.095	4.137	4.178	4.219	4.261	4.302	4.343	4.384	4.426	4.467	4.508	100
110	4.508	4.549	4.590	4.632	4.673	4.714	4.755	4.796	4.837	4.878	4.919	110
120	4.919	4.960	5.001	5.042	5.083	5.124	5.164	5.205	5.246	5.287	5.327	120
130	5.327	5.368	5.409	5.450	5.490	5.531	5.571	5.612	5.652	5.693	5.733	130
140	5.733	5.774	5.814	5.855	5.895	5.936	5.976	6.016	6.057	6.097	6.137	140
150	6.137	6.177	6.218	6.258	6.298	6.338	6.378	6.419	6.459	6.499	6.539	150
160	6.539	6.579	6.619	6.659	6.699	6.739	6.779	6.819	6.859	6.899	6.939	160
170	6.939	6.979	7.019	7.059	7.099	7.139	7.179	7.219	7.259	7.299	7.338	170
180	7.338	7.378	7.418	7.458	7.498	7.538	7.578	7.618	7.658	7.697	7.737	180
190	7.737	7.777	7.817	7.857	7.897	7.937	7.977	8.017	8.057	8.097	8.137	190
200	8.137	8.177	8.216	8.256	8.296	8.336	8.376	8.416	8.456	8.497	8.537	200
210	8.537	8.577	8.617	8.657	8.697	8.737	8.777	8.817	8.857	8.898	8.938	210
220	8.938	8.978	9.018	9.058	9.099	9.139	9.179	9.220	9.260	9.300	9.341	220
230	9.341	9.381	9.421	9.462	9.502	9.543	9.583	9.624	9.664	9.705	9.745	230
240	9.745	9.786	9.826	9.867	9.907	9.948	9.989	10.029	10.070	10.111	10.151	240
250	10.151	10.192	10.233	10.274	10.315	10.355	10.396	10.437	10.478	10.519	10.560	250
260	10.560	10.600	10.641	10.682	10.723	10.764	10.805	10.846	10.887	10.928	10.969	260
270	10.969	11.010	11.051	11.093	11.134	11.175	11.216	11.257	11.298	11.339	11.381	270
280	11.381	11.422	11.463	11.504	11.546	11.587	11.628	11.669	11.711	11.752	11.793	280
290	11.793	11.835	11.876	11.918	11.959	12.000	12.042	12.083	12.125	12.166	12.207	290
300	12.207	12.249	12.290	12.332	12.373	12.415	12.456	12.498	12.539	12.581	12.623	300
310	12.623	12.664	12.706	12.747	12.789	12.831	12.872	12.914	12.955	12.997	13.039	310
320	13.039	13.080	13.122	13.164	13.205	13.247	13.289	13.331	13.372	13.414	13.456	320
330	13.456	13.497	13.539	13.581	13.623	13.665	13.706	13.748	13.790	13.832	13.874	330
340	13.874	13.915	13.957	13.999	14.041	14.083	14.125	14.167	14.208	14.250	14.292	340
350	14.292	14.334	14.376	14.418	14.460	14.502	14.544	14.586	14.628	14.670	14.712	350
360	14.712	14.754	14.796	14.838	14.880	14.922	14.964	15.006	15.048	15.090	15.132	360
370	15.132	15.174	15.216	15.258	15.300	15.342	15.384	15.426	15.468	15.510	15.552	370
380	15.552	15.594	15.636	15.679	15.721	15.763	15.805	15.847	15.889	15.931	15.974	380
390	15.974	16.016	16.058	16.100	16.142	16.184	16.227	16.269	16.311	16.353	16.395	390
400	16.395	16.438	16.480	16.522	16.564	16.607	16.649	16.691	16.733	16.776	16.818	400
410	16.818	16.860	16.902	16.945	16.987	17.029	17.072	17.114	17.156	17.199	17.241	410
420	17.241	17.283	17.326	17.368	17.410	17.453	17.495	17.537	17.580	17.622	17.664	420
430	17.664	17.707	17.749	17.792	17.834	17.876	17.919	17.961	18.004	18.046	18.088	430
440	18.088	18.131	18.173	18.216	18.258	18.301	18.343	18.385	18.428	18.470	18.513	440
450	18.513	18.555	18.598	18.640	18.683	18.725	18.768	18.810	18.853	18.895	18.938	450
460	18.938	18.980	19.023	19.065	19.108	19.150	19.193	19.235	19.278	19.320	19.363	460
470	19.363	19.405	19.448	19.490	19.533	19.576	19.618	19.661	19.703	19.746	19.788	470
480	19.788	19.831	19.873	19.916	19.959	20.001	20.044	20.086	20.129	20.172	20.214	480
490	20.214	20.257	20.299	20.342	20.385	20.427	20.470	20.512	20.555	20.598	20.640	490

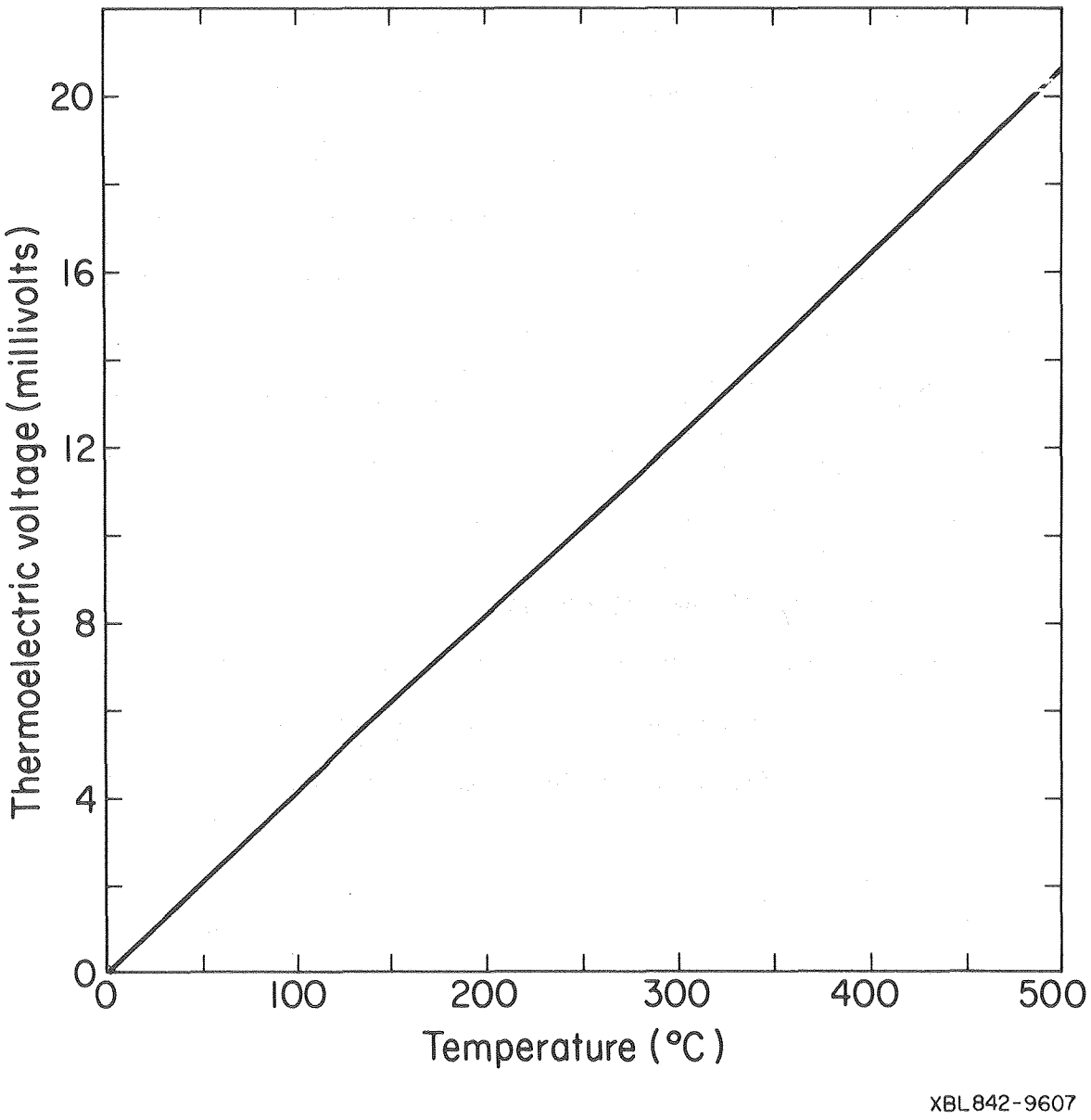

Fig. A-1. NBS voltage-versus-temperature graph for Chromel-Alumel (ANSI type-K) thermocouples.

resistances of 99.98, 138.44 and 198.15 ohms, respectively. Additional points calculated for each °F are listed in Table A-2.

The RTD was recalibrated by the Swedish Bureau of Standards on 18 May 1978. Calibrations were performed at 0°C in ice water, at 60°C in a water bath, at 120 and 180°C in an oil bath, at 250°C in a sand bath, and again at 0°C in ice water. RTD currents were maintained at 1 mA during calibrations. The resulting calibration data is listed in Table A-3 and is shown graphically in Fig. A-2 illustrating the nearly linear characteristics. Figure A-3 shows the deviation between the calibrations from Omega and the Swedish Bureau of Standards.

At the conclusion of the experiment the RTD was again compared with two accurate temperature standards at the University of California's Richmond Field Station. Figure A-4 illustrates the deviations that were found. This final calibration is discussed in Section 3.3.

Table A-2. Omega Engineering's calibration data for RTD S/N 1116, dated 12 August 1977.

°F	Sensor resistance in Ohms									
	0	1	2	3	4	5	6	7	8	9
30			99.98	100.20	100.41	100.63	100.85	101.06	101.28	101.50
40	101.71	101.93	102.15	102.36	102.58	102.79	103.01	103.23	103.44	103.66
50	103.88	104.09	104.31	104.52	104.74	104.96	105.17	105.39	105.60	105.82
60	106.03	108.25	106.47	106.68	106.90	107.11	107.33	107.54	107.76	107.97
70	108.19	108.41	108.62	108.84	109.05	109.27	109.48	109.70	109.91	110.13
80	110.34	110.56	110.77	110.99	111.20	111.42	111.63	111.85	112.06	112.28
90	112.49	112.71	112.92	113.14	113.35	113.57	113.78	113.99	114.21	114.42
100	114.64	114.85	115.07	115.28	115.50	115.71	115.92	116.14	116.35	116.57
110	116.78	116.99	117.21	117.42	117.64	117.85	118.06	118.28	118.49	118.71
120	118.92	119.13	119.35	119.56	119.77	119.99	120.20	120.41	120.63	120.84
130	121.05	121.27	121.48	121.69	121.91	122.12	122.33	122.55	122.76	122.97
140	123.19	123.40	123.61	123.83	124.04	124.25	124.46	124.68	124.89	125.10
150	125.32	125.53	125.74	125.95	126.17	126.38	126.59	126.80	127.02	127.23
160	127.44	127.65	127.87	128.08	128.29	128.50	128.72	128.93	129.14	129.35
170	129.56	129.78	129.99	130.20	130.41	130.62	130.84	131.05	131.26	131.47
180	131.68	131.89	132.11	132.32	132.53	132.74	132.95	133.16	133.38	133.59
190	133.80	134.01	134.22	134.43	134.64	134.85	135.07	135.28	135.49	135.70
200	135.91	136.12	136.33	136.54	136.75	136.96	137.18	137.39	137.60	137.81
210	138.02	138.23	138.44	138.65	138.86	139.07	139.28	139.49	139.70	139.91
220	140.12	140.33	140.54	140.75	140.97	141.18	141.39	141.60	141.81	142.02
230	142.23	142.44	142.65	142.86	143.07	143.28	143.49	143.70	143.90	144.11
240	144.32	144.53	144.74	144.95	145.16	145.37	145.58	145.79	146.00	146.21
250	146.42	146.63	146.84	147.05	147.26	147.47	147.68	147.88	148.09	148.30
260	148.51	148.72	148.93	149.14	149.35	149.56	149.76	149.97	150.18	150.39
270	150.60	150.81	151.02	151.23	151.43	151.64	151.85	152.06	152.27	152.48
280	152.68	152.89	153.10	153.31	153.52	153.73	153.93	154.14	154.35	154.56
290	154.77	154.97	155.18	155.39	155.60	155.81	156.01	156.22	156.43	156.64
300	156.84	157.05	157.26	157.47	157.68	157.88	158.09	158.30	158.50	158.71
310	158.92	159.13	159.33	159.54	159.75	159.96	160.16	160.37	160.58	160.78
320	160.99	161.20	161.41	161.61	161.82	162.03	162.23	162.44	162.65	162.85
330	163.06	163.27	163.47	163.68	163.89	164.09	164.30	164.50	164.71	164.92
340	165.12	165.33	165.54	165.74	165.95	166.16	166.36	166.56	166.77	166.98
350	167.19	167.39	167.60	167.80	168.01	168.21	168.42	168.63	168.83	169.04
360	169.24	169.45	169.65	169.86	170.07	170.27	170.48	170.68	170.89	171.09
370	171.30	171.50	171.71	171.91	172.12	172.32	172.53	172.73	172.94	173.14
380	173.35	173.55	173.76	173.96	174.17	174.37	174.58	174.78	174.99	175.19
390	175.40	175.60	175.81	176.01	176.22	176.42	176.62	176.83	177.03	177.24
400	177.44	177.65	177.85	178.05	178.26	178.46	178.67	178.87	179 08	179.28
410	179.48	179.69	179.89	180.09	180.30	180.50	180.71	180.91	180.11	181.32
420	181.52	181.72	181.93	182.13	182.33	182.54	182.74	182.95	183.15	183.35
430	183.56	183.76	183.96	184.16	184.37	184.57	184.77	184.98	185.18	185.38
440	185.59	185.79	185.99	186.19	186.40	186.60	186.80	187.01	187.21	187.41
450	187.61	187.82	188.02	188.22	188.42	188.63	188.83	189.03	189.23	189.44
460	189.64	189.84	190.04	190.24	190.45	190.65	190.85	191.05	191.26	191.46
470	191.66	191.86	192.06	192.26	192.47	192.67	192.87	193.07	193.27	193.47
480	193.68	193.88	194.08	194.28	194.48	194.68	194.89	195.09	195.29	195.49
490	195.69	195.89	196.09	196.29	196.50	196.70	196.90	197.10	197.30	197.50

Table A-3 Swedish Bureau of Standards' calibration data for RTD S/N 1116, dated 18 May 1978.

°C	RTD Resistance in Ohms									
	0	1	2	3	4	5	6	7	8	9
0	100.010	100.401	100.792	101.182	101.572	101.963	102.353	102.743	103.133	103.522
10	103.912	104.302	104.691	105.080	105.469	105.858	106.247	106.636	107.024	107.413
20	107.801	108.190	108.578	108.966	109.354	109.741	110.129	110.516	110.904	111.291
30	111.678	112.065	112.452	112.839	113.226	113.612	113.998	114.385	114.771	115.157
40	115.543	115.929	116.314	116.700	117.085	117.470	117.856	118.241	118.626	119.010
50	119.395	119.780	120.164	120.548	120.932	121.316	121.700	122.084	122.468	122.851
60	123.235	123.618	124.001	124.384	124.767	125.150	125.533	125.916	126.298	126.680
70	127.063	127.445	127.827	128.208	128.590	128.972	129.353	129.735	130.116	130.497
80	130.878	131.259	131.640	132.020	132.401	132.781	133.161	133.542	133.922	134.302
90	134.681	135.061	135.440	135.820	136.199	136.578	136.957	137.336	137.715	138.094
100	138.472	138.851	139.229	139.607	139.985	140.363	140.741	141.119	141.497	141.874
110	142.251	142.629	143.006	143.383	143.760	144.136	144.513	144.890	145.266	145.642
120	146.018	146.394	146.770	147.146	147.522	147.897	148.273	148.648	149.023	149.398
130	149.773	150.148	150.523	150.897	151.272	151.646	152.020	152.395	152.769	153.142
140	153.516	153.890	154.263	154.637	155.010	155.383	155.756	156.129	156.502	156.874
150	157.247	157.619	157.992	158.364	158.736	159.108	159.480	159.851	160.223	160.595
160	160.966	161.337	161.708	162.079	162.450	162.821	163.191	163.562	163.932	164.303
170	164.673	165.043	165.413	165.782	166.152	166.522	166.891	167.260	167.630	167.999
180	168.368	168.737	169.105	169.474	169.842	170.211	170.579	170.947	171.315	171.683
190	172.051	172.418	172.786	173.153	173.521	173.888	174.255	174.622	174.989	175.355
200	175.722	176.088	176.455	176.821	177.187	177.553	177.919	178.285	178.650	179.016
210	179.381	179.746	180.111	180.476	180.841	181.206	181.571	181.935	182.300	182.664
220	183.028	183.392	183.756	184.120	184.484	184.848	185.211	185.574	185.938	186.301
230	186.664	187.027	187.389	187.752	188.115	188.477	188.839	189.201	189.564	189.925
240	190.287	190.649	191.011	191.372	191.733	192.095	192.456	192.817	193.178	193.538

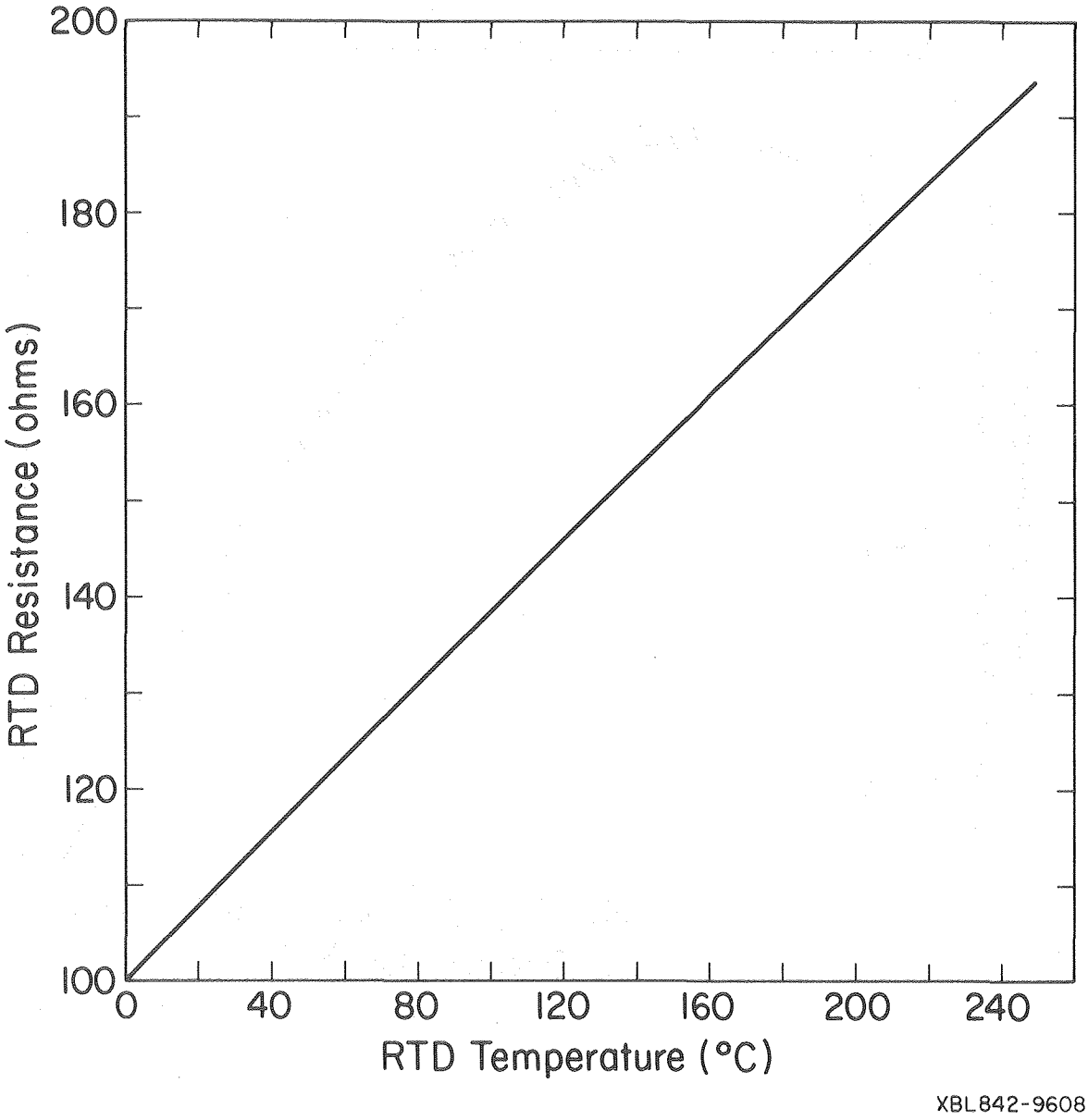

Fig. A-2. RTD resistance-versus-temperature from the Swedish Bureau of Standards calibration.

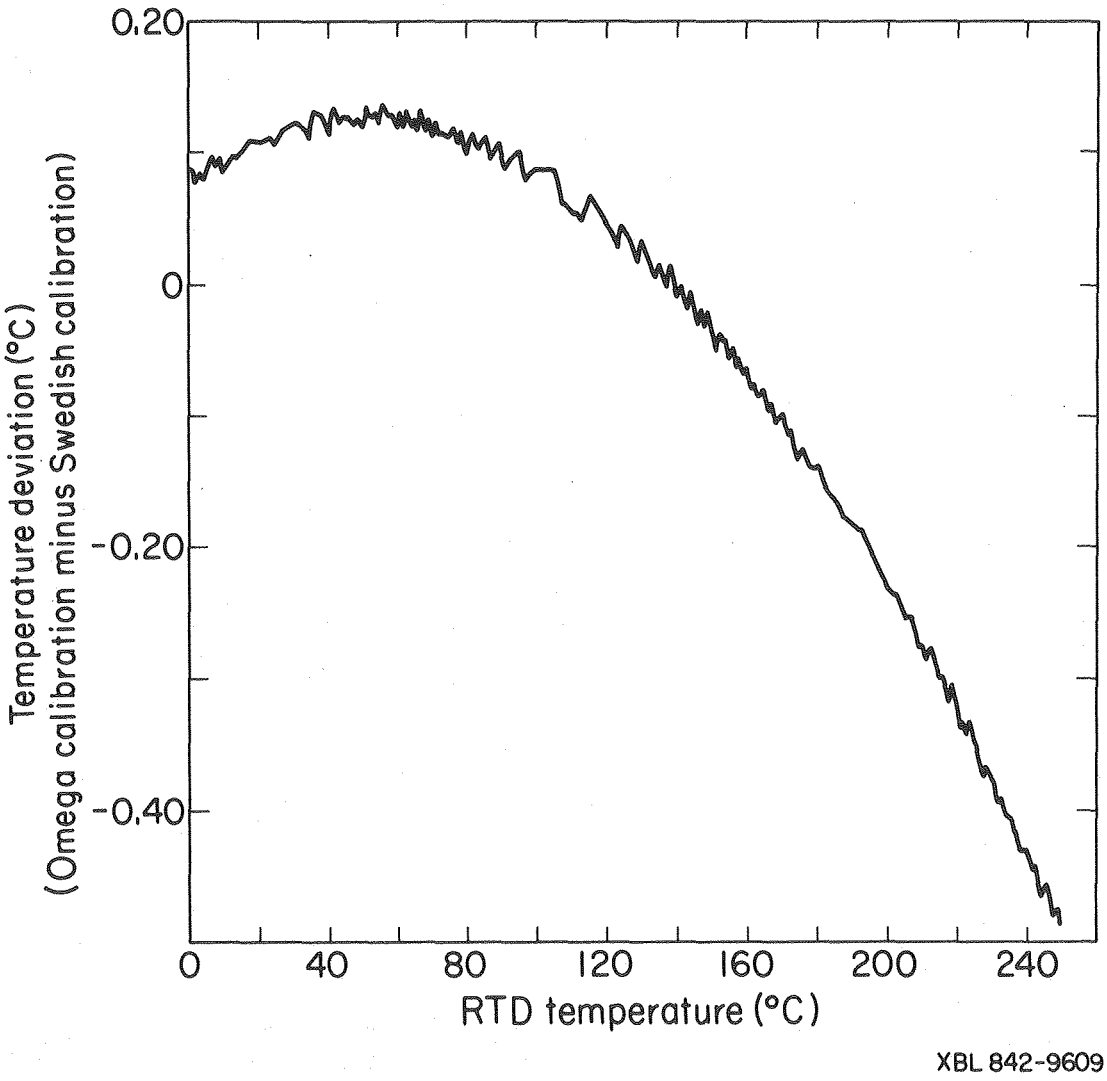

Fig. A-3. Deviation between RTD calibrations from Omega Engineering and the Swedish Bureau of Standards.

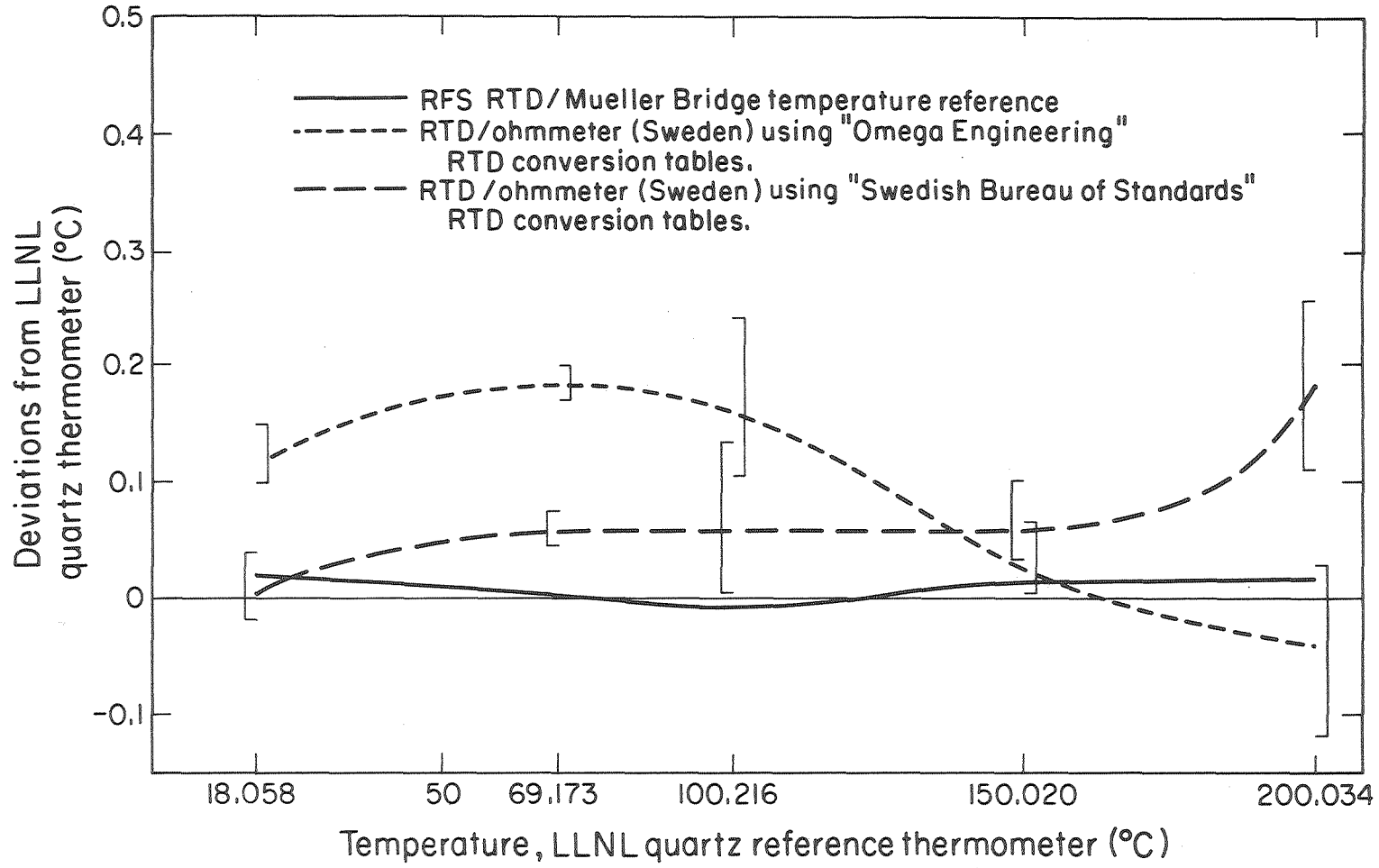

Fig. A-4. Richmond Field Station Calibration of RTD (S/N 1116) and Fluke 8500A ohmmeter (S/N 805003) used in Sweden for thermocouple calibrations.